

Durham E-Theses

Surface Functionalised Emulsion- Templated Porous Polymers for In- Vitro Cell Culture

CAROLINE MARGARET ZEYFERT

How to cite:

ZEYFERT, CAROLINE MARGARET (2010) Surface Functionalised Emulsion- Templated Porous Polymers for In- Vitro Cell Culture. Doctoral thesis, Durham University.

Use policy

The full-text may be used and/or reproduced, and given to third parties in any format or medium, without prior permission or charge, for personal research or study, educational, or not-for-profit purposes provided that:

- a full bibliographic reference is made to the original source
- a <https://etheses.durham.ac.uk/id/eprint/794/> is made to the metadata record in Durham E-Theses
- the full-text is not changed in any way

The full-text must not be sold in any format or medium without the formal permission of the copyright holders.

Please consult the [full Durham E-Theses policy](#) for further details.

Surface Functionalised Emulsion- Templated Porous Polymers for *In- Vitro* Cell Culture

Submitted in Fulfillment for the Degree of PhD
University of Durham
December 2010

Caroline M. Zeyfert

“The copyright of this thesis rests with the author. No quotation from it should be published without the prior written consent and information derived from it should be acknowledged.”

Surface Functionalised Emulsion-Templated Porous Polymers for In-Vitro Cell Culture

Caroline M. Zeyfert

ABSTRACT: “PolyHIPE” is an acronym for **poly**merized high internal phase emulsions. The nature of the formation of PolyHIPEs creates a highly porous, interconnected monolith structure, the architecture of which can be tightly controlled. Styrene-2-ethylhexylacrylate-divinylbenzene PolyHIPEs with defined architecture of voids between 80 - 100 μm have been previously investigated as suitable supports for *in-vitro* cell culture, but the highly hydrophobic nature of the predominantly polystyrene scaffold requires extra processing steps to hydrate the surface before use as a support for cell culture.

This thesis addresses routes to surface functionalise these PolyHIPEs for the specific aim of optimising 3D *in-vitro* cell culture materials. Specific routes to this include chemical modification, plasma treatment and chemical adsorption. Of these three routes to surface functionalisation, the plasma processing appears to give the best results, with further attachment of biologically-directing molecules, possible.

This thesis presents oxygen plasma treatment as a route to increase the hydrophilicity of these materials, with a reasonable shelf-life, which both reduces the processing steps before cell culture, and increases cell viability when grown on the functionalised PolyHIPE. The ultimate aim in this project is to create smart “off-the-shelf” materials that can control cell behaviour *in-vitro*. Chemical attachment to the surface of the PolyHIPE with synthetic retinoid EC23 has been proposed, and initial chemical tests obtained to suggest attachment, with future testing with mammalian cells envisaged.

Table of Contents

Title Page.....	i
Abstract.....	iii
Table of Contents.....	iv
List of Figures	ix
List of Tables.....	xiv

Chapter 1 - Introduction

1.1 Introduction and Aims	1
1.2 Polymers	1
1.2.1 Emulsion Polymerisation.....	2
1.2.2 PolyHIPE Manufacture.....	5
1.2.3 In-Vitro Cell Culture.....	7
1.2.4 PolyHIPEs as Scaffolds for Cell Culture.....	10
1.3 Retinoids	14
1.4 Plasma	16
1.5 References	20

Chapter 2 - Experimental and Techniques

2.1 PolyHIPE Synthesis	26
2.1.1 Materials	26
2.1.2 Standard PolyHIPE Preparation.....	26
2.1.3 Stirrer Variation	27
2.1.4 Variation of Aqueous Phase Temperature	27
2.1.5 Swelling of PolyHIPE Slices.....	28
2.2 PolyHIPE Chemical Modification.....	28

2.2.1	Bromination of PolyHIPE.....	28
2.2.2	Titration of bromine vs. PolyHIPE	28
2.2.3	Amination.....	29
2.2.4	Thiolation	29
2.2.5	Dopamine Treatment	29
2.2.6	Further Reactivity of Dopamine Coated Substrates	30
	2.2.6.1 Thiolation.....	30
	2.2.6.2 Aiamine Attachment	30
	2.2.6.3 Ninhydrin Test	30
	2.2.6.4 Fluorine Attachment	30
2.2.7	Plasma treatment.....	30
2.2.8	Fluorine functionalisation	31
	2.2.8.1 Carboxyl Derivatisation Procedure	31
	2.2.8.2 Carbonyl Derivatisation Procedure	31
	2.2.8.3 Hydroxyl Derivatisation Procedure	31
	2.2.8.4 Cysteamine Derivatisation Procedure	32
2.3	Cell Culture	32
	2.3.1 Cell Preparation	32
	2.3.2 PolyHIPE Preparation	33
	2.3.3 Histology	33
	2.3.4 Preparation for SEM.....	34
	2.3.5 MTS Assay.....	34
	2.3.6 STF Investigation	34
2.4	Sample Preparation for Physical Analysis.....	35
	2.4.1 SEM	35
	2.4.2 Wet Mode ESEM.....	35
2.5	Retinoids:	35
	2.5.1 Solution Phase Thio-ester Formation.....	35
	2.5.2 Solid Phase Thio-ester Formation.....	36
2.6	Analytical Techniques	37
	2.6.1 XPS.....	37
	2.6.2 Tof-SIMS.....	37

2.7	Background theory of Analytical Techniques.....	37
	2.7.1 Elemental Analysis.....	37
	2.7.2 ToF-SIMS.....	38
	2.7.3 XPS.....	39
	2.7.4 (E)SEM	40
2.8	References	41

Chapter 3 - PolyHIPE Manufacture

3.1	Introduction.....	42
3.2	Stirrer Variation	44
3.3	Sectioning PolyHIPE Monoliths.....	46
3.4	Swelling of PolyHIPE Slices	47
3.5	Surface Topological Features (STF).....	49
3.6	MG63 <i>In-Vitro</i> Cell Culture on PolyHIPE Slices.....	54
3.7	ToF-SIMS	56
3.8	XPS	60
3.9	Conclusions.....	64
3.10	References	65

Chapter 4 - Wet Chemical Functionalisation of PolyHIPEs

4.1	Introduction.....	66
4.2	Bromination	66
4.3	Amination	69
4.4	Thiolation.....	69
4.5	Bromination of 100 % DVB PolyHIPE.....	70
4.6	Poly-Dopamine Coating of PolyHIPEs.....	71

4.7	Contact Angles	75
4.8	XPS	76
4.9	Tof-SIMS	79
4.10	<i>In-Vitro</i> Cell Culture on Polydopamine Treated PolyHIPEs	84
4.11	Histology.....	85
4.12	Conclusions.....	86
4.13	References	87

Chapter 5 - Plasma Treatment

5.1	Introduction.....	88
5.2	Optimisation (machine)	88
5.3	Optimisation (Parameters).....	93
5.4	Chemical Markers	96
5.5	Contact Angles and Wet Mode SEM	97
5.6	X-ray Photoelectron Spectroscopy (XPS).....	101
5.7	Cell Culture.....	110
5.8	Comparison with Commercial TCPS	113
5.9	Conclusions.....	114
5.10	References	115

Chapter 6 - Further Functionalisation

6.1	Introduction.....	116
6.2	Thiol Attachment to Dopamine Treated Substrates.....	116
6.3	Diamine attachment	118
6.4	Fluorine Attachment	121
6.5	Solvent Effects	123

6.6	Introduction to Retinoids.....	124
6.7	Adsorption of EC23 onto PolyHIPE slices.	125
6.8	Solution Phase Thio-ester Formation.	129
6.10	Conclusions.....	134
6.11	References	134

Chapter 7 - Conclusions and Future Work

7.1	Conclusions.....	136
7.2	Future Work.....	136

List of Figures

Figure 1.1	Schematic of a stabilised emulsion.....	3
Figure 1.2	Schematic of the steps requires to make a PolyHIPE material from an emulsion.	4
Figure 1.3	SEM image of a “typical” PolyHIPE including definitions of void and interconnect.	5
Figure 1.4	Structure of natural retinoids and synthetic retinoid EC23	15
Figure 1.5	Definitions of water droplet behaviour on a rough surface	20
Figure 2.1	Very simplified diagram of a Tof-SIMS instrument.....	39
Figure 2.2	Very simplified diagram of an XPS instrument.....	40
Figure 2.3	Very simplified diagram of a SEM instrument	41
Figure 3.1	Schematic of PolyHIPE manufacture.....	42
Figure 3.2	Reaction of monomeric components to form the PolyHIPE	43
Figure 3.3	Photograph of a Tornado/Starfish stirrer set up	44
Figure 3.4	Average void diameter comparison with stirrer variation.....	45
Figure 3.5	Photograph of thin sections of PolyHIPE	46
Figure 3.6	SEM images and graph showing the void diameter difference between swollen and non swollen PolyHIPE slices	48
Figure 3.7	SEM images of STF present on a washed PolyHIPE	49
Figure 3.8	SEM images of the separated phase formed alongside the PolyHIPE upon curing.....	51
Figure 3.9	SEM images illustrating monoliths formed with subtly different processing parameters	53

Figure 3.10.	Photograph of PolyHIPE slices in the bottom of a typical tissue-culture six-well plate	54
Figure 3.11	SEM micrographs at 7 day time point, showing cells growing on PolyHIPE scaffold with, and without STF present.....	55
Figure 3.12	MTS assay results showing no significant difference in viability between cells grown on PolyHIPE slices with or without STF.....	56
Figure 3.13	Tof-SIMS spectra of the lower region negative ions of unfunctionalised PolyHIPE slices	57
Figure 3.14	Tof-SIMS spectra of the lower region positive ions of unfunctionalised PolyHIPE slices.....	58
Figure 3.15	Composite 500 μm^2 ion images of the Tof-SIMS of unfunctionalised PolyHIPE slices	59
Figure 3.16	Carbon high resolution peak from XPS analysis showing typical C 1s assymetry and carbon carboxylic acid peak	61
Figure 3.17	Oxygen high resolution peak from XPS analysis showing carboxylic acid-type groups.	62
Figure 3.18	XPS Analysis of the wide scan of the Sulfur peak.....	63
Figure 4.1	IR spectrum showing nP blank spectrum and brominated nP PolyHIPE	68
Figure 4.2	Infrared spectra of 100 % DVB PolyHIPE slice	71
Figure 4.3	Figure adapted from Messersmith et al showing a possible route to the polydopamine coating	72
Figure 4.4	Photograph of the setup of the polydopamine experiment.....	73
Figure 4.5	Photograph of colour change indicating polydopamine coating on mesh supports, PolyHIPE slices and flat bacteriological plate.....	74

Figure 4.6	Photograph of three PolyHIPE slice illustrating increased polydopamine coverage due to pre-wetting	74
Figure 4.7	Photograph of three slices of PolyHIPE showing difference in polydopamine deposition over time	75
Figure 4.8	Example photographs showing the difference in contact angles by 100 μ l droplets of water on the untreated and dopamine treated substrates.....	76
Figure 4.9	XPS wide scans showing increase in nitrogen and oxygen content upon treatment of blank PolyHIPE slices and bacteriological plates with the polydopamine treatment.....	77
Figure 4.10	High resolution oxygen peak scans taken from the XPS analysis...	78
Figure 4.11	The positive spectra taken from ToF-SIMS data of a polydopamine coated PolyHIPE	79
Figure 4.12	Positive peaks from dopamine coated PolyHIPE.....	81
Figure 4.13	ToF-SIMS composite images and corresponding ion assignments for blank PolyHIPE slices.....	82
Figure 4.14	ToF-SIMS composite images and corresponding ion assignments for dopamine coated PolyHIPE slices.....	83
Figure 4.15	Graph showing results of the MTS viability assay over time.....	84
Figure 4.16	SEM images of cells growing through PolyHIPE slices.....	85
Figure 4.17	Photographs taken down a microscope of H&E stained PolyHIPE slices.....	86
Figure 5.1	Glass centrifuge tube with PolyHIPE slice inside. Photographs of PolyHIPE slices shown before treatment and after treatment.....	89

Figure 5.2	Photograph of water droplet behaviour on plasma treated PolyHIPE slices	90
Figure 5.3	Glass and PTFE sample holder developed for plasma treatment of PolyHIPE slices.	91
Figure 5.4	Plasma treated samples burned through by the TePla Plasma Asher.	92
Figure 5.5	Photograph of stages of plasma treatment of PolyHIPE	93
Figure 5.6	Photographs of 3 different PolyHIPE slices, showing effects of plasma treatment by initial stage thinning and final stage burning .	95
Figure 5.7	SEM images of PolyHIPEs showing mass loss	95
Figure 5.8	Three dyed PolyHIPE slices as seen under a UV light	96
Figure 5.9	Structure of Rhodamine B.....	96
Figure 5.10	Setup of a Peltier stage within the ESEM	98
Figure 5.11	ESEM images taken in wet mode	99
Figure 5.12	Blank and plasma treated PolyHIPE SEM images showing water droplet formation.....	100
Figure 5.13	Schematic of how surface roughness affects contact angle	100
Figure 5.14	High resolution oxygen 1s scans from XPS analysis	102
Figure 5.15	XPS graph of 1s peaks showing the very little difference of oxygen composition with variation of time of treatment.....	103
Figure 5.16	Schematic of the derivatisation procedures of the surface oxygen-containing groups on the PolyHIPE and plasma treated PolyHIPE	106
Figure 5.17	MTS assay showing a significant difference between blank PolyHIPE and wet plasma treated PolyHIPE slice.....	111

Figure 5.18	SEM images of 7 day time points showing increased cell coverage on the wet plasma treated polyHIPE slice compared to the blank polyHIPE	112
Figure 5.19	Bar chart with table showing comparison of XPS results of PolyHIPE with commercial samples	113
Figure 6.1	Photographs illustrating contact angles of polystyrene squares before and after thiolation	117
Figure 6.2	Photographs of ninhydrin treated PolyHIPE slices after reaction with octanediamine and ethanediamine.....	119
Figure 6.3	Photographs of ninhydrin treated powders after reaction with octanediamine and ethanediamine	120
Figure 6.4	Graph of Percentage change of each component before and after reaction with fluorine containing molecules	122
Figure 6.5	2D structure of EC23 and all-trans-retinoic-acid (ATRA)	124
Figure 6.6	UV curve of 0.1 mg / ml EC23 in DMSO	126
Figure 6.7	Concentration curves for absorbance of EC23 in DMSO at 308 nm.....	127
Figure 6.8	UV absorption by solvent at 308nm	128
Figure 6.9	2D structures of EC23 acid form and EC23 Ester form.....	129
Figure 6.10	Reaction scheme reaction to form a EC23-thioester in solution....	130
Figure 6.11	Sample NMRs showing spectra of EC23 and EC23-thiol product.	131
Figure 6.12	Schematic of EC23 functionalisation of PolyHIPE surfaces.....	132

List of Tables

Table 3.1	Elemental analysis of the composition of monolith material compared to the microdroplet/STF material.....	51
Table 3.2	Corresponding table of negative peaks for the Tof-SIMS spectra shown in figure 3.13.....	57
Table 3.3	Tof-SIMS peak list of the lower region positive ions of an unfunctionalised PolyHIPE	59
Table 3.4	Table of quantification of the wide scan XPS analysis of the sulfur peak.....	63
Table 4.1	Quantity of bromine from a radical addition and an electrophilic addition reaction analysis of sulfur peak	67
Table 4.2	Elemental analysis values from amination experiments	69
Table 4.3	Bromination data showing the difference in amount of bromine incorporation between nP and PolyHIPE made by the Mercier paper route	71
Table 4.4	Corresponding table of values from the XPS wide scans plotted in figure 4.9.....	77
Table 4.5	Table of peak assignation from Tof-SIMS data analysis of the dopamine treated PolyHIPE.....	80
Table 5.1	Hydrophobic recovery of the plasma treated PolyHIPE slices assessed over time.....	93
Table 5.2	Table of mass loss of PolyHIPE slices after different time points of plasma treatment.....	94

Table 5.3	Percentage compositions of the plasma treated PolyHIPE over four weeks	102
Table 5.4	XPS table of oxygen percentage composition with variation of time of treatment.....	103
Table 5.5	XPS analysis of plasma treated slices before and after ethanol immersion	104
Table 5.6	XPS data showing the degree of attachment for each functional fluorine containing molecule	106
Table 5.7	XPS data showing the degree of attachment calculated from the amount of fluorine present	108
Table 5.8	XPS data of PolyHIPE slices after derivatisation reactions	108
Table 6.1	XPS analysis of dopamine coated PolyHIPE substrate before and after thiolation	117
Table 6.2	Averaged surface components after diamine attachment taken from XPS analysis	120
Table 6.3	XPS assigned percentages from plasma treatment and polydopamine treatment reaction with fluorine containing molecules	122
Table 6.4	XPS analysis of solvent effects of DMF on plasma treated PolyHIPE slices	124
Table 6.5	UV absorption at 308 nm	128
Table 6.6	Comparative UV readings at 308 nm of amount of free EC23 in solution for each of the functionalised surfaces	133

Chapter 1 - Introduction

1.1 Introduction and Aims

This thesis sets out to create, and optimise a porous, polymeric scaffold for *in-vitro* cell culture. The cell type used throughout this thesis (MG63) is an osteoblast-like cell line which is known for its robustness, tolerance and its reasonably short cell cycle. This cell line however is used here as a demonstrator, as the scaffold is being developed for a support to culture a variety of cell lines within the laboratory setting.

The first aim is to simplify, and exemplify the use of the scaffold for in-vitro cell culture. The second aim is to demonstrate by surface analysis that an adlayer could be created on the surface of the polyHIPE, whilst keeping the polymeric material morphology the same. The third aim was to demonstrate that these adlayers formed in aims 1 and 2 could be further functionalised with reactive molecules. The final, overall aim, is to attach, and release, with at least some semblance of control, bioactive molecules to the surface of the polymeric scaffold, to influence cell growth, proliferation and/or attachment in an *in-vitro* laboratory setting.

1.2 Polymers

No thesis, or polymer tract, would be without the almost obligatory definition of a polymer, taken from the Greek, *poly* = *many* and *meros* = *particles* or *units*.

A brief history of polymers should then follow, to include events such as Jons Jacob Berzelius defining the word "*polymer*" in 1832 to describe substances that are identical in chemical composition but have differing molecular weights. Classic

examples are acetylene, benzene and styrene, having the formula C_nH_n with $n = 2, 6$ and 8 , respectively).

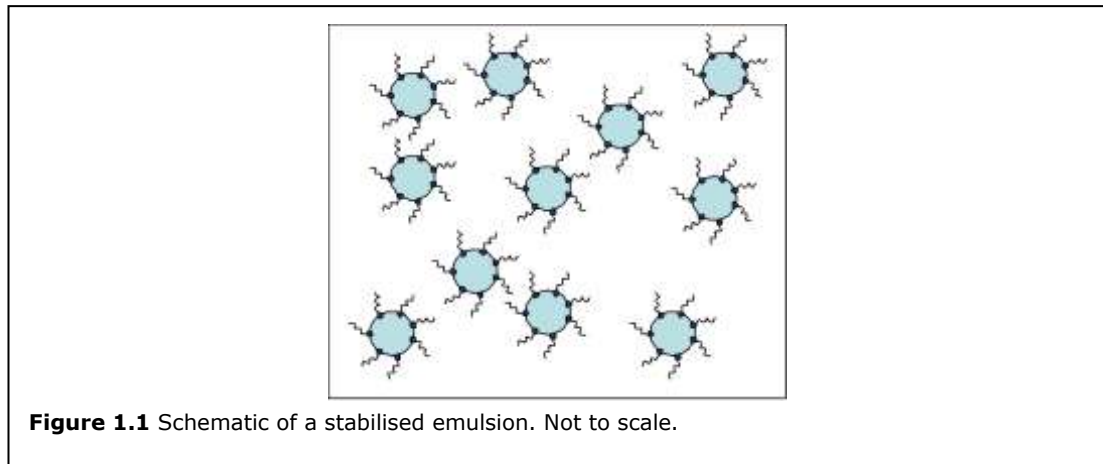
A mention must also be given to key developments in the birth of the plastics industry, such as Alexander Parkes's nitrocellulose "Parkesine"¹ (1855) or Celluloid (1872); the composition of which is predominantly Parkesine with a camphor plasticiser. An extension of the cellulose (a natural polymer) based products were also used as a bases for fabrics, coming through the names of "Chardonnay Silk" in 1885 (although nitrocellulose based material was soon removed from the clothing market due to its extreme flammability) to "Rayon", introduced in 1905, made up of a regenerated cellulose fibre, still in use today, under the more generic name of "viscose" fibre.

Citing the differences between "natural" and "synthetic" polymer materials leads to an unavoidable mention to Bakelite - the first commercially produced synthetic polymer, (although the phenol component can be sourced "naturally"). Bakelite was patented in 1909 Belgian chemist Dr. Leo Baekeland.² and the material's development is recognised by the American Chemical Society (ACS) as a "Chemical Landmark".³ Bakelite is a very versatile, moldable material, predominantly for a cheaper, lighter, tougher wood replacement in commodity items such as radios in the 1920s and 30s. It was almost exclusively replaced with further synthetic polymers, such as acrylic, in the 1950s.

1.2.1 Emulsion Polymerisation

An emulsion can be defined as a dispersal of immiscible liquids. Usually the emulsion can be kept in a quasi-stable state with use of suitable surfactants. A schematic of a simple, stabilised emulsion is shown in figure 1.1. The classic

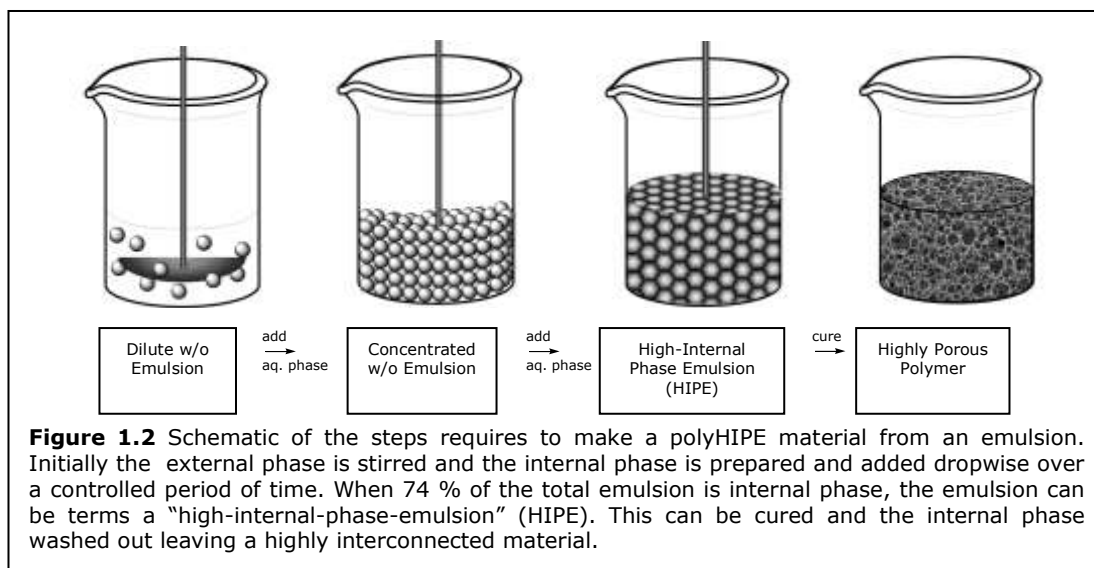
example of an emulsion is milk - where fat droplets are kept suspended in an aqueous external phase, stabilised by milk phospholipids.



Emulsion polymerisation can describe two methods of forming polymers. One way to form polymer particles, is for an emulsion to be formed of a monomer mixture in a immiscible solvent, for example water. The polymer emulsion is then cured, by heat, UV, redox as examples, and the internal phase of the emulsion is polymerised, forming discrete particles. If the emulsion is formed in such a way as to control the size and distribution of these particles, then particles of a controlled size and shape can be formed. Conversely, if an emulsion is formed with the monomer mixture as the external phase, which is then cured, the water droplets are then suspended in a enclosed polymer structure.

A high internal phase emulsion (HIPE) is an emulsion in which the internal (or dispersed) phase occupies more than 74 % of the volume. This figure is reached by the calculation of the space filling properties of regular, monodispersed spheres. Once above this limit the maximum packing fraction is reached and the droplets are forced into non-uniform polyhedral shapes, separated by a thin continuous film. This external monomeric phase can then be cured, again by UV, heat, redox reactions as examples. The curing of the emulsion causes a porous structure to be formed, allowing the internal (usually aqueous) phase to be washed

out, along with the surfactant and any unreacted monomeric components. The final material, the polymerised high internal phase emulsion (polyHIPE) is a highly porous material with a defined internal structure. The stages of polyHIPE formation are shown in figure 1.2.

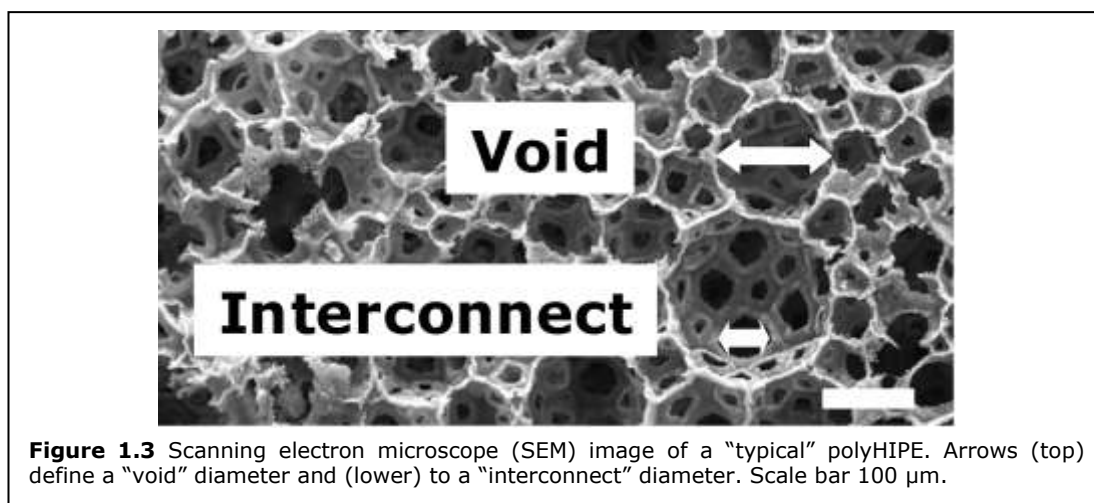


The term polyHIPE was first used by Unilever Research Port Sunlight Laboratory (Cheshire, UK).⁴ PolyHIPE is now a well recognized name for polymerised high internal phase emulsions.

The focus in this thesis are emulsions formed by an aqueous internal phase containing stabilizing salt(s) and water soluble initiator(s) being added to a continuous phase containing monomer(s), cross-linker, surfactant/emulsifier and optional plasticizer.⁵ The emulsion then can be poured into a suitable size/shape mould and be cured (in this case by heat). Upon curing the monomer polymerises. During this process holes form in the continuous film separating the droplets. This has been shown to be due to the retraction of the continuous phase (shrinkage) during the polymerization.⁶

After curing the aqueous phase can be removed, leaving a highly porous, interconnected monolithic structure. This can then be washed (soxhlet), in a

suitable solvent then dried in-vacuo. An example of the structure of the final material is shown in figure 1.3.



Terminology of polyHIPEs vary between research groups. The spherical cavities caused by the water droplets are called “voids”,⁷ “cells”,⁸ “pores”,⁹ and the interconnecting holes between these called, “holes”,¹⁰ “interconnects”,⁵ “windows”,¹¹ “pore throats”,¹² “channels”,¹³ etc.

1.2.2 PolyHIPE Manufacture

PolyHIPEs can be formed from a wide range of monomers, for example aromatic hydrocarbons such as styrene, or methacrylates¹⁴ and with a large variation of morphologies.¹⁵ A novel way of incorporating a methacrylic anhydride modified gelatin into a polyHIPE for proposed biomaterial development has also been published.¹⁶ The final morphology of polyHIPE structure is different to that of a blown foam due to its smaller pore size and interconnected structure.

PolyHIPEs, as previously stated, are formed by emulsion templating. The final structure of the polymer depends on the form and stability of the parent emulsion and parameters such as curing time and temperature. The size and dispersity of the voids in the final material are directly linked to that of the parent emulsion, and by varying the emulsion formation parameters, and the composition of monomer or

additives, the void and interconnect sizes of the polyHIPE can be changed. Tuning the parent emulsion in order to define and control emulsion parameters and to produce a stable emulsion, with defined void size, shape and architecture is discussed further in the literature.¹⁷ It must be remembered that the documented instability of emulsions also has a case here, as any instability in the emulsion can lead, in extreme circumstances, to the emulsion settling out, forming two (or more) layers and preventing polyHIPE formation. Causes of instability in the parent emulsion are due to two main effects - droplet coalescence and Ostwald ripening, these effects lead to a coarsening of the emulsion and increase in droplet size.⁷ Coalescence is where two droplets meet and merge, and Ostwald ripening is a thermodynamically driven effect where larger, more energetically favoured, droplets grow larger at the expense of smaller droplets, due to the migration of molecules of the dispersed phase from smaller droplets to larger droplets through the continuous phase, leading to an overall minimisation of total surface area.

Important parameters in the emulsion stability include the composition of each phase and the amount and type of surfactant and stabilising salts. As previously mentioned, this has been investigated in previous papers, and monolithic polyHIPE material with defined void and interconnect sizes has been prepared and this composition is fixed throughout.⁷ A main advantage to this process, with respect to making easily utilisable scaffolds, is that the emulsion often has low enough viscosity to be cured into a mould of the desired shape of the final monolith prior to curing, which introduce opportunities to create materials of desired size and shape.

Suggested uses for polyHIPEs in the literature include; ion exchange systems,¹⁸ heat resistant structural foams,¹⁹ adsorbents,²⁰ damping materials,²¹ to support initiators for catalysis,²² as supports for sensors,²³ for TEMPO immobilisation,²⁴ as

well as for *in-vitro* cell culture.¹¹ PolyHIPEs have been investigated for supports for cell growth, with the scaffolds affecting proliferation, differentiation and mineralised matrix formation in osteoblasts.²⁵ Biodegradable polyHIPE scaffolds have also been investigated, but this is outside the main scope of this thesis.²⁶

1.2.3 In-Vitro Cell Culture

“*In-vitro cell culture*”, often termed “*tissue culture*” when using eukaryotic cells, is used as a routine tool to culture cells outside the *in-vivo* environment. This thesis focuses on human cells, which have been immortalised into a cell line.

In-vitro cell culture materials have been routinely used for many years. Not only are *in-vitro* cell studies used for toxicology testing, they are also used to study cancerous cell tissue growth, interactions between cells, promoting differentiation (particularly in the case of stem cell research) and to help understand how cells grow and develop. Knowledge gained from culturing cells in engineered environments has the potential to contribute to the design of better systems for the *in-vitro* study of cell biology.

Cells grown *in-vitro* often respond differently to cells grown *in-vivo*. It is a current problem especially when cells are challenged with ranges of potential drug therapies, which fail when pushed onto clinical trials due to specific responses not being identified in the early stages of testing in the laboratory (*in-vitro*) trials.²⁷ It is a recognised fact that cells are affected by the environment in which they are grown.²⁸ The basic mechanisms by which cells adhere, spread and communicate is an active area of research, but by understanding the “basic mechanisms” the aim in this thesis is to create surfaces to control cell behaviour, and to grow cells in a three-dimensional scaffold closer to *in-vivo* conditions as possible with fewer cost and ethical implications than growing *in-vivo*.

When cells are grown *in-vivo* they are exposed to a three dimensional space surrounded by appropriate media, growth factors and at optimum temperatures, humidity and CO₂ levels. Currently the most common substrate for cell culture is tissue-culture-polystyrene (TCPS) which is prevalent in most tissue culture laboratories. The “standard” type of TCPS is made by several manufacturers (eg. Corning, Falcon, Nunc) and generally is a hard, flat polymer base within a vented cap to the container, with a one (hydrophilic) surface to which cells attach and proliferate. Cells are grown inside the TCPS vessels in specialised, optimised, cell culture media, which may contain a balance of salt, glucose, amino acids, vitamin and growth factors. Standard growing conditions are controlled temperature (37 °C), humidity (100 %), and CO₂ levels (5 %). Many studies have shown that *in-vitro* cultured cells grow better and closer to their *in-vivo* counterparts if grown in three dimensions.²⁹ There are several approaches to growing cells in three-dimensions. namely cell aggregates,³⁰ gels and a variety of non-biodegradable and biodegradable scaffolds.^{25,31} Also proposed are ways to prepare solid, non-degradable 3D base scaffolds for cell culture, including porous materials prepared by emulsion templating (as mentioned previously), electrospinning,³² and more novel methods such as creation of 3D porous scaffolds by casting polystyrene mixtures and generating pores within this structure by decomposing ammonium bicarbonate (to ammonia, CO₂ and water) by heating.³³

In-vitro cell culture is used to assess many variables, such as the effect on the cell cycle of cell cycle disrupters, promoters and to also assess the effect of different materials on a given cell type. It has been quoted that there are at least 411 different types of cells within an adult human body, with 145 of these being neurons.³⁴ Recent literature attempts to address the issue of how topology of a substrate affects cell growth, proliferation and development. A predominant theme

within this is comparisons of patterning on flat substrates, for example microtopography³⁵ and nanotopography.³⁶ Another strong vein of research is into the development of 3D substrates or gels, such as the development of dextran hydrogels with macroporous interconnecting structures.³⁷ One example, of many in the literature,³⁸ demonstrates the effect that the flexibility/malleability of a material has on cell growth and development. This can be extended into chemical modification on quartz slides to demonstrate different moduli affects macrophages.³⁹ PDMS has been investigated as a modified substrate for which to control cell behaviour by changing the modulus of the surface material and identifying links to cell attachment.⁴⁰ The modulus of polymeric materials has been shown to influence the cell growth, but the research in this area focuses predominantly on interconnected polymer gel networks. Changing the surface chemistry of the polyHIPE is unlikely to have a great effect on the overall modulus of the material.

Functionalised surfaces to culture cells are a large area of research, with specific motifs being presented to different cell types. Attachment motifs that encourage cell attachment can be classified into several general categories: firstly adsorption onto a surface, this would include dip coating of collagen⁴¹ to increase cell attachment, and there is also far ranging literature dealing with the adsorption of proteins from extracellular matrix (ECM) at solid-liquid interfaces,⁴² and the effect on cell proliferation. Secondly, chemical, covalent, attachment of defined attachment molecules, for example self-assembling monolayers (SAMS) incorporating Arg-Gly-Asp (RGD) peptides,⁴³ to promote cell adhesion. Also there is research that shows deposition of polymer film by RF plasma, for example methylmethacrylate, to influence cell attachment.⁴⁴

1.2.4 PolyHIPEs as Scaffolds for Cell Culture

Biodegradable polyHIPE scaffolds (primarily investigated for the concern of tissue engineering for implantation) have been investigated in the literature for cell culture,⁴⁵⁻⁴⁶ but predominantly are outside the main scope of this thesis, as these are designed for *in-vivo* use.

Recent publications have shown that polyHIPEs, with a well-defined structure, can be used as a three-dimensional scaffold on which to grow cells *in-vitro*.⁴⁷ Slices from the monoliths have been investigated for supports for cell growth, with the scaffolds affecting proliferation, differentiation and mineralised matrix formation in osteoblasts.⁴⁸ PolyHIPEs made with this method have been studied in detail and the morphology of the resulting monoliths characterised.¹⁶

To create a suitable material for cell growth, high porosity and high connectivity with the scaffolds are important, in terms of surface area for cell attachment, but also to allow sufficient diffusion of oxygen to, and waste from, the growing cells. Scaffolds for cell growth/tissue engineering have to be robust in order to be used for handling, including lab-sterilisation procedures, media changes, and removal of cells from the scaffold, often using a protease such as trypsin. Another requirement of scaffolds for cell growth is that they are non-toxic, and stable enough to undergo processing to visualise the cells growing in/on the substrate. Typically, when polyHIPEs are prepared for cell culture, they are immersed in a solution of coating material in an aqueous media, for example collagen in water, and allowed to dry. These can be dip coated several times, to create a thicker layer. This is a standard protocol in biology, whether it is for flat, or 3D substrates. The dip coating creates an undefined surface, where the final conformation of the collagen is not controlled, and not usually chemically analysed. Collagen, for

example can denature onto the surface, so the motifs presented to the cells for binding (for example RGD) cannot be assured. This effect has been demonstrated by immobilizing fibronectin onto an untreated plastic surface and observing the cell behaviour. When these proteins (such as fibronectin) are immobilised, attachment and spreading of cells occur. Cells applied to the dishes coated with the matrix proteins attach “almost quantitatively” to the dish, whereas no cell attachment occurs on control dishes.⁴⁹ However, whether the same binding motif was presented to the cells from each molecule of fibronectin, is open to interpretation.

There also have been papers that suggest fibronectin, (which is also abundant in plasma, tissue fluids) needs a high concentration if attached to a solid substrate in order to promote cell attachment.⁴⁴

Proteins will adsorb to the polyHIPE scaffold from solution. This is a very non-specific technique, and can lead to denaturation of the protein due to non-controlled attachment. Most ECM proteins have several different cell binding regions and the proteins can adsorb onto the surface in multiple conformations, masking or exposing different peptide sequences. This leads to a sub-optimal, heterogeneous substrate for cell attachment. This process also leads to intrinsically unstable substrates as the process is dependent on non-covalent bonding between the protein and the scaffold surface.

Cell recognition and attachment is a huge topic and one that is still an active research area. Within each recognition event (eg cell-cell, cell-substrate) there are a large host of factors, and these factors are not necessarily unique, or common, to each cell type and line.

Most cells attach to supporting substrates through extracellular matrix (ECM), which is excreted by certain cells. The exact composition of the extracellular matrix

(ECM) is still being actively studied.⁵⁰⁻⁵¹ The signalling between the extracellular matrix and the cell is usually mitigated by integrins, (which are one group of glycoproteins which are one group of cell adhesion molecules (CAMs)) and are used by the cell to detect changes in the composition of ECM on the culture surface and can illicit a response to modify the cell behaviour. The levels of integrins can also be changed at the cell surface to alter cell adhesion, an example being in motility or adhesion to a surface.⁵²⁻⁵³ The ECM is predominantly composed of three types of macromolecules: collagens (especially types IV and V)⁵⁴⁻⁵⁵ and glycoproteins (such as fibronectin and laminin)⁵⁶⁻⁵⁷. Lack of attachment usually leads the cell to apoptosis (cell suicide).⁵⁸

In many *in-vitro* cell culture media ECM is already present in the added serum. With the *in-vitro* cultures, cell attachment and spreading is preceded by adsorption of the ECM onto the matrix surface, and therefore cells are unlikely to proliferate on surfaces that resist the adsorption of these molecules. The ECM-cell communication is not limited to the attachment and spreading of cells, but also communication between the ECM and the cell regulates events including cell survival, increase or decrease of migration, differentiation and stimulated or arrested growth, cell metabolism, protein synthesis and gene expression.⁵⁹ The macromolecular components are secreted by the cell and self-aggregate in order to form the insoluble ECM, which *in-vivo* would then be used to prompt signalling between cells and their environment. Cell-ECM adhesion is both dynamic and tightly regulated. Most cells, in order to grow at all *in-vitro*, require attachment proteins from serum,⁶⁰ which contains, amongst other things, fibronectin and vitronectin. Serum-free media will usually have to be supplemented with one of these proteins to be supportive of cell growth.⁶¹

With respect to the increased cell attachment due to the immobilisation of fibronectin on surfaces it has been shown that by isolating progressively smaller cell attachment promoting fragments of fibronectin and by synthesizing peptides according to the amino acid sequence of the smallest active fragment, it has been shown that cell attachment-promoting activity of fibronectin is dependent on the arginine-glycine-aspartic (RGD) acid tripeptide sequence.^{62,63}

It therefore follows that short synthetic peptides can be made that contain the RGD motif and be immobilised onto the surface in some respect to promote cell attachment on that surface. This would allow a larger functionalisation of the surface, and a greater chance of cell attachment.

Biological cells have diameters in the range of microns to tens of microns. Due to the optimisation of void size for cell culture the morphology of the polyHIPE is not going to be changed at a fundamental level but the study will concentrate on the surface functionalisation of these materials.

These polyHIPE scaffolds have, in previous studies, been exposed to fibronectin, which, as most proteins, will adsorb to the surface of the polyHIPE, creating a fibronectin layer. Such coating appeared to promote the growth of neurons into the PolyHIPE, but adsorption is a non-specific process, and the fibronectin could have adsorbed in different conformations and also may have desorbed upon addition of the media, or in the ethanol sterilisation step.⁶⁴

As adsorption is ruled out as a controllable reaction route, most of the focus of this project will be on the covalent linkage of chemical and/or biological moieties to the surface of PolyHIPE materials to develop surface chemistries that permit bio-specific association of protein but prevent non-specific adsorption of proteins.

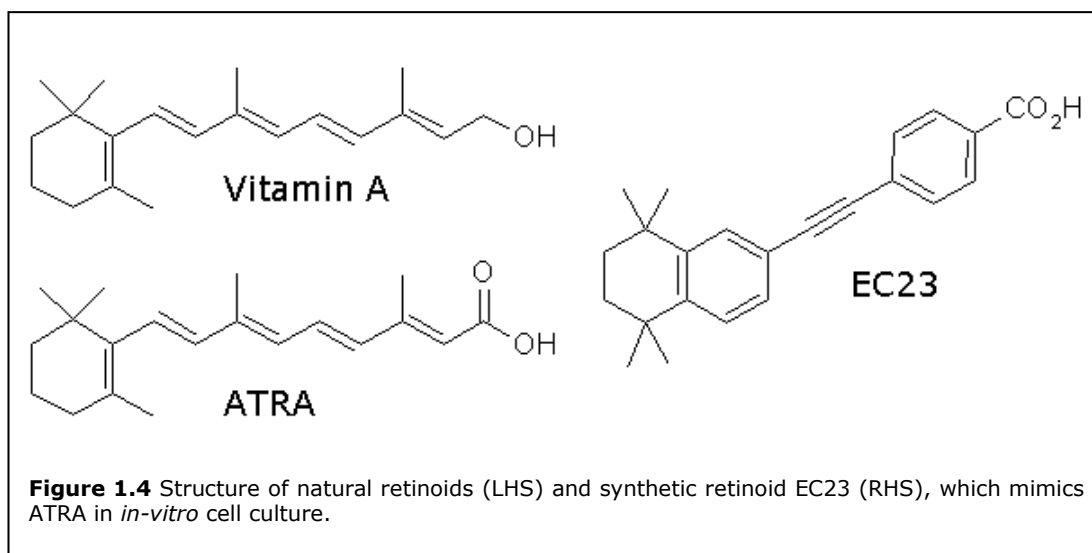
In this thesis we are looking for possible motifs to bind to the PolyHIPE substrate in order to increase cell attachment, growth and proliferation, and possibly differentiation. There are many studies on many different types of substrate to demonstrate exactly what motifs are preferential for cell attachment. In order to attach any motifs to the surface of the polyHIPE it must be shown that controlled, covalent, binding to the surface the polyHIPE is possible.

1.3 Retinoids

Retinoids are a class of chemical compounds, the most well known of which is vitamin A. They have a diverse function on the human body and are thought to be involved in regulation of cell proliferation and differentiation, as well as being involved in the growth of bone tissue and activation of certain genes.⁶⁵ They are used in some cases for treatment of skin disorders.⁶⁶ Retinoids have also been identified as preventative and therapeutic anticancer agents.⁶⁷

The basic structure of a retinoid, in the simplest sense, is a cyclic end group, a polyene side chain and a polar end group. Retinoids are also used within a laboratory environment for studying the differentiation of stem cells. Natural retinoids degrade and dimerise easily and therefore have to be kept away from UV, and often visible, light.

All-trans retinoid acid (ATRA), as shown in figure 1.4, is the acid form of vitamin A and is used in treating leukemia and skin diseases.



The effect of the retinoid on the cells is controlled by cellular nuclear receptors. There are two major classes of retinoid nuclear receptors; retinoic acid receptors (RAR) and retinoid-X-receptors (RXR). There are also variation subtypes within each of these classes. Each of these types of receptors have different functions in different tissues. There is a growing trend towards the synthesis of stable retinoids, that mimic the outcomes of natural retinoids. An outcome of the synthesis of chemically distinct molecules is that by variation of the structure of the retinoid, the receptor orientation can be probed and elucidated.⁶⁸ Different retinoid drugs work by binding to different receptors; which, in turn, affect cell growth and differentiation. With respect to ATRA, in a laboratory setting, it is used to induce the *in-vitro* differentiation of stem cells. A synthetic retinoid, EC23 has been shown to direct differentiation in stem cells (embryonal carcinoma cell line TERA2.cl.SP12).⁶⁹ The EC23 is stable to UV and visible light for at least 3 weeks, and is shown to induce a similar pathway of differentiation to ATRA. Advantages of using EC23 over natural ATRA molecules are that as the EC23 is more stable, reproducibility and accountability are increased, along with an observation that much lower levels of EC23 are needed to illicit similar response to ATRA in stem cells. With the stability and defined chemistry, these are ideal molecules to attach

to a polyHIPE substrate as a “proof-of-concept”, in order to demonstrate that surface functionalisation via covalent attachment to the polyHIPE is a possible route to controlling the fate of mammalian cells.

1.4 Plasma

Plasma is accredited to being first identified in 1878 by William Crookes,⁷⁰ but the word “plasma” only came to name Crookes’s “radiant matter”, with the publication of Irving Langmuir’s paper “Oscillations in ionized gases”, published in *PNAS* in 1928.⁷¹ The name “plasma” refers to a ionised gas and is often referred to as the “4th state of matter”, with properties sitting between the other three states of gas, solid and liquid.

Plasma is typically an ionised gas formed by high energy generation of atoms stripped of electrons. The degree of ionization represents the ratio of ionized atoms/molecules over the total amount of particles. The degree of ionization is depicted as α . Two types of plasmas are usually described, “true” plasma where α is close to 1, and a weakly ionized plasma “cold” with α values typically between 10^{-7} and 10^{-4} .⁷² The very high reactivity of “cold” plasma is ideal for treating polymeric surfaces as the reactive excited species it generates, from collisions in the gas phase between the high energy electrons and the reaction species, enable functionalisation of the surfaces without the need for processing temperatures greater than the decomposition point of the polymers surfaces.

Low temperature plasma is versatile and the discharge can be generated by several different source (for example AC, DC, RF, HF) at different powers and using different gasses (for example, oxygen, argon, nitrogen), as well as other monomeric materials. There are two main types of cold plasma processing; vacuum process, which is a batch technique which has the advantages of a highly

controlled atmosphere, and atmospheric which has the main advantage of being able to “in-line” (continuously) run.

Plasma is therefore made up of high energy, highly mobile, highly reactive, independently acting ions, radicals and other reactive species. It can be generated by many different energy sources and with a large number of parameters. For the scope of this thesis low-temperature, radio-frequency generated plasmas, plasma processing and the types of desired functionality will be discussed.

The plasma process is used in industrial processes such as car bumper modification (in batch processes) and in preparation of tissue culture polystyrene (TCPS) for in-vitro cell growth.⁷³ Atmospheric plasma treatment is used in industry to improve surface for adhesion, eg. in coating technologies. This generates polar groups on the surface and removes barrier/loose layers.

The plasma treatment can change the surface properties of a material in different ways; by deposition, etching, functionalisation (from reactive gasses) and also surface roughening. Plasma treatment has also been shown to increase cross-linking at the material surface⁷⁴ and can be used to modify surfaces for better adhesion, surface cleaning (removal of organic residues). Many plasma processes are used for removal of hydrocarbon residues from metals and silicon surfaces, this process being of particular interest and use in the semiconductor industry, where it is used to remove the photoresist from an etched silicon wafer.⁷⁵⁻⁷⁶ It can also be used as a combustion technique for asbestos disposal.⁷⁷

The term “plasma-processing” can be applied to several applications. Plasma treatment is used in a wide variety of research and industrial applications, and plasma reactors can vary hugely in terms of size, power and impaired properties.

Plasma is a popularly used industrial process, and is used to surface engineer or modify the surface without affecting the bulk material. This can be used to influence properties such as frictional behaviour, lubricity, heat resistance, cohesive strength of films, surface electrical conductivity, or dielectric constant, or it can be used to make materials hydrophilic or hydrophobic. Advantages of using plasma processes include an easy modification of the mechanical, electrical, chemical properties of materials,⁵⁷ the process is environmentally friendly with negligible health and disposal hazards. The process variables are usually computer controlled so this increases the repeatability of the studies. The plasma treatment has to be optimised for each type of polymer and each plasma system, as too much plasma treatment can affect the bulk material, burning or deforming it, if too harsh parameters are used.

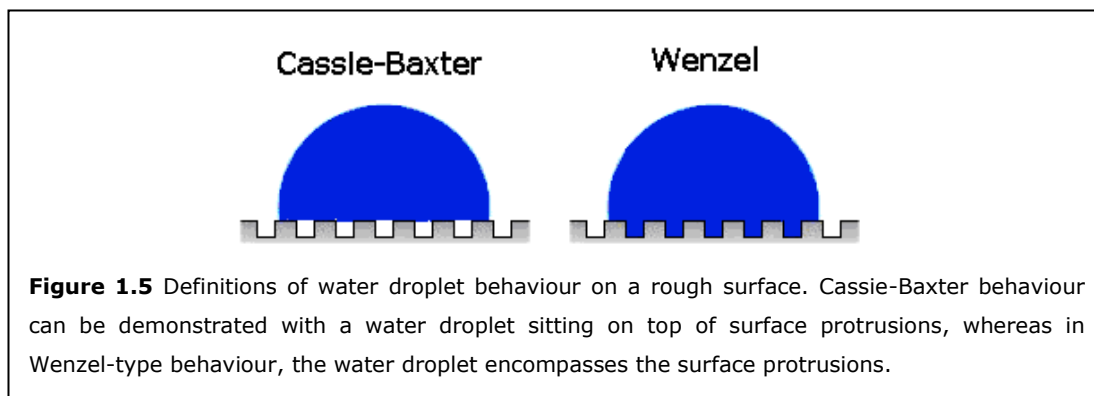
Other plasma processes such as plasma deposition, in which larger molecules (eg polymers) are deposited on a surface, will not be discussed in great detail. The limitation with a “off-the-shelf” batch process is that specialist power control is needed to pulse plasma bursts in order to create specific step growth and orientation of monomeric or polymeric components.⁷⁸

The processes described in this thesis are vacuum plasma treatment chambers which have a low temp process (generally 40 - 120 °C). Modification of the surfaces can be varied due to different concentrations of reactive species and the application methods. The low vacuum chamber process is a controlled, low temperature process with low energy densities, thus avoiding excessive damage to the materials. Plasma generated photons are thought to penetrate bulk polymers to a depth of about 10 µm.⁵⁷

The hydrophilicity of a surface is a good indication of the type of groups that remain on the surface and therefore the observation of change (or non-change) in hydrophobicity can be an indication of the stability of the surface. Hydrophobic recovery, in which the surface gradually “regains” its hydrophobicity over time is a documented process. This is due to the mobility of species at the surface of the materials, which is rearranged over time.⁷⁹

To visually observe the degree of hydrophilicity, contact angles are often used. There are several methods to observe this, namely sessile drop method; traditionally measured using a static goniometer, dynamic sessile drop method; measuring the contact angle hysteresis by comparing the receding and advancing contact angles and Dynamic Wilhelmy method; measuring the wetting force on a uniform solid by immersing and withdrawing the solid from a liquid of known surface tension. Other, less traditional, methods used to measure contact angle include using the wet-mode on an environmental scanning electron microscope (ESEM).

With a porous material, the droplet is affected by the roughness of the surface. One way around this is just to compare the surfaces against each other of the same roughness or dynamic readings over time have to be taken, but this is often not practicable without specialist high-speed equipment.⁸⁰ How a droplet of water behaves on a hydrophobic rough surface is defined in two ways: Wenzel⁸¹ in which the droplet follows the contours of the material or Cassie-Baxter⁸² where the droplet is suspended on a composite surface of the material and air pockets. (Figure 1.5). This will be discussed in more detail in Chapter 5.



In this thesis the main aim is to identify conditions that will functionalise the surface (including the inside of the porous material) of the polyHIPE without affecting the morphology of the bulk material. The aim is to functionalise the surface sufficiently in order to produce oxygen containing groups to modify the hydrophilicity of the surface, but also to enable the material to retain this hydrophilicity over time and not to be subsequently altered by washing or sterilisation techniques. The stability of the functionalisation needs to be monitored over time, as a commercial product must have a long shelf-life. Stability of plasma-treated surfaces can be monitored by x-ray photoelectron spectroscopy (XPS).⁸³

If stable, functional, chemical groups are present on the material surface there would be the possibility of further functionalisation of the oxygen-containing groups with chemical/biological moieties.

1.5 References

- ¹ D.R. Wiggam, W.E. Gloor *Ind Eng Chem* (1934) **26** (5) 551
- ² L.H. Baekeland *Ind Eng Chem* (1909) **1** 149
- ³ www.acs.org » education » explore chemistry » Chemical Landmarks
- ⁴ D. Barby, Z. Haq, *Eur. Pat.* 0,060,138 (1982) (to Unilever)
- ⁵ G. Akay, M.A. Birch, M.A. Bokhari *Biomaterials* (2004) **25**(18) 3991

-
- ⁶ N.R. Cameron, D.C. Sherrington, L. Albiston, D.P. Gregory *Colloid Polym Sci* (1996) **274** 592
- ⁷ R.J. Carnachan, M. Bokhari, S.A. Przyborski, N.R. Cameron *Soft Matter* (2006) **2** 608
- ⁸ C. Lucchesi, S. Pascual, G. Dujardin, L. Fontaine *React Funct Polym* (2008) **68**(1) 97
- ⁹ E.M. Christenson, W. Soofi, J.L. Holm, N.R. Cameron, A.G. Mikos *Biomacromolecules* (2007) **8**(12) 3806
- ¹⁰ N.R. Cameron, D.C. Sherrington, L. Albiston, D.P. Gregory *Colloid & Polymer Science* (1996) **274**(6) 592
- ¹¹ A. Desforges, M. Arpontet, H. Deleuze, O. Mondain-Monval *React Funct Polym* (2002) **53**(2-3) 183
- ¹² V.O. Ikem, A. Menner, T.S. Horozov, A. Bismarck *Adv Mat* (2010) **22**(32) 3588
- ¹³ H. Deleuze, B. Maillard and O. Mondain-Monval *Bio Med Chem Lett* (2002) **12**(14) 1877
- ¹⁴ P. Krajnc, N. Leber D. Štefanec, S. Kontrec, A. Podgornik *J Chrom A* (2005) **69**(1) 1065
- ¹⁵ H. Tai, A. Sergienko, M.S. Silverstein *Poly Eng Sci* (2001) **41**(9) 1540
- ¹⁶ A. Barbetta, M. Dentini, E. Zannoni, M. De Stefano *Langmuir* (2005) **21**(26) 12333
- ¹⁷ R.J. Carnachan, M. Bokhari, S.A. Przyborski, N.R. Cameron *Soft Matter* (2006) **2** 608
- ¹⁸ B.C. Benicewicz, G.D. Jarvinen, D.J. Kathios, B.S. Jorgensen *J Radioanal Nucl Chem* (1998) **236** 31

-
- ¹⁹ J.R. Duke, M.A. Hoisington, D.A. Langlois, B.C. Benicewicz *Polymer* (1998) **39**
4369
- ²⁰ T.A. Desmarais *PCTInt Appl* (1999) WO 9947183
- ²¹ H. Tai, A. Sergienko, M.S. Silverstein *Poly Eng Sci* (2001) **41** 9
- ²² S. Cetinkaya, E. Khosravi, R. Thompson *J Mol Cat A: Chem* (2006) **254** 138
- ²³ M.S. Silverstein, H. Tai, A. Sergienko, Y. Lumelsky, S. Pavlovsky *Polymer*
(2005) **46** 6682
- ²⁴ A. Desforges, M. Arpontet, H. Deleuze, O. Mondain-Monval *React Funct Polym*
(2002) **53** 183
- ²⁵ M.A. Bokhari, G. Akay, S. Zhangd, M.A. Birch *Biomaterials* (2005) **26** 5198
- ²⁶ W. Busby, N.R. Cameron C.A.B. Jahoda *Polym Int* (2002) **51** 871
- ²⁷ K. Bhadiraju, C.S. Chen *Drug Discov Today* (2002) **7** 612
- ²⁸ J.P. Mather, P.E. Roberts *Introduction to Cell and Tissue Culture* Plenum Press,
New York (1998) 6
- ²⁹ E.H. Lee, W.H. Lee, C.S. Kaetzel, G. Parry, M.J. Blssell *Proc Nat Acad Sci*
(1985) **82** 1419
- ³⁰ K. Rubin, M. Hook, B. Obrlnk, R. Timpl *Cell* (1981) **24** 463
- ³¹ J.R. Fuchs, B.A. Nasser, J.P. Vacanti *Ann Thorac Surg* (2001) **72** 577
- ³² S.C. Baker, N. Atkin, P.A. Gunning, N. Granville, K. Wilson, D. Wilson, J.
Southgate *Biomaterials* (2006) **27**(16) 3136
- ³³ K.Cheng, Y.Lai, W. S. Kisaalita *Biomaterials* (2008) **29** 2802
- ³⁴ M.K. Vickaryous, B.K. Hall *Biol Rev* (2006) **81**(3) 425
- ³⁵ A.F. Von Recum, T.G. Van Kooten *J Biomat Sci* (1996) **7**(2) 181-198
- ³⁶ T.P. Kunzler, C. Huwiler, T. Drobek, J. Vörös, N.D. Spencer *Biomaterials* (2007)
28 5000

-
- ³⁷ S.G. Lévesque, R.M. Lim, M.S. Shoichet. *Biomaterials* (2005) **26**(35) 7436
- ³⁸ H.P. Hohn, U. Steih, H.W. Denker *In Vitro Cell Dev Biol* (1995)**31** 37
- ³⁹ E.F. Irwin, K. Saha, M. Rosenbluth , L.J. Gamble, D.G. Castner, K.E. Healy *J. Biomat Sci* (2008) **19**(10) 1363
- ⁴⁰ X.Q. Brown, K. Ookawa, J.Y. Wong *Biomaterials* (2005) **26** 3123
- ⁴¹ H.K. Kleinman, E.B. McGoodwin, S.I. Rennard, G.R. Martin *Anal Biochem* (1979) **94**(2) 308
- ⁴² J.J. Ramsden *Chem Soc Rev* (1995) **24** 73
- ⁴³ B.T. Houseman, M. Mrksich *Biomaterials* (2001) **22** 943
- ⁴⁴ J.G. Steele, G. Johnson, H.J. Griessert, P.A Underwood *Biomaterials* (1997) **18** 1541
- ⁴⁵ R.P. Lanza, R. Langer, W.L. Chick *Principle of Tissue Engineering* Academic Press, London (1997) 405
- ⁴⁶ W. Busby, N.R. Cameron, C.A.B. Jahoda *Polym Int* (2002) **51** 871
- ⁴⁷ M.A. Bokhari, R.J. Carnachan, N.R. Cameron, S.A. Przyborski *Biochem Biophys Res Comm* (2007) **354** 1095
- ⁴⁸ M.A. Bokhari, G. Akay, S. Zhangd, M.A. Birch *Biomaterials* (2005) **26** 5198
- ⁴⁹ E. Ruoslahti, E.G. Hayman *Arterioscler Thromb Vasc Bio* (1985) **5** 581
- ⁵⁰ M.O. Klein, C. Reichert, D. Koch, S. Horn, B. Al-Nawas *Clin Oral Impl Res* (2007) **18** 40
- ⁵¹ K. Macfelda, B. Kapeller, I. Wilbacher, U.M. Losert *Artificial Organs* (2007) **31**(1) 4
- ⁵² C.S. Elangbam, C.W. Qualls Jr, R.R. Dahlgren *Vet Pathol* (1997) **34** 61
- ⁵³ R.O. Hynes *Cell* (1992) **69** 11
- ⁵⁴ F.J. Roll, J.A. Madri, J. Albert, H. Furthmayr *J Cell Biol* (1980) **85** 597

-
- ⁵⁵ S.C.G Tseng, N. Savlon, D. Gospodarowicz, R. Stern *J Biol Chem* (1981) **256**
3361
- ⁵⁶ J.A. Madri, F.J. Roll, H. Furthmayr, J-M Foldart *J Cell Biol* (1980) **86** 682
- ⁵⁷ P.J. Courtoy, R. Timpl, M.G. Farquhar *J Histochem Cytochem* (1982) **30**(9) 874
- ⁵⁸ C.S. Chen, M. Mrksich, S. Huang, G.M. Whitesides, D.E. Ingber *Science* (1997)
276 1425
- ⁵⁹ M.A. Schwartz, M.D. Schaller, M.H. Ginsberg *Annu. Rev. Cell Dev. Biol* (1995)
11 549
- ⁶⁰ H.M. Tern *J Natl Cancer Inst* (1966) **37** 167
- ⁶¹ D. Barnes, G. Sato *Cell* (1980) **22** 649
- ⁶² M.D. Pierschbacher, E. Ruoslahti, J. Sundelln, P. Und, P.A. Peterson *J Biol Chem* (1982) **257** 9593
- ⁶³ M.D. Pierschbacher, E. Ruoslahti *Nature* (1984) **309** 30
- ⁶⁴ M.W. Hayman, K.H. Smith, N.R. Cameron, S.A. Przyborski *Biochem Biophys Res Comm* (2004) **314** 483
- ⁶⁵ M.B. Sporn, N.M. Dunlop, D.L. Newton, J.M. Smith *Fed Proc* (1976) **35**(6) 1332
- ⁶⁶ C.E. Orfanos, C.C. Zouboulis, B. Almond-Roesler, C.C. Geilen *Drugs* (1997)
53(3) 358
- ⁶⁷ S.M. Lippman, J.F. Kessler, F.L. Meyskens *Cancer Treat Rep* (1987) **71**(4) 391
- ⁶⁸ J. Barnard, J. Collings, A. Whiting, S. Przyborski, T. Marder *Synth Chem* (2009)
15 11430
- ⁶⁹ D.J. Maltman, V.B. Christie, J.C. Collings, J.H. Barnard, S. Fenyk, T.B. Marder, A. Whiting, S.A. Przyborski *Mol BioSyst* (2009) **5** 458
- ⁷⁰ W. Crookes *Phil Trans* (1878) **170** 135
- ⁷¹ I. Langmuir *Proc Nat Acad Sci* (1928) **14** 628

-
- ⁷² N. Vandencastele, F. Reniers *J Elect Spect* (2010) **178** 394
- ⁷³ S. Tachi, K. Tsujimoto, S. Okudaira *Appl Phys Lett* (1988) **52**(8) 616
- ⁷⁴ J.R. Hall, C.A.L. Westerdahl, A.T. Devine, M.J. Bodnar *J App Poly Sci* (1969) **13**(10) 2085
- ⁷⁵ G.S. Oehrlein *Surf Sci* (1997) **386** 222
- ⁷⁶ G.S. Oehrlein, J.F. Rembetski *IBM J Res Develop* (1992) **36** 140
- ⁷⁷ H.H. Zaghoul, L.J. Circeo Final report: *Defense Technical Information Center* (1993) available online at <http://stinet.dtic.mil>
- ⁷⁸ B. Gupta, C. Plummer, I. Bisson, P. Frey, J. Hilborn *Biomat* (2002) **23**(3) 863
- ⁷⁹ H. Yasuda, H.K. Sharma, T. Yasuda *J Polym Sci* (1981) **19**(9) 1285
- ⁸⁰ A.M. Peters, C. Pirat, M. Sbragaglia, B.M. Borkent, M. Wessling, D. Lohse, R.G.H. Lammertink *Eur Phys J E* (2009) **29** 391
- ⁸¹ R.N. Wenzel *Ind Eng Chem* (1936) **28** 988
- ⁸² A.B.D. Cassie, S. Baxter *Trans Faraday Soc* (1944) **40** 546
- ⁸³ F.M. Petrat, D. Wolany, B.C. Schwede, L. Wiedmann, A. Benninghoven *Surf Interface Anal* (1994) **21** 274

Chapter 2 - Experimental and Techniques

2.1 PolyHIPE Synthesis

2.1.1 Materials

Styrene (Aldrich; 99 %), divinylbenzene (Aldrich; 80 vol % divinylbenzene, the remainder being m- and p-ethylstyrene), 2-ethylhexyl acrylate (Aldrich; 99 %) and were freed of inhibitor by passing through a short column of basic alumina (Aldrich; Brockmann). The inhibitors removed were 4-tert-butylcatechol for styrene and divinylbenzene and hydroquinone / monomethyl ether hydroquinone for 2-ethylhexyl acrylate. Potassium persulfate (Aldrich), sorbitan monooleate (SPAN 80, Aldrich), were used as supplied.

2.1.2 Standard PolyHIPE Preparation

Poly(styrene-EHA-DVB) polyHIPEs (aqueous:organic phase ratio = 9:1 w/w) were prepared according to a procedure taken from the literature.¹ An external ("oil") phase consisting of styrene (6.0 g, 58 mmol), 2-ethylhexyl acrylate (3.0 g, 16 mmol), divinylbenzene (1.0 g, 6 mmol DVB), sorbitan monooleate (Span 80) (2.5 g, 25 % w/w of monomer phase) was added to a 250 ml two-necked round bottomed flask (RBF).

A separate aqueous solution was prepared, in a 250 ml beaker, consisting of 90 ml deionised water with an excess of potassium persulfate (1 % w/w of aqueous phase), heated up to 80 °C.

The external phase was then stirred at 300 rpm using an overhead IKA stirrer fitted with a D-shaped PTFE stirrer, while the aqueous phase was added via syringe pump to the external phase in the RBF, over a period of 2 minutes (45 ml/min), until a HIPE is formed. After the complete addition of the aqueous phase, the

emulsion was stirred for a further 1 min. After this time, the HIPE was poured gently into two 50 ml polycarbonate centrifuge tubes and placed in an oven (at 60 °C) for 24 h. The resulting monolith was removed from the tube and washed in Soxhlet apparatus in acetone for 24 h, and then allowed to air dry.

Monolithic materials formed have average pore diameter of between 80 - 100 µm and with an average interconnect diameter of 20 µm. Disks were predominantly cut from the monolith using a Leica 100 vibrotome to defined thicknesses, typically 200 µm.

2.1.3 Stirrer Variation (tP)

The Tornado is used for parallel processing, and with the “Starfish” setup, can stir six 250 ml RBF simultaneously. To make polyHIPEs using this process, only one port was used. As the stirring D-shaped paddles from the IKA stirrer cannot be used on the Tornado, paddles were made by Radleys for this purpose. To make the monolith on the Tornado stirrer, starting materials used as above, with the stirring speed set to 300 rpm. The stirring was undertaken in a multi-well plate, with the Radleys Tornado/StarFish setup with similar PTFE stirrers in a 250 ml round bottomed flask with minimal gap between the bottom of the flask and the bottom of the stirrer. There was the same length addition and stirring times as above. Monoliths formed by this procedure were characterised by SEM images, processed using Image J software.

2.1.4 Variation of Aqueous Phase Temperature

Procedure was followed as above, but the aqueous phase temperature was set to heat to 60 °C rather than 80 °C. This has the effect of reducing the Oswald ripening and coalescence, leading to a monolith with smaller voids.

2.1.5 Swelling of PolyHIPE Slices

Slices cut (200 μm) from 60 $^{\circ}\text{C}$ monoliths, as formed through the above procedure (2.1.4), and placed on a watchglass. 5 ml THF was gently added to the watchglass, covering the slices. This was then left for 20 minutes, and the remaining THF decanted off. The slices were then left on the watchglass and allowed to slowly air-dry over 18 h.

2.2 PolyHIPE Chemical Modification

2.2.1 Bromination of PolyHIPE

Powdered PS-DVB-EHA polyHIPE (2.00 g) was placed in dry toluene with anhydrous lithium bromide (1.0 g, 12 mmol), chlorotrimethylsilane (1.4 ml, 13.4 mmol), water (0.12 ml, 6 mmol) and AIBN (recrystallised from MeOH) (0.2 g, 1.2 mmol) was heated to 70 - 80 $^{\circ}\text{C}$ for 24 h. The powder was washed with hot acetonitrile, then rinsed with diethyl ether. Secondary washings were done by extraction with acetonitrile in a Soxhlet apparatus for 48 h then dried in-vacuo overnight. Polymer turned pale yellow after reaction and retained pale colour upon drying.

2.2.2 Titration of Bromine vs. PolyHIPE

Powdered, weighed, polyHIPE was suspended in DCM. The end point was defined as when the first colour appeared in the solution. Different strengths of bromine solution were investigated but the colour disappeared within a short period of time after addition. Large excess of bromine was added and the mixture stirred overnight. This was then washed with hot acetonitrile and diethyl ether and submitted for elemental analysis, the data shown in Chapter 4. The solution decolourised overnight.

2.2.3 Amination

This procedure was followed from the literature.² Powdered PolyHIPE (1.0 g) was suspended in DMF and 0.18 g (1.23 mmol) Tris(2-aminoethyl)amine. The mixture was stirred at 45 °C for 24 h, then extracted then washed (6 x 20 ml) with DMF, MeOH, MeOH : H₂O (1 : 1), MeOH and THF. The powder was then dried *in-vacuo* overnight (18 h).

2.2.4 Thiolation

Small cubes of (vinyl)polystyrene polyHIPE (1.0 g suspended in 20 ml of DMF). Five equivalents of aminoethanethiol (0.6 g, 15 mmol) and azobisisobutyronitrile (AIBN) (2.5 g, 15 mmol) were added. The suspension was then heated to 70 - 80 °C, under gentle stirring and nitrogen atmosphere for 48 h. The polymer was isolated and extracted in IPA (soxhlet) further 48 h. The cubes obtained were dried *in-vacuo* overnight.

2.2.5 Dopamine Treatment

“Polydopamine” was laid down as a coating as described in the paper by Messersmith et al.³ Dopamine (2 mg / ml) (as dopamine hydrochloride - Sigma) was dissolved in 10 mM Tris-HCl (pH 8.5), and substrates (either polyHIPE, bacteriological plate (BP) or glass) were immersed in the dopamine solution for between 18 - 24 h. Stirring was necessary to prevent non-specific microparticle deposition on surfaces. Substrates were either skewered onto needles (for polyHIPE) or placed within two metal meshes to prevent hydrophobic interaction between the substrates, or scratching by the mechanical action of the stirrer bar. The coated surfaces were rinsed with distilled water and dried by N₂ gas before storage or further treatment. During the reaction the solution turns from colourless

to a dark brown. The polydopamine coated samples are also a dark brown/black in colour.

2.2.6 Further Reactivity of Dopamine Coated Substrates

2.2.6.1 Thiolation

Squares of dopamine treated BP and slices of polyHIPE were immersed overnight in solutions of 1-dodecanethiol (1 mg/ml) in DCM. As a control BP squares were also immersed in DCM overnight.

2.2.6.2 Amine Attachment

PolyHIPE slices were submerged in a solution containing either a large excess (1 mg/ml) of ethylenediamine or 1,8-octanediamine in ethanol. These were then thoroughly rinsed in ethanol and were dried *in-vacuo*.

2.2.6.3 Ninhydrin test

Ninhydrin (1 mg/ml) dissolved in ethanol, which was then added (3ml) to polyHIPE slices or polyHIPE powders and left for 5 minutes. The slices in solution were then placed in a water bath at 60 °C for 15 minutes. All the substrates were then thoroughly washed in ethanol (4 x 20 ml) and allowed to air dry. A dark blue - grey colour on the polyHIPE slice indicated amine reactive groups.

2.2.6.4 Fluorine Attachment

2,2,2-trifluoroethanethiol or 2,2,2-trifluoroethylamine were made up into a 1 mg/ml solution in DMF. PolyHIPE slices were immersed in this solution for 4 h. Samples were then thoroughly washed with DMF (4 x 20 ml) and dried *in-vacuo*.

2.2.7 Plasma Treatment

Plasma treatment was run using a Quorum-Emitech K1050X Plasma Asher. Studies were carried out differing power, time and oxygen flow settings. The

“standard” treatment being 10 W, 30 ml/min O₂ flow rate for a period of 15 min, unless otherwise stated.

2.2.8 Fluorine Functionalisation

Reactions 1, 3, 5: Three slices of PolyHIPE were placed on a watchglass inside a sealed flat bottomed container.

Reactions 2, 4, 6: Three slices of PolyHIPE were placed in a flat bottomed container.

After all treatments, samples were left in a *in-vacuo* for 18 h at ambient temperature to remove unreacted/adsorbed reactants.

2.2.8.1 Carboxyl Derivatisation Procedure

1. Trifluoroethanol (TFE) (0.9 ml), pyridine (0.4 ml) and *N,N*-Di-*tert*-butylcarbodiimide (Di-tBuC) were injected down the sides of the sealed container at 15 minute intervals. This was left to proceed at ambient temperature for 18 h.
2. TFE (0.9 ml), pyridine (0.4 ml) and *N,N*-Di-*tert*-butylcarbodiimide (Di-tBuC) were injected down the sides of the sealed container into 1 ml ethanol containing the material slices, at 15 minute intervals. This was left to proceed at ambient temperature for 18 h.

2.2.8.2 Carbonyl Derivatisation Procedure

3. Pentafluorophenyl hydrazine (PPH) was dissolved in ethanol (4 % w/w) (0.5 g in 10 ml) was placed in a dessicator under samples for 12 h at 50 °C.
4. PPH was dissolved in ethanol (4 % w/w) (0.5 g in 10 ml) was placed in sealed flat bottomed container in contact with the material slices for 12 h at 50 °C.

2.2.8.3 Hydroxyl Derivatisation Procedure

5. 2 ml of trifluoroacetic anhydride (TFAA) was injected into the bottom of the container, without any direct contact with the material slices. This was left to proceed for 40 min at 35 °C.

6. 2 ml TFAA was injected at the side of the container and allowed contact with the polyHIPE slices. This was left to proceed for 40 mins at 35 °C.

2.2.8.4 Cysteamine Derivatisation Procedure

Slices of polyHIPE were plasma treated (10 W, 15 min, 30 ml/min O₂). The slices were then placed on a watchglass within a sealed container and 2 ml cysteamine (4 % in ethanol) was added to the bottom of the container and left at 60 °C temperature overnight.

2.3 Cell Culture

Culture media and supplements were obtained from Invitrogen (Paisley, UK).

2.3.1 Cell Preparation

In-vitro cell experiments, unless otherwise stated, were performed with the well-documented human osteoblast-like cell line MG63, that was originally isolated from an osteosarcoma and exhibits many osteoblastic traits characteristic of bone forming cells.³⁻⁴

MG63 cells were suspended in Dulbecco's modified Eagle's medium (DMEM) supplemented with 10 % fetal calf serum (FCS), 100 mg/ml streptomycin, 100 µl penicillin, and then plated into a 75 cm² flask (T75). These were statically cultured at 37 °C in a humidified atmosphere with 5 % CO₂, until confluent. A flask can be termed confluent at the point at which at least 80 % of the growing surface of the growing flask is covered by a single layer of cells.

2.3.2 PolyHIPE Preparation

In preparation for growing cells, untreated disks of polyHIPE were sterilized using absolute ethanol, hydrated through a series of graded ethanol solutions and subsequently washed (x 3) with sterile phosphate buffered saline (PBS) prior to use. All disks were then irradiated with UV for 15 mins prior to use. Although the ethanol wash sterilised the polyHIPE slices, the primary purpose of this was to hydrate the polyHIPE slices, which are very hydrophobic, and cell ingress is very limited on an untreated polyHIPE slices. As the plasma treated polyHIPE slices did not need to be hydrated by ethanol wash, sterilisation with the UV light was sufficient.

Trypsinised MG63 osteoblastic cells from the confluent 75 cm² flasks were resuspended in DMEM at a cell seeding density allowing distribution of 1 x 10⁶ cells per scaffold. This suspension was then transferred onto a prepared scaffold placed in the bottom of a 6 well plate and allowed to rest for 20 minutes, then 2ml of supplemented DMEM added.

The cell-seeded polyHIPE slices were statically cultured at 37 °C in a humidified atmosphere with 5% CO₂, for a set period of days, usually 1, 4, 7 days for a MTS assay, and 14 - 28 days for histological evaluation. Medium, including supplements, was replaced every 2 - 3 days depending on confluence.

2.3.3 Histology

Cell seeded scaffolds were prepared for histology after 14 - 28 days in culture. Samples were fixed in 4 % formaldehyde. The samples were then dehydrated using graded ethanol solutions. Following dehydration, samples were “end-on” paraffin-embedded, sectioned at 7 – 10 µm and stained with Haematoxylin and

Eosin (H&E) stain. Digital images were captured on a computer controlled light microscope. Images from the H&E sections were used to observe cell penetration.

2.3.4 Preparation for SEM

After the specific growth periods, the seeded scaffold were washed in PBS and fixed at 4 °C for 90 min in Karnovsky's fixative. Fixed cells were then stained at 4 °C for a further 60 min using 1 % (w/v) osmium tetroxide in phosphate buffer (pH 7.2). Samples were dehydrated using a graded series of ethanol solutions and dried using CO₂ critical point drying. These were then gold-coated for SEM imaging using a sputter coater for six periods of 30 seconds, as described below.

2.3.5 MTS Assay

MTS assay was performed using Promega Cell Titer 96 ® Aqueous One Solution Cell Proliferation Assay. This was run with 1 ml of media with 200 µl reagent per well in a 12 well plate. The incubation time was between 2 and 4 h and the resulting solution was either diluted 10:1 in order to read the absorbance at 490 nm using a standard UV photospectrometer (PerkinElmer) or used undiluted using 2 µl of the solution and read with a Nanodrop 1000 spectrophotometer (Leica).

2.3.6 Surface Topological Features (STF) Investigation

As in these investigations it was essential to observe whether STF were present on each of the slices. MG63 cells were prepared as above, but each polyHIPE scaffold quartered, and these quartered slices placed in 12 well plates, with 25 x 10⁴ cells (¼ of cells seeded onto whole slices) seeded on each quarter scaffold.

2.4 Sample Preparation for Physical Analysis

2.4.1 SEM

PolyHIPE slices were thinly cut and scanning electron microscopy (SEM) was performed with a Philips/FEI XL30 ESEM on samples sputter-coated in gold (Edwards S150B sputter coater) using the secondary electron detector (SE).

2.4.2 Wet Mode ESEM

Wet mode ESEM was performed with the XL30 using ESEM mode with Peltier stage set at 5 °C with recirculating water. Samples were not gold-coated before insertion. Very thin samples were attached to the stage using a thin tacky layer of quick drying conductive silver paint (AGAR). Carbon cement was evaluated, but was not sufficiently conductive. A GSE detector was used, using a 500 µm aperture adapter. The sample was left to equilibrate on the Peltier stage for 30 minutes before the chamber was purged for 10 cycles from 3 Torr to 10 Torr, equilibrating at 4 Torr. The water pressure and temperature was balanced in order to form micro droplets on the surface of the polyHIPE slices. Droplets were confirmed by increasing the water pressure, with images taken at each stage of development, and reducing the pressure, and observation of the droplets reducing in size. Time focussed on a single sample was limited due to the destructive nature of the electron beam.

2.5 Retinoids:

2.5.1 Solution Phase Thio-ester Formation

EC23 was synthesised in-house.

To a stirred solution of EC23 (10 mg, 0.03 mmol) in 10 ml anhydrous CH₂Cl₂ at 0 °C, was added DCC (Sigma) (7.4 mg, 0.036 mmol) which is stirred for 5 minutes at

0 °C , then allowed to reach room temperature (RT) and stirred for a further hour. DMAP (3 - 10 % w/w, 0.1 - 0.36 mg) and 20 - 40 mmol 1-dodecane thiol (13.5 mg, 0.06 mmol) was added to the solution and the reaction was stirred, under an inert atmosphere, for 6 - 8 h. Reaction conditions were monitored by tlc (85% hexane : 15 % ethyl acetate). Further developing agents for the tlc were not required as EC23-containing spots fluoresced under UV light. Column separation was attempted, but sufficiently anhydrous conditions were not found. **NMR:** EC23 Acid: ¹H NMR (400 MHz, CDCl₃) δ 8.09 (d, *J* = 8.3 Hz, 2H), 7.62 (d, *J* = 8.3 Hz, 2H), 7.50 (s, 1H), 7.31 (d, *J* = 0.8 Hz, 2H), 1.70 (s, 4H), 1.28 (t, *J* = 11.2 Hz, 12H). 1-dodecanethiol: ¹H NMR (400 MHz, CDCl₃) δ 2.54 (dd, *J* = 14.7, 7.5 Hz, 2H), 1.67 - 1.57 (m, 2H), 1.43 - 1.28 (m, 19H), 0.90 (t, *J* = 6.9 Hz, 3H). EC23 Thio-ester (unpurified - excess thiol): ¹H NMR (400 MHz, CDCl₃) δ 7.96 (d, *J* = 8.7 Hz, 2H), 7.60 (d, *J* = 8.7 Hz, 2H), 7.34 - 7.26 (m, 3H), 3.14 - 3.05 (t, *J* = 2 Hz, 2H), 1.71 (d, *J* = 7.1 Hz, 6H), 1.57 (s, 5H), 1.45 (d, *J* = 2.1 Hz, 4.4H), 1.35 - 1.24 (m, 35.1H) (*excess thiol*)

2.5.2 Solid Phase Thio-ester Formation

EC23 (10 mg, 0.03mmol) was reacted with DCC (Sigma) (7.4 mg, 0.036 mmol in dry DCM, for 1 hour. Meanwhile plasma treated polyHIPEs have been plasma treated (10 W, 15 min, 30 ml. min O₂) and functionalised using the vapour phase method described above (**Cysteamine derivatisation procedure**), either using cysteamine, ethylamine or ethylenediamine in the same procedure.

The EC23-DCC solution was transferred via vacuum to a clean flask and diluted to required dilution (0.1 mg/ml). 3 ml of the solution was transferred to a vessel containing the linker-attached polyHIPE slices. These were analysed at timepoints after immersion using the Leica Nanodrop.

2.6 Analytical Techniques

2.6.1 XPS

XPS was run on a Kratos AXIS ULTRA XPS using mono-chromated Al $K\alpha$ X-ray source (1486.6eV) operated at 15mA emission current and 12kV anode potential - 180W.

The XPS analysis, and initial data evaluation, was performed by Emily Smith at Nottingham University, enabled by ESPRC grant EP/F019750/1 "A Coordinated Open-Access Centre for Comprehensive Materials Analysis" which funded the analysis. The XPS data was charge corrected by 2 eV. XPS data was analysed using an evaluation copy of CasaXPS and evaluated using: Beamson, G.; and Briggs, D.; XPS Database of Polymers in High Resolution High resolution XPS of organic polymers : the Scienta ESCA300 database Chichester [England] ; New York : Wiley, 1992.

2.6.2 Tof-SIMS

Tof-SIMS was also run at Nottingham University under the above grant by David Scurr.

2.7 Background Theory of Analytical Techniques

2.7.1 Elemental Analysis

This measures percentage composition of a sample for the elements tested for.

The instrument used was an Exeter Analytical CE440 Elemental Analyser.

The samples are loaded into disposable capsules and the sample is combusted in a high temperature furnace under pure oxygen. The combustion products pass through purification steps that create compounds (usually oxidised) of the CHN components, and remove any trace elements such as sulfur, phosphorous or

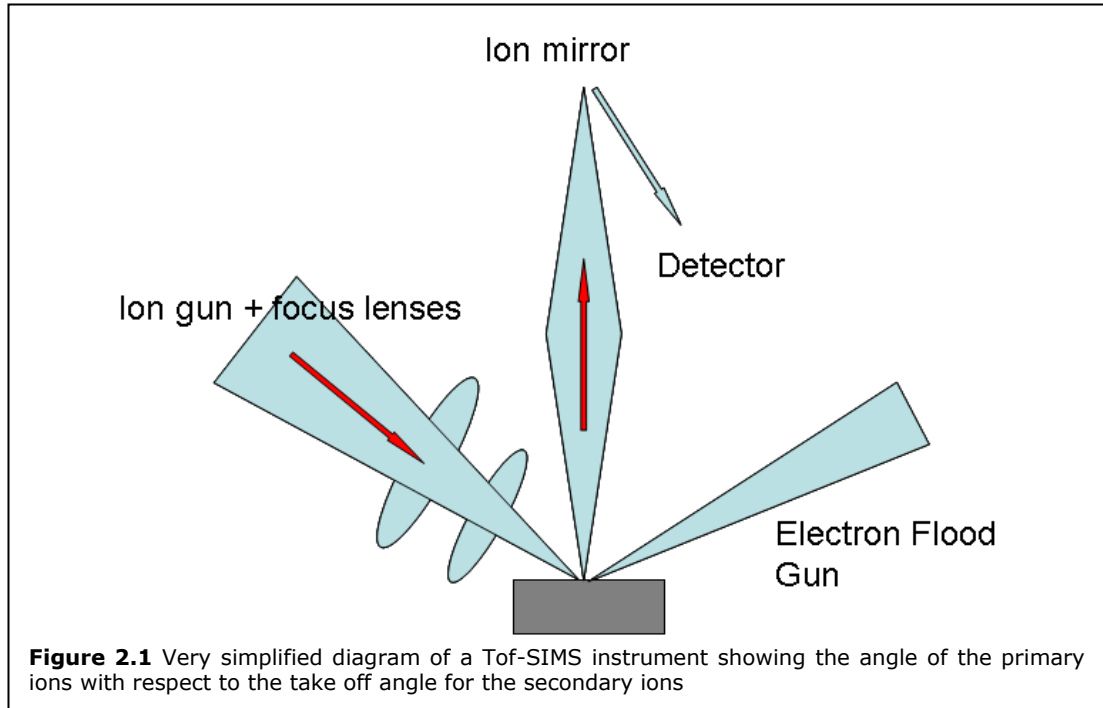
halogens. These compounds are then pass over copper wire and the composition of the mixture of gasses is then detected with precision thermal conductivity detectors. Hydrogen is detected by analysing the amount of water present, carbon is measured as carbon dioxide and nitrogen is measured against a helium reference. Using this technique, the amount of CHN in the sample is measured as a percentage composition of the original sample. The stated accuracy of the machine is for the error of the measurements being $\pm 0.15\%$ absolute plus $\pm 0.15\%$ relative.⁵

2.7.2 Time-of-Flight Secondary Ion Mass Spectrometry (ToF-SIMS)

Time-of-Flight Secondary Ion Mass Spectrometry (TOF-SIMS) is a surface sensitive technique that uses short, (< 1 ns) pulsed primary ion beams to desorb and ionize species from a sample surface in a “collision cascade”. Only about 1 % of the secondary ions desorbed from the surface are charged and the surface analysed is usually only the top 1 - 2 atomic layers, making this a very surface sensitive technique, but qualitative at best. The resulting ionized secondary ions are accelerated (by applying a high voltage potential) into a mass spectrometer, where they are mass analyzed by measuring their time-of-flight from the sample surface to the detector. For each primary ion pulse, a full mass spectrum is obtained by measuring the arrival times of the secondary ions at the detector and performing a simple time to mass conversion

The data acquired from the spectrometer, can either be arranged as a “traditional” mass spectra plot, or alternatively they can be “imaged” where each individual mass spectra for each ion is converted into a pixel of differing colour depth, and the surface is rastered over an area of (for example) 200 μm , creating a image of individual ion distributions over the surface. This gives an image of ion patterns

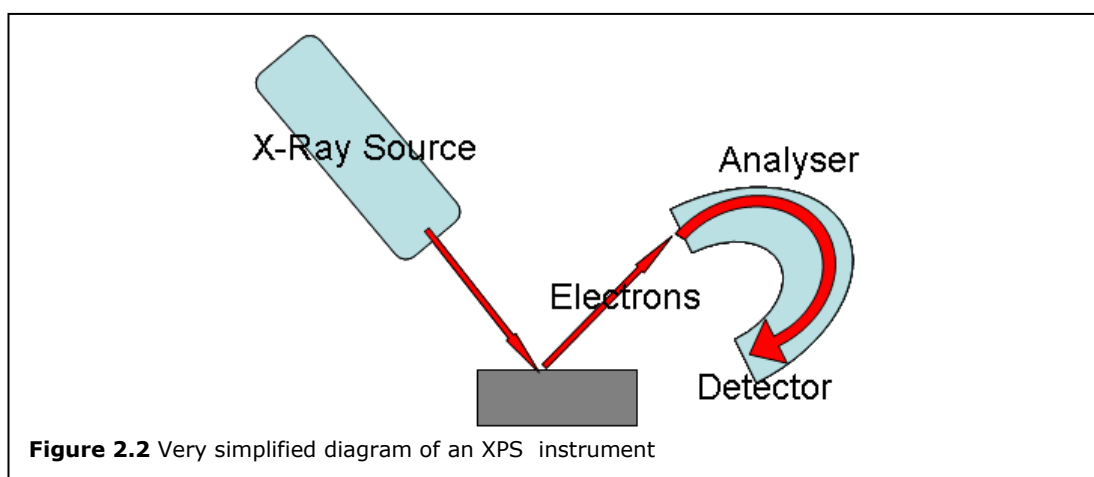
over the surface, but is limited where the surface is not flat, such as in polyHIPE slices, where the surface is “lost” in craters due to the incident angle of the ion beam. The angles are demonstrated in figure 2.1.



2.7.3 X-ray Photoelectron Spectroscopy (XPS)

X-ray photoelectron spectroscopy is a surface technique that utilises x-ray to ionize surface atoms and measuring the energy of ejected photoelectrons. The method requires the sample to be bombarded with low energy x-rays, produced from an aluminum (in this case), with an energy of $h\nu$. These x-rays cause electrons to be ejected from either a valence or inner core electron shell. The energy of the electron, E , is given by $E = h\nu - E_1 - \Phi$, where E_1 is the binding energy of the atom and Φ is the work function of the sample. It is therefore possible to calculate the binding energy of each type of ejected electron, and therefore identify the atom (and its chemical state) from which the electron originates, by comparison with known data.

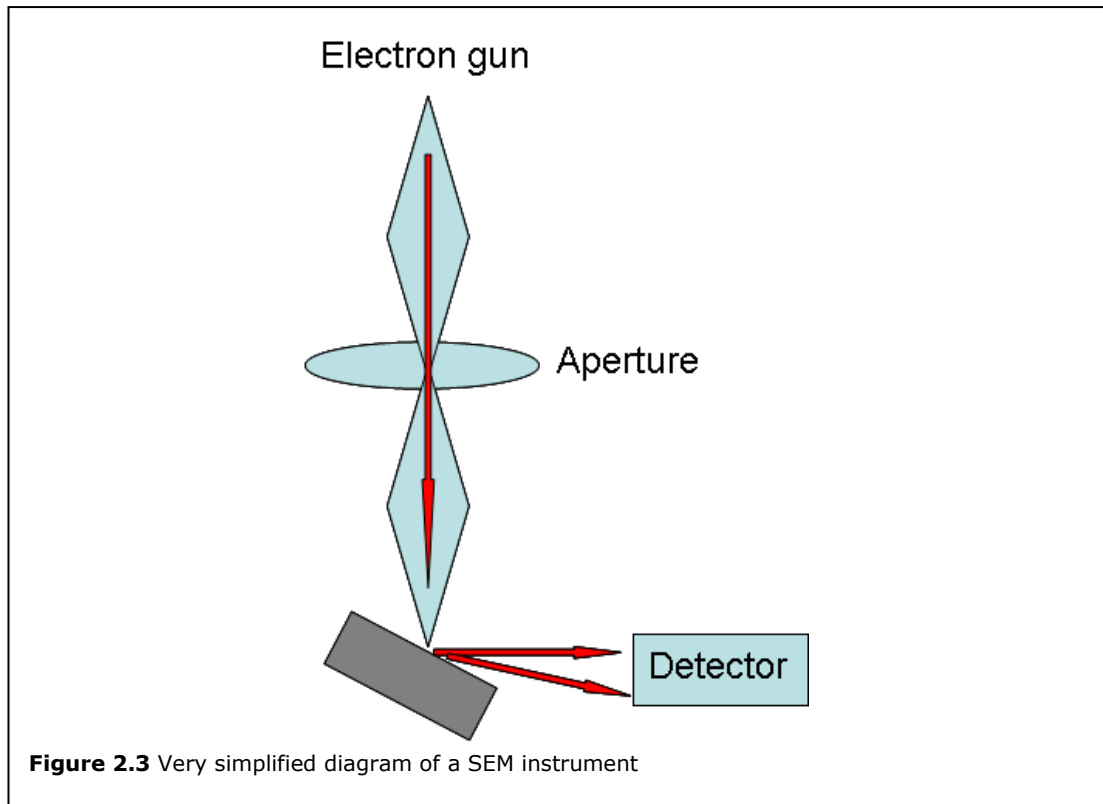
The XPS machine works by directing x-rays from the source to the sample surface, and the resulting photoelectrons are focused onto the concentric hemispherical analyzer, where a potential range is applied over the inner and outer cylinders to create a line of zero potential. By variation of the potential, certain energy levels of electrons are allowed through, and therefore certain energy bands can be investigated in greater depth. For a simplified diagram, see figure 2.2.



2.7.4 (Environmental) Scanning Electron Microscopy (E)SEM

The scanning electron microscope works by electrons produced using an electron gun which is then focused down onto the sample through several electromagnetic coils. A set of scan coils are used to raster the spot over the surface of the sample and reflected electrons are collected, amplified and converted into a video signal. This video signal has the ability to be paused, and still images taken of the surface (in 2D). Electrons can be accelerated to energies in the range of 0 to 30 keV (in this thesis between 15 - 25 keV, with a spot size of 5 nm). The spot size can be set to various values, and the dimensions observed are dictated by this setting. In the “SEM” mode, samples are usually coated with a conducting material (usually Au) to prevent electrical charging. Using the “environmental mode” (ESEM), water vapour is pumped into the chamber with a variable pressure of 1 - 10 Torr. This

allows hydrated, non-sputter coated samples to be imaged, although not to the same resolution as “dry” SEM. A simplified figure is shown in figure 2.3.



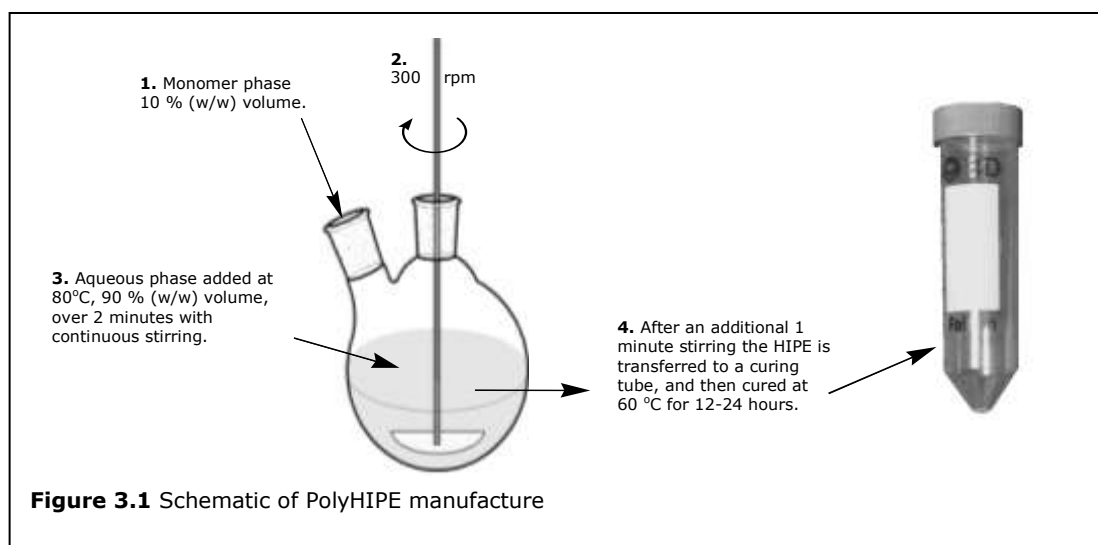
2.8 References

-
- ¹ R.J. Carnachan, M.A. Bokhari, S.A. Przyborski, N.R. Cameron *Soft Matter* (2006) **2** 608
 - ² G. Boissier, J. Dubois *Makromol Chem* (1981) **182** 2075
 - ³ M. Bachle, R.J. Kohal *Clin Oral Implants Res* (2004) **15** 683
 - ⁴ B.D. Boyan, Z. Schwartz, C.H. Lohmann, V.L. Sylvia, D.L. Cochran, D.D Dean, J.E. Puzas *J Orthop Res* (2003) **21** 638
 - ⁵ <http://www.exeteranalytical.co.uk/ce440.htm>

Chapter 3 - PolyHIPE Manufacture

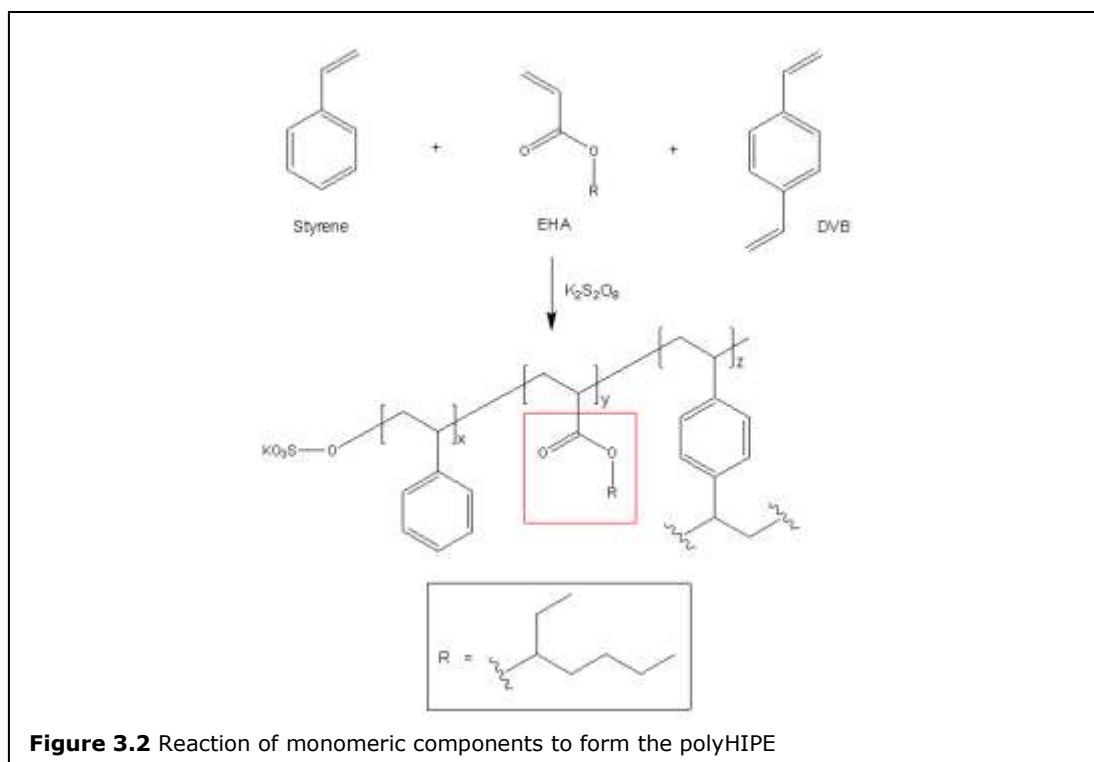
3.1 Introduction

PolyHIPE is the acronym for a polymerised high internal phase emulsion (HIPE). A high internal phase emulsion is where the internal phase of the parent emulsion is above 74 % of the total volume. A *poly*HIPE is where one phase consists of a monomer, or mixture of monomers, which is then cured, and the non-polymerisable phase removed. Briefly polyHIPEs are made here by adding a 90 % (w / w) aqueous phase to a 10 % (w / w) monomer phase and stirring to form a HIPE. This is then poured into a mould, in this case a 50 ml falcon tube which is then sealed and cured, in this case thermally, at 60 °C for 12 - 24 hours. This is represented in Scheme 3.1.



The polyHIPEs made with relation to this project were 90 % internal phase emulsions, unless stated otherwise. The material preparation was followed as set out in the paper by Carnachan et al.¹ with the aqueous phase temperature set at 80 °C. The monomer phase consisted of a styrene : divinylbenzene : 2-ethylhexyl

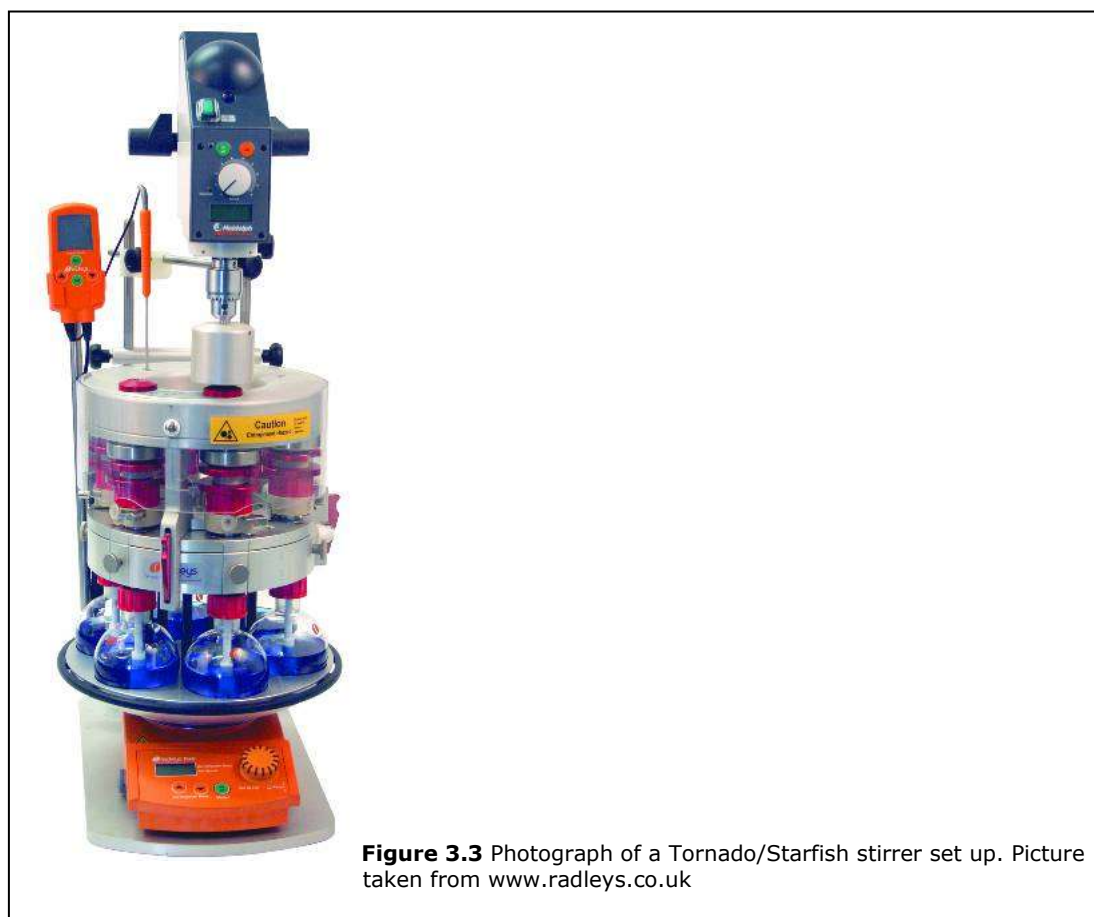
acrylate mixture in the ratio of 6 : 1 : 3 respectively, the schematic of which is shown in Figure 3.2.



The surfactant used was Span 80 in a ratio of 2.5 % (w/w) to the total HIPE volume. Potassium persulfate was used at a 1 % (w/w) of the aqueous phase. The polyHIPEs formed by this method have an average void diameter of 80-100 μm and an average interconnect diameter of 10-20 μm . The large interconnect diameter in the monoliths is due to the instability of the parent emulsion, promoting coalescence and Ostwald ripening. Typical polyHIPEs have a much smaller void diameter as they are formed from reasonably stable parent emulsions. Due to this emulsion being designed to be on the limits of instability, (ie. if left it would separate in a very short space of time) the polyHIPE formed has larger pores and interconnects, and therefore have suitable morphology for use as cell culture supports.

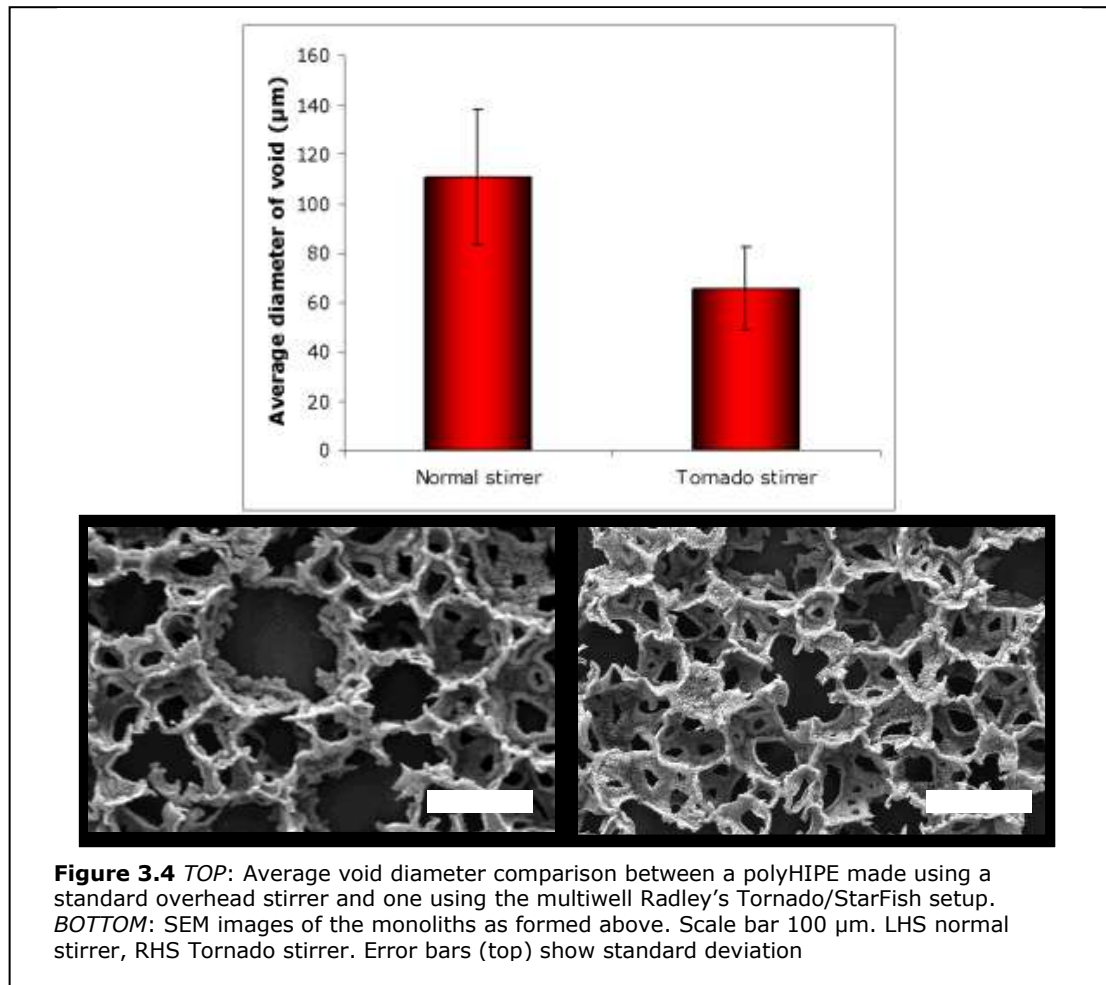
3.2 Stirrer Variation

In an attempt to increase efficiency of polyHIPE manufacture a multi-stirrer (Radleys Tornado/StarFish) was used as shown in figure 3.3. The PTFE stirrers were re-designed to be used with a 250 ml round bottomed flask with minimal gap between the bottom of the flask and the bottom of the stirrer. A polyHIPE was made at the same time with a normal overhead stirrer. Both stirrers were set to the same stirring speed (300 rpm) and with the same length of addition (2 minutes) and stirring (1 minute) times.



Both methods produced stable emulsions which were cured at 60 °C for 24 h. Qualitatively it was observed upon pouring into the mould that the HIPE formed by the Tornado stirrer was more viscous than the HIPE made using the traditional method. The Tornado HIPE appeared to be a more stable emulsion and upon

curing did not shrink as much as the traditionally made polyHIPE, and as such had to be cut from the mould without damaging the outer layer of polyHIPE, instead of sliding smoothly out. Both polyHIPEs were washed in soxhlets, cut, and analysed from three SEM images using image analysis software. The results can be seen in figure 3.4.

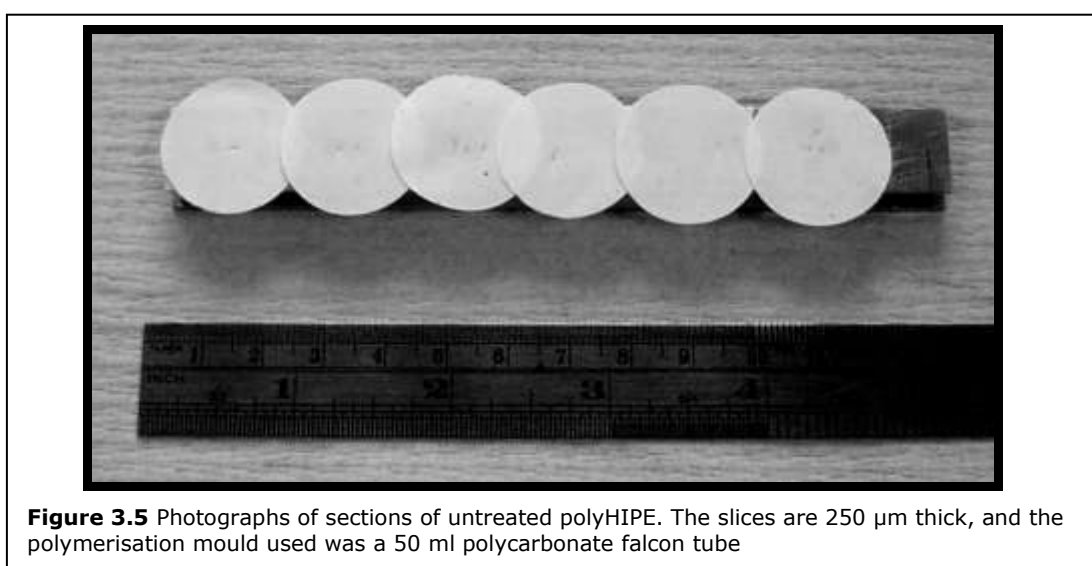


The interconnect diameter is significantly larger in the normal stirrer polyHIPE (nP) and has a larger standard deviation. The Tornado stirrer polyHIPE (tP) has a lower average interconnect diameter than the nP. This would indicate that the tP parent emulsion is more stable than the nP made emulsion. In most instances this would be advantageous, but in this case, where the void diameter has been optimised to a larger, specific diameter, it is a disadvantage. Although there are potential time

saving issues with adopting the multi-mixing Tornado stirrer, in this case it is not appropriate. It is interesting to note that, although it appeared to be a more stable monolith, upon curing, microdroplets were still seen on the surface of the tP surface (figure 3.3), the appearance of which will be discussed later.

3.3 Sectioning PolyHIPE Monoliths

In order to grow cells on the polyHIPE material, the monoliths were sectioned into thin slices (see figure 3.5).



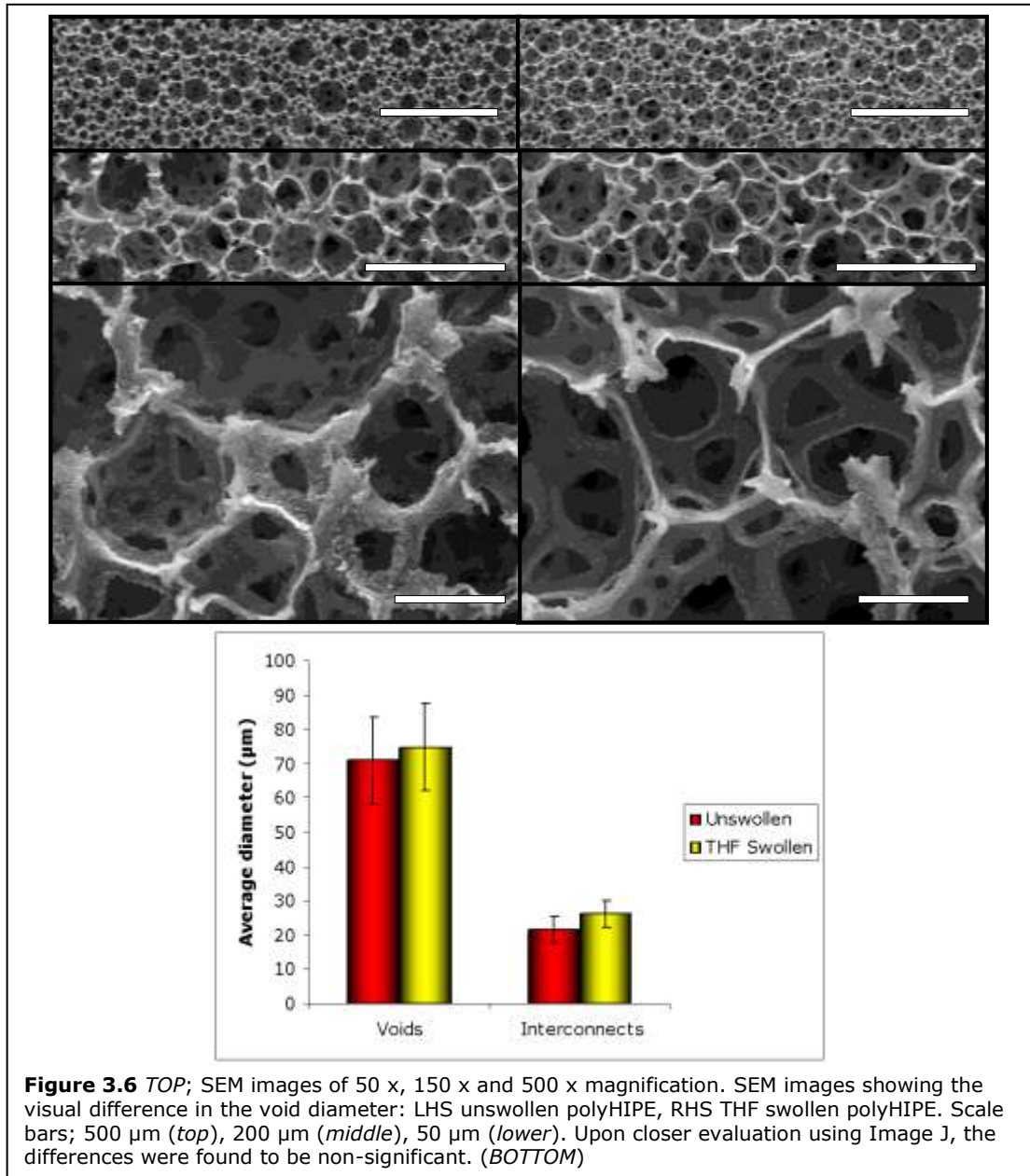
Previously, and initially in this project, cutting was done on a standard histology microtome (such as a LEICA RM 2135), with the range of thicknesses from 1 - 60 μm , but with a “doubler” button, which when pressed, approximately doubled the active slicing depth, so a slice of approximately 120 μm was able to be cut. The procedure to cut a slice was to rotate manually a handle to cut each slice. The minimum thickness that could be cut was determined by the material properties of the polyHIPE monolith. This was partially determined by the void diameter but also the polymeric composition of the polyHIPE. The lower limit of cutting a slice of nP was 30 μm . Predictably the thinner the material was cut the more the material was

prone to tearing. Upon processing the material for biological analysis, for example transferring the cell-containing polyHIPE, a 30 μm polyHIPE slice was prone to ripping. The disadvantage with using a thicker slice was that the thicker the slice, the further nutrients and oxygen had to diffuse in terms of providing the cells with nutrients and removing waste.

The initial maximum thickness of the polyHIPE slice was constrained by the limitations of the cutting machine. Acquisition of the Leica VT1000S vibratome allowed a greater versatility and partial automation of the cutting process. The limitation of the thickness to be used was the diffusion ability of the oxygen and nutrients to, and waste from, the cells in culture. A thicker slice of 200 or 250 μm was used, and the viability of cells did not decrease due to the thickness of the slice (data not shown). These were determined as the “standard” thicknesses for cell culture after this time.

3.4 Swelling of PolyHIPE Slices

A possible alternative to the unstable emulsion method, is to make a more stable emulsion and then swell the resulting polyHIPE slices in a suitable solvent, giving rise to a subsequently larger void diameter. This was demonstrated with a polyHIPE made with the aqueous phase temperature at 60 $^{\circ}\text{C}$, which was then sliced to 200 μm and the slices were swollen in THF. The slices were left in THF for 20 minutes, removed from the THF and allowed to air-dry on an evaporating dish overnight. The slices were then analysed by SEM and image analysis. The results are shown in figure 3.6. The THF swelling had a noticeable visual effect by SEM of increasing the void and interconnect diameter as well as having the added effect of reducing the number of surface topological features (STF), as discussed in the next section.

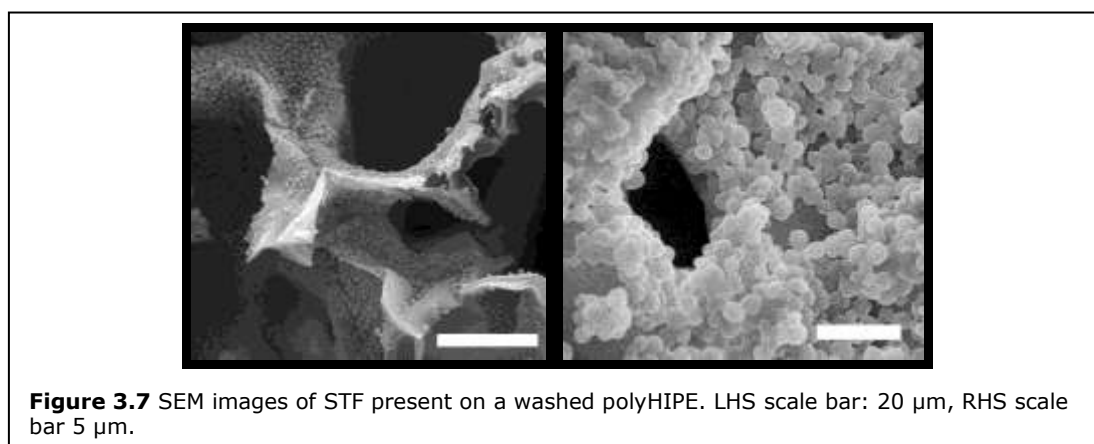


Although the polyHIPE slice was swollen by the THF, and the dried diameter of the swollen polyHIPE was 120 % of the diameter of the original polyHIPE, the SEM images of the unswollen and swollen polyHIPE do not show a great significance. There is a difference appearing in the thicknesses of the walls of the voids, but statistically the difference in the diameter of the voids and interconnects is not significant. The average void diameter only varies between the unswollen and THF swollen by 3.8 μm and the interconnect diameter by 4.8 μm . The standard deviation is 25.5 and 7.7 (unswollen) and 26.2 and 10.7 (THF swollen) for the void

diameter and the interconnect diameters respectively. The swelling, although altering the appearance of the polyHIPE, and reducing the number of surface topological features (see below), did not have as great an effect on void diameter as phase temperature.

3.5 Surface Topological Features (STF) / Microdroplets

Small “microdroplets” of material were seen on the surface of some polyHIPEs, even after extensive washing, as shown in figure 3.6. These were named surface topological features (STF) until the cause and composition could be determined.



Microdroplets, similar in diameter and shape to the STF seen in figure 3.7, were observed in the washing residue after extracting the polyHIPE monolith in a soxhlet. Solvents such as acetone, iso-propyl alcohol (IPA), ethanol, ethanol : water, water, THF and diethyl ether were used to wash out unattached STF from the polyHIPE. Acetone was found to (qualitatively) remove more of the STF from the polyHIPE. This is suggested to be because the acetone swells the polyHIPE monolith more than a solvent such as IPA, without collapsing the porous structure of the monolith which occurs with solvents such as THF.

Upon curing the parent emulsion, these small microdroplets also adhered to the sides of the curing tubes, and were very hard to remove. If the tubes were re-used,

large craters were seen on the surface of the monolith, due to the different surface of the tube, in contact with the unstable emulsion. Polycarbonate curing tubes (50 ml falcon centrifuge tubes) were therefore only used once, and then disposed of.

Some separation upon curing can be seen in which an aqueous layer forms on top of the polyHIPE. The separated layer is cream in colour and when dried out onto a suitable substrate, such as a glass slide, can be examined using SEM. Figure 3.7 shows a micrograph of the dried residue from the “creamed” layer. This contains many spherical microdroplets but also larger areas of less defined material. To investigate whether the microdroplets were polymeric material, the creamed layer was subjected to 3 x 40 ml warm water : ethanol washes and centrifugation of the resulting suspension to dissolve and remove any non-polymeric components, such as Span 80 or potassium persulfate (KPS). The remaining microdroplets were analysed by SEM (“c” in figure 3.8) and by elemental analysis. The CHN analysis is shown in table 3.1. The composition was shown to be the same as the bulk polyHIPE. The balance of the CHN analysis is assumed to be the oxygen component.

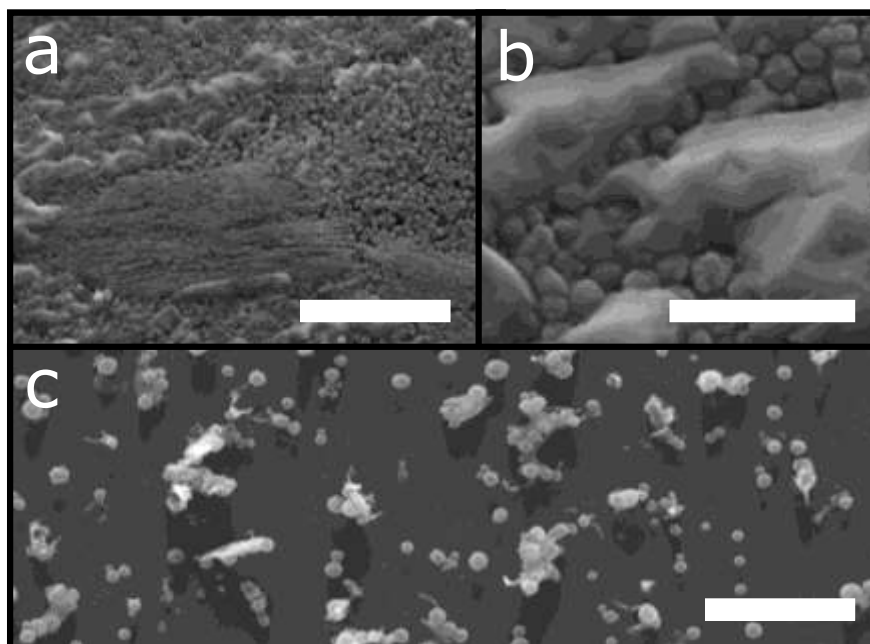


Figure 3.8 TOP: Top images: SEM images of the separated phase formed with the polyHIPE upon curing. Small microdroplets of cured polymer can clearly be seen, along with residue from the emulsion. Lower image: Image shows extracted microdroplets with the soluble residue removed. Scale bars: **a**; 20 μm , **b**; 5 μm , **c**; 10 μm

Table 3.1 Elemental analysis of the composition of monolith material compared to the microdroplet (STF) material

	C %	H %	N %	Balance %
Monolith material	83.5	9.1	-	7.4
Microdroplet material	83.3	9.1	-	7.6

To investigate subtleties in the manufacture of the polyHIPE that could be causing the microdroplets/STF to form, repeats of the nP were made with different experimental parameters. See figure 3.9 for SEM images of the monoliths formed.

The variables were as follows:

Age of monomer: (a) The monomers are passed through basic alumina to remove the inhibitors. After filtration they are kept at 4 °C which should minimise the amount of polymerisation. To see if this had an effect, monomers were filtered and left in the fridge for 10 days prior to use. The polyHIPEs were observed to have only a few STF on the surface.

“Standard” polyHIPE: (b) Freshly filtered monomers were used to make a monolith, this was shown in figure b.

KPS degradation: (c) KPS decomposes to radicals at temperatures less than 50 °C,² consequently a batch of polyHIPE was made with the aqueous phase containing KPS left for 1 hour at 80 °C before use. The resulting monolith is shown in image c.

Inhibitors: (d) Batches of polyHIPE were made with the inhibitors present (chemicals used as sold). This is shown in image d. These have many STF on the monolith.

Oxygen content of H₂O: To see if the oxygen content of the water being used had any effect on the STF formation, nitrogen was bubbled through the aqueous phase prior to use. This formed a polyHIPE, which when sliced, showed large holes unevenly distributed through the slice. This is shown in image g.

This group of polyHIPEs (shown in figure 3.9) appear to show that, although many more STF are seen on the monoliths with extremes of variables (b and d), the STF cannot be eradicated entirely, as the repeats (e and f) show that STF are present even when appearing to have the same manufacturing procedure.

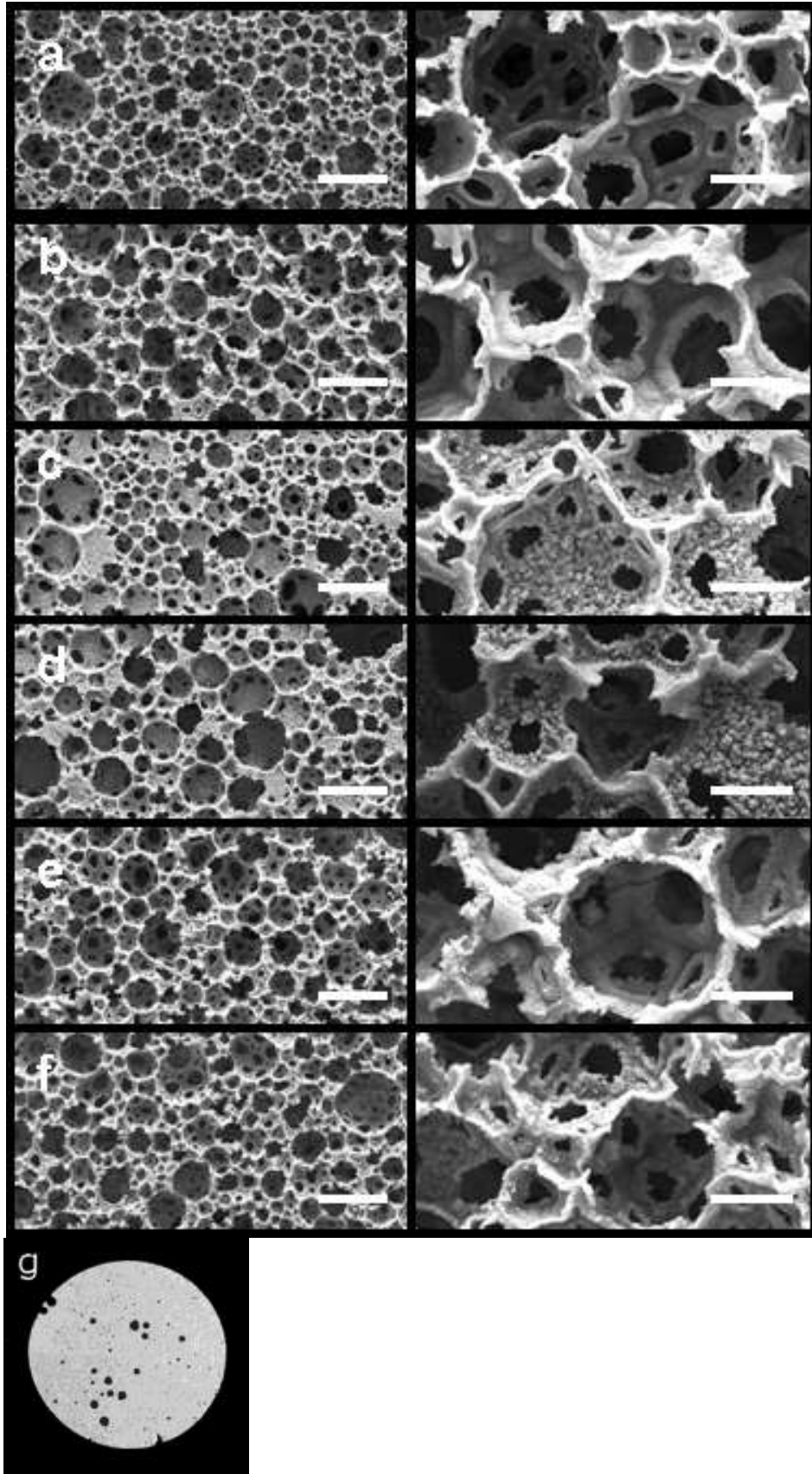
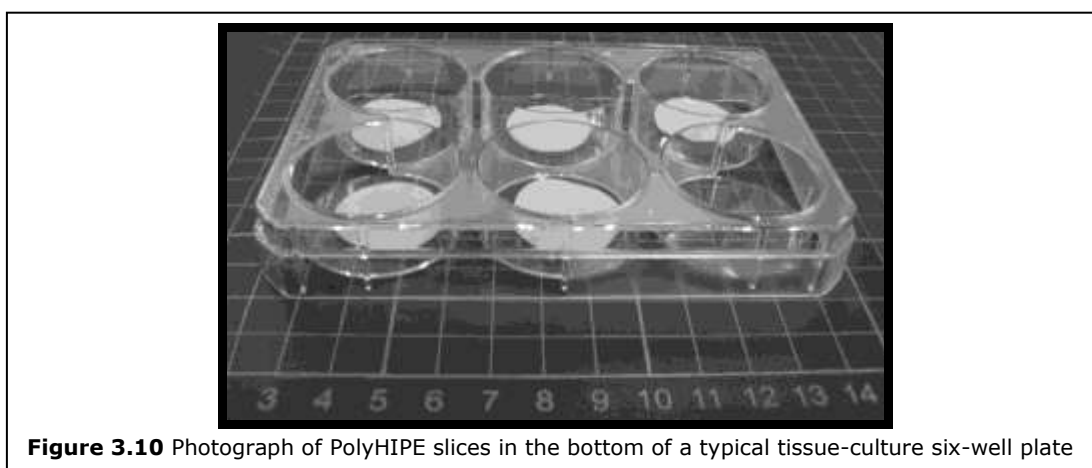


Figure 3.9 a-f: SEM images at 100 x and 500 x magnification. Scale bar LHS 200 μm , RHS, 50 μm . Each row shows the resulting monolith with the following subtleties; a: 10 day old styrene, b: aqueous phase with KPS present left at 80 $^{\circ}\text{C}$ for 1 hour, c: freshly filtered unrefrigerated monomers, d: inhibitors present (chemicals used as received), e: repeat of "standard conditons": refrigerated filtered monomers used within 24 hours of filtering, aqueous phase/KPS used with no delay f: second repeat as "e". g: photograph of large uneven holes formed through the polyHIPE slice

It is proposed that the STF are formed by micelles of monomer being formed by inversion of the emulsion, due to the inherent instability of the parent emulsion, and upon curing, form polymeric micelles. The unattached micelles are predominantly washed out in the soxhlet, but due to their lower surface area: total area ratio, will cure more quickly than the monolith, and may embed into the uncured surface of the polyHIPE. Other than changing the composition and temperature of the parent emulsion, there appeared not to be a easily solvable route to removing the STF.

3.6 MG63 *In-Vitro* Cell Culture on PolyHIPE Slices

As the STF on the polyHIPEs do not appear to be easily controlled, cell work was undertaken on the polyHIPE slices to see whether the “microtopology” of the surface affected the cell growth and viability. There have been many studies on the microtopology of the surface affecting cell growth, in which the cell growth, or attachment, is enhanced by an increase in (order/disorder) of the surface.³ To investigate this, MG63 osteoblast-like cells were cultured on slices of substrates with, and without STF.



To grow cells on the polyHIPE slices, slices are placed into the bottom of 6 well plates (as shown in figure 3.10), sterilised with 70 % aqueous ethanol solution

washes and irradiated with UV light to ensure sterility before washing with a buffer solution (PBS), then seeding the cells onto the slices. In this case, to ensure the slices had, or lacked, STF, slices were cut, and before the sterilisation step, each slice was cut into four pieces. One quarter of each slice was examined under SEM to confirm the presence/absence of STF. The three other quarter slices were then sterilised and placed into the bottom of 12-well plates and cells were grown for a period of up to 7 days.

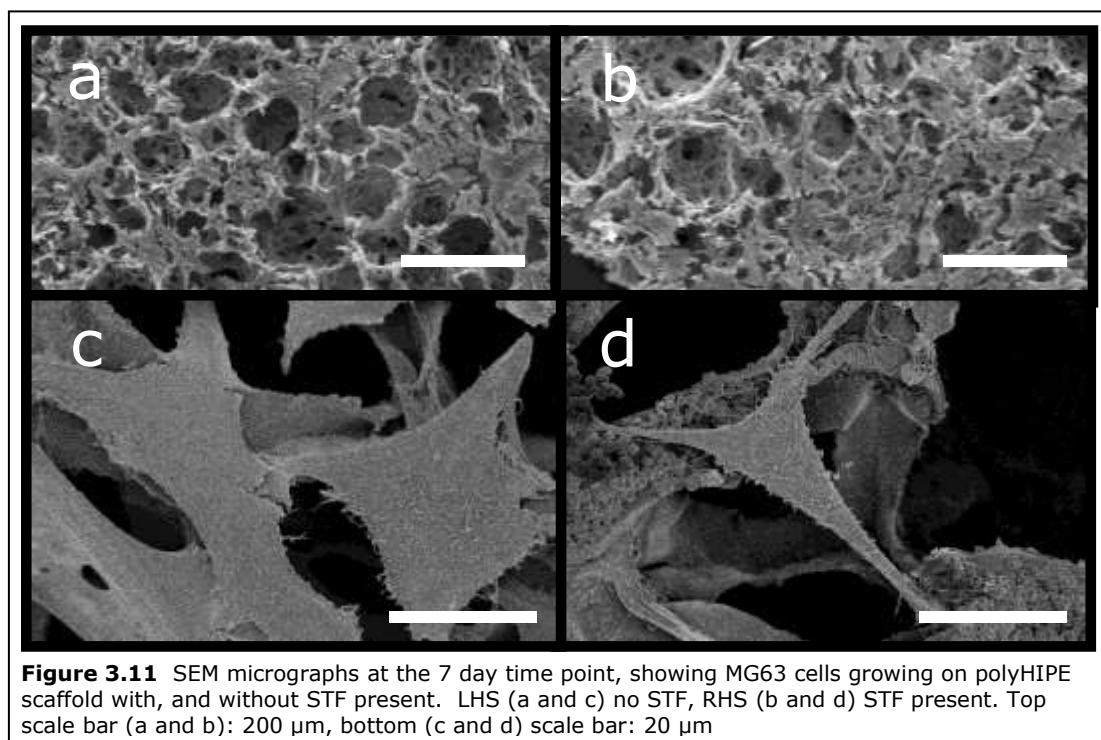
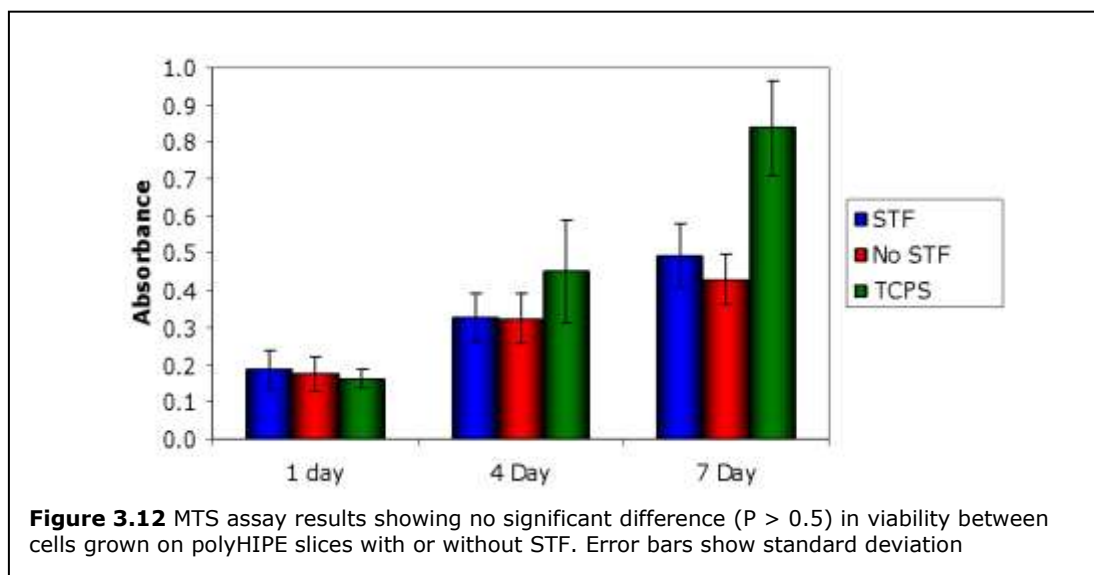


Figure 3.11 show SEM micrographs of the cells grown on the polyHIPE at a low magnification (a and b) and at a higher magnification (c and d). There appear to be no significant difference at the 7 day timepoint in terms of coverage or the number of rounded, dead cells, observed. The cells appear to be spreading and attaching to the polyHIPE, whether STF were present or not. To quantify this, a MTS assay was undertaken at 1, 4 and 7 day timepoints, the results of which are shown in figure 3.12. The MTS assay is a quantitative test for the viability of cells. The term 'viability' refers to the quantification of metabolic activity - a higher reading can be

interpreted as either a higher metabolic activity due to increase in cell number, or increase in metabolic activity of individual cells. The results show that there is no significant difference between the samples, confirming that the STF do not significantly affect MG63 cell viability despite affecting the microtopology.



3.7 Time-of Flight Secondary Mass Spectroscopy (ToF-SIMS)

With thanks to David Scurr at Nottingham University.

Samples were analysed at Nottingham University. ToF-SIMS was run on unfunctionalised polyHIPE, primarily to investigate the usefulness as a surface analysis technique for three-dimensional surfaces. ToF-SIMS is often used for surface analysis of flat plaques of polymers, and expected ions from the polystyrene backbone can often be identified. The “fingerprint region” of the ions in a polymer is usually less than 200 m/z and can indicate molecular structures. The spectra are shown in figures 3.13 and 3.14 (negative and positive respectively). Expected peaks listed below the spectra show the polystyrene backbone, peaks also at 15.9943 and 17.0023 show that oxygen is present from the EHA, as well as possibly some nitrogen. The individual ions can be mapped over a surface, in this

case an area of 500 μm^2 was used, and the resulting chemical maps are a good indicator of the homogeneity of the surface. The corresponding tables are shown in tables 3.2 and 3.3.

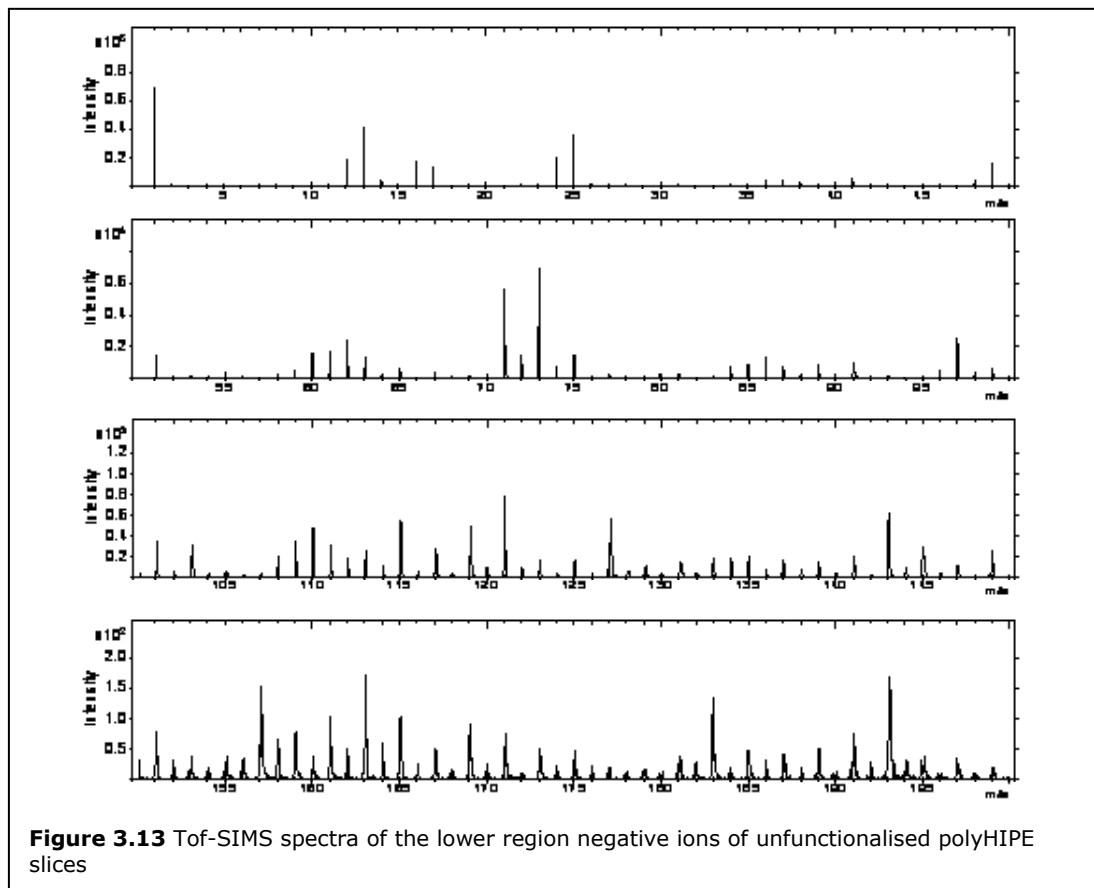


Table 3.2 Corresponding table of negative peaks for the Tof-SIMS spectra shown in figure 3.13 for the unfunctionalised polyHIPE

Ion	Mass	Deviation (ppm)
O	15.9943	-37.4
OH	17.0023	-25.8
F	18.9983	-4
C ₂ H	25.0072	-26.1
Cl	34.9686	-8.6
C ₃ H	37.0071	-19.4
C ₄ H	49.0087	18.3
C ₅ H ₂	62.0155	-2.9
C ₆ H	73.0071	-9.4

	=	Polystyrene
	=	Polystyrene ring structure
	=	Possible contamination

If we take the expected ion peaks from the polystyrene, (for example C_8H_7 at 103.0472 and C_9H_7 at 115.0442 - both expected structures from the polystyrene aromatic ring) and plot them over an area, the resulting maps show that the prevalence of styrene is homogenous over the surface, as expected. Selected maps are shown in figure 3.15. The peaks for oxygen and OH groups show that the acrylate in the base polymer can be detected. Sulfur, in its elemental state (m/z at 31.97207, 33.96787 - 4.4 %), was not detected, showing that the initiator concentration is too low to be detected.

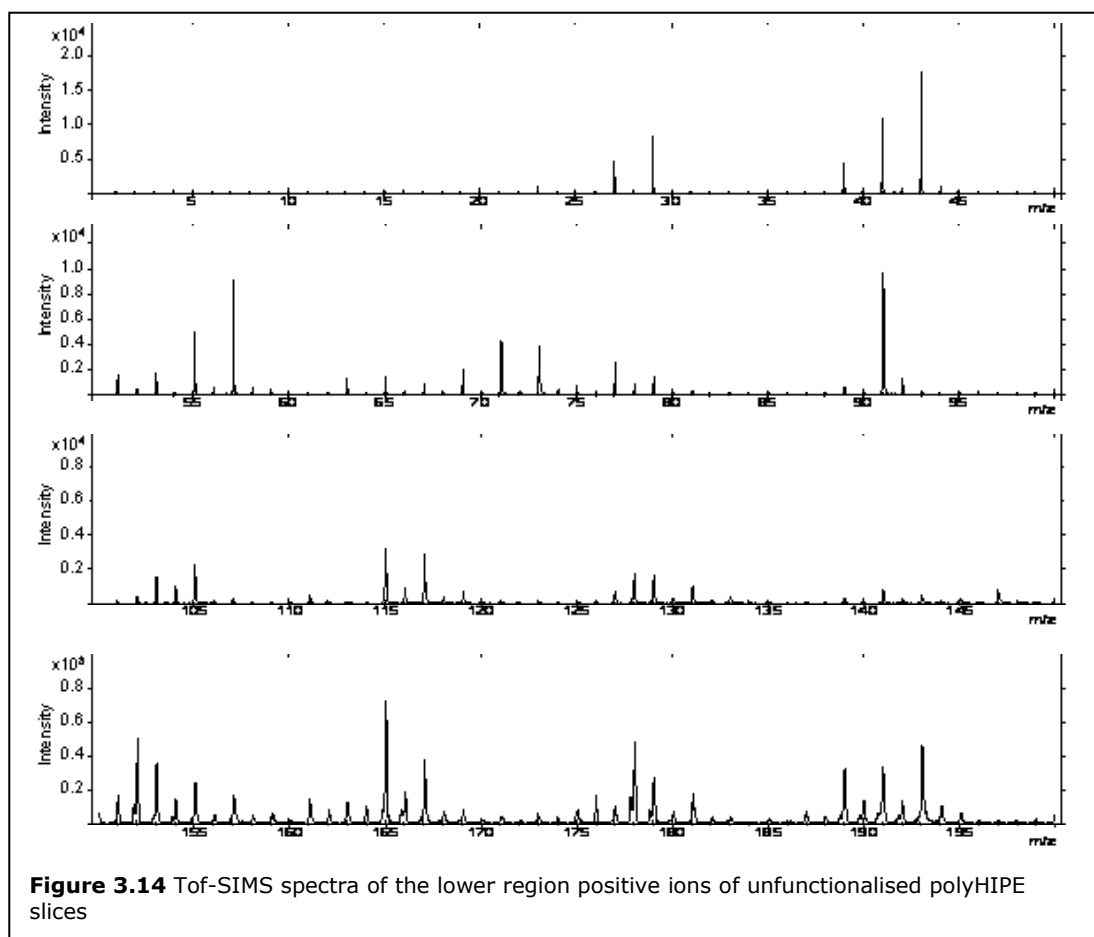
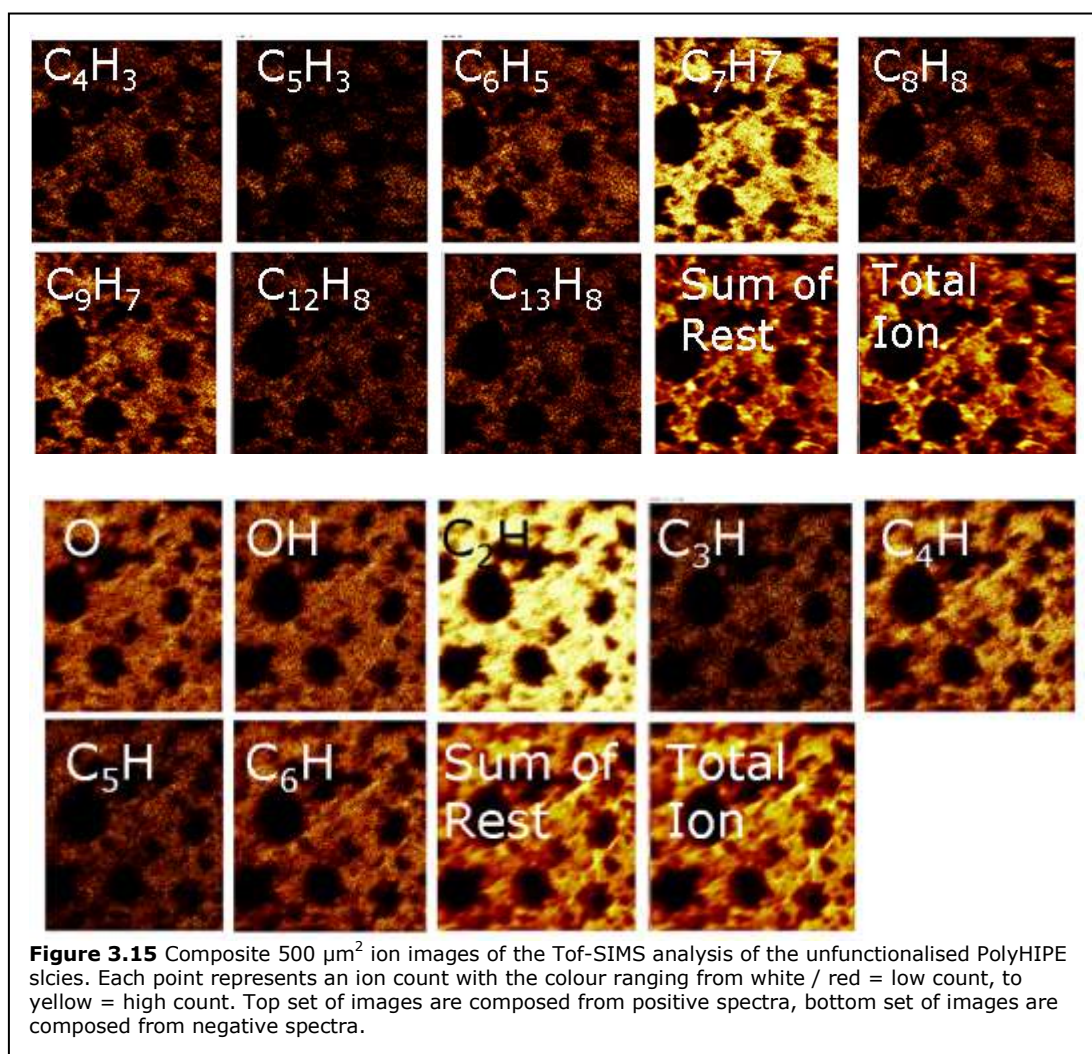


Table 3.3 ToF-SIMS peak list of the lower region positive ions of an unfunctionalised polyHIPE

Ion	Mass	Deviation (ppm)
CH ₃	15.026	170.9
Na	22.9917	81.8
C ₄ H ₃	51.0223	-23.9
C ₅ H ₃	63.0235	0.7
C ₆ H ₅	77.0353	-49
C ₇ H ₇	91.0581	36.6
C ₈ H ₇	103.0472	-73.9
C ₉ H ₇	115.0442	-92.1
C ₁₂ H ₈	152.0443	-120.6
C ₁₃ H ₉	165.0517	-113.6

	=	Polystyrene
	=	Polystyrene ring structure
	=	Possible contamination



As shown in figures 3.13 - 3.15, the expected peaks for polystyrene are shown clearly, and the surface (shown by the composite images) is homogeneous as

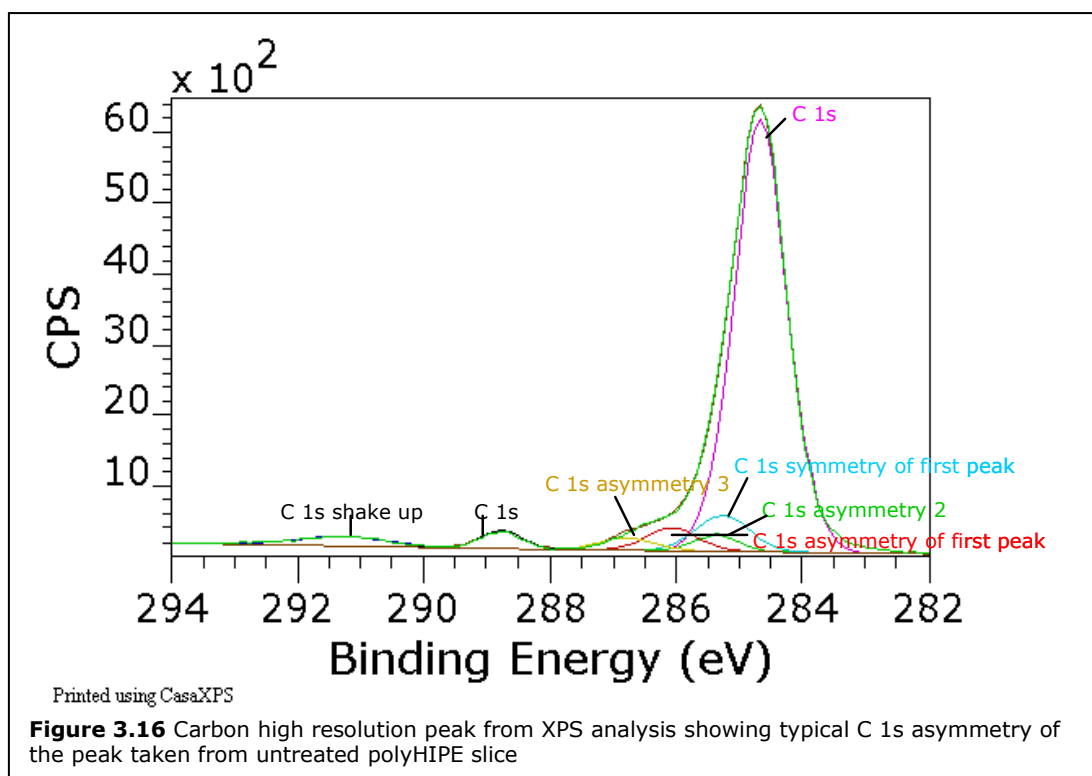
expected. This shows that ToF-SIMS is a potentially useful tool in being able to identify surface groups on the polyHIPE. Although less sensitive than X-ray photoelectron spectroscopy (XPS), the fragmentation of groups may be a useful method to identify the types of functionality present on the surface of the polyHIPE. There is some possible contamination on the surface, seen in the positive spectrum, with peaks appearing at 79.0422 and 111.0684 assigned to $C_5H_5N^+$ and $C_6H_9NO^+$ respectively, but with there being no nitrogen in the polyHIPE composition, this can be accredited to contamination, and the sensitivity and error margins now take into account the magnitude of contamination expected. An alternative assignment of these peaks could be $C_2H_7O_3^+$ (deviation of 22 ppm) and $C_3H_{11}O_4^+$ (deviation of 5 ppm), although it is not presently clear the mechanism for which the oxygen (from the EHA) reacts to form fragments with greater than 2 oxygen moieties.

3.8 X-ray Photoelectron Spectroscopy (XPS)

With thanks to Emily Smith at Nottingham University.

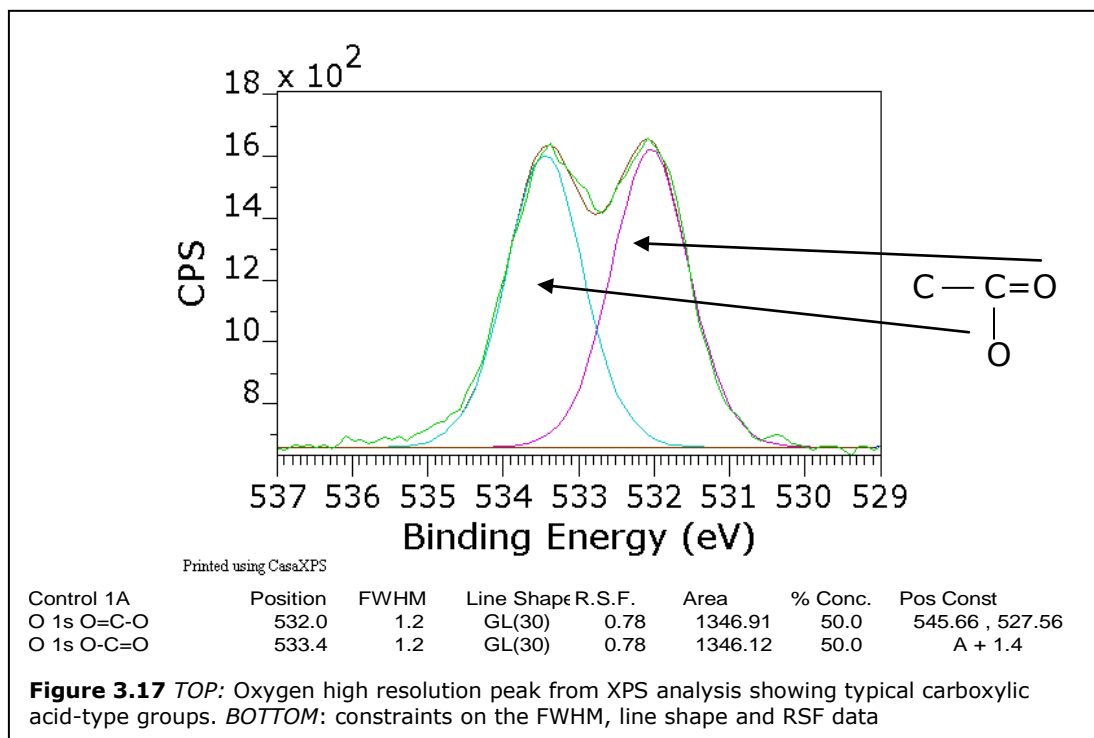
Samples were analysed at Nottingham University. The wide scan of the blank polyHIPE surface shows the surface only contains C and O species. These are in the ratios of 94.75 : 5.25 % correspondingly. This is slightly lower than expected. The composition of the monomer mixture is calculated at C 83.57 %, O 7.34 % and H 9.09 %, when taking into account the non inclusion of hydrogen in the XPS spectrum, the expected composition would be C 91.93 %, O 8.07 %.

The high resolution scan of the carbon and oxygen peaks is shown in figure 3.16 and 3.17. All values are taken from the XPS of polymers database.⁴



For the carbon peak fitting the C 1s main peak was initially set to 284.7 eV due to the assumption that it is mostly aromatic carbon, even though it is slightly broader than it may be expected to be for a pure aromatic peak. The broadening of the peak suggests partial aliphatic content, which can then be related to the monomer mixture used. A shake up peak at 291 eV can be seen, which is caused by exiting photoelectrons from C 1s interacting with the π orbitals of the aromatic species ($n \rightarrow \pi^*$ transition). This shake up peak area covers approximately 3 % of the main peak, which is reasonably low, so an estimate of approximately half of the main peak can be assigned to aliphatic species. The main aromatic peak is usually asymmetric so in this case it has been modelled with a set of four diminishing components to the high binding energy side of the main peak. A peak also appears in the C 1s spectrum at + 4 eV which can be attributed to carbon in carboxylic acid. The carboxylic acid carbon is due to the 2-ethylhexylacrylate (EHA) in the base polyHIPE. This peak is roughly the size expected from the EHA carboxylic acid

contribution so correlates well with the oxygen high resolutions scans that the EHA carboxylic acid group is present on the surface of the polyHIPE (see next section) For future analysis, the C 1s peak was set to 285 eV.



High resolution oxygen scans were charge-corrected to the main C 1s peak = 285 eV. The di-modal peak has a ratio of approximately 1 : 1 between peaks so the high resolution scan can be fitted with two synthetic components, which then relates very closely to the predicted two distinct peak energies for the COO structure of oxygen on the surface, with the difference in binding energy (BE) being due to the different binding states of the oxygen. The synthetic components are shown in blue (LHS) and purple (RHS) respectively. In this fitting the FWHM, areas and splitting are constrained and linear background and GL(30) components shapes are used in all cases. The oxygen peak fits correspond well with the expected oxygen peaks from the carboxylic acid type group in the EHA. There is no immediate trace of any sulfur on the surface.

In terms of oxygen contribution from the sulfur from the KPS initiator, the area where the sulfur peak is found was analysed on the wide scan. In a routine scan, the peak shown in figure 3.18 would be not be analysed, as it is very weak, it is probably attributable to noise. Upon detailed re-analysis the maximum amount of sulfur would be 0.02 % as shown in table 3.4.

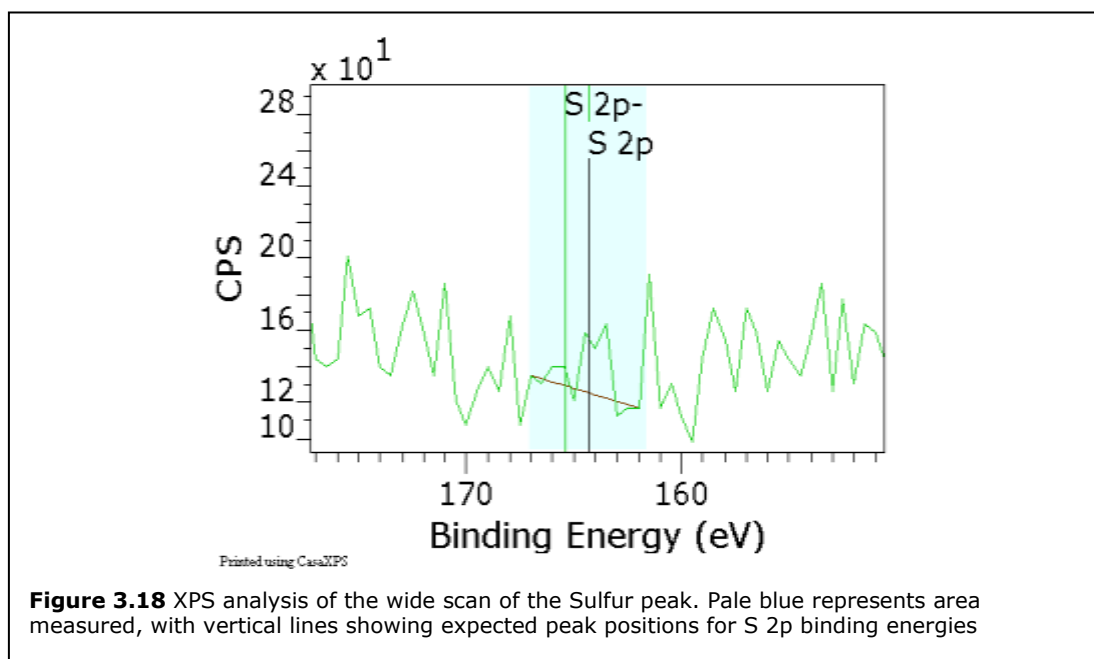


Table 3.4 Analysis of sulfur peak. Composition of wide scan if sulfur is taken into account

	% composition
C 1s	94.75
O 1s	5.23
S 2p	0.02

If there was sulfate present, then one sulfur atom would be attached to 3 oxygen atoms and $0.02\% \text{ S} \times 3 = 0.06\%$ of total elements O 1s signal is SO_3 . That is $0.06 / 5.23 = \text{approx } 1\%$ of the total of the O 1s envelope could possibly be sulfates. There is no obvious K 2p peak (overlaps into the C 1s region). Detection levels for this would be typically ~ 0.05 atomic % or better. This shows that sulfur is not present in any great quantity on the surface of the polyHIPE and predominantly

the oxygen present on the surface is due to the EHA, not from the persulfate initiator.

The XPS data clearly shows that the polyHIPE monolith can be analysed and interpreted, with the results that the polyHIPE is composed of carbon and oxygen, and also being able to confirm the expected composition of the monomers - with particular reference to the clear identification of the carboxylic acid group from the EHA being present in the monolith.

3.9 Conclusions

PolyHIPEs have been made using previously investigated methods, and analysed using a variety of techniques, including x-ray photoelectron spectroscopy (XPS) and time-of-flight secondary-ion-mass-spectrometry (ToF-SIMS). The analysis revealed no real surprises but has demonstrated that the surface-specific techniques can be accurately and specifically used to analyse the top surface of the three dimensional porous materials. Various techniques to speed up the manufacture of polyHIPEs were investigated, with the dismissal of some (Tornado stirrer) and the adoption of others (LEICA vibratome). Steps were taken to identify the microdroplets found on the surface (STF) of some of the monoliths, and control them. As total control was not achieved, cell work was taken to observe the effect on cell viability. Cells were not adversely affected by the STF, so whereas polyHIPE manufacture tightened up control, the appearance of the STF was not a continuing issue.

With retrospect, the formation of the STF does not come as a surprise. The initial emulsion formulation was envisaged as a room temperature system, and a suitable surfactant with a low HLB was chosen to create a water in oil (W/O) emulsion. Upon heating up the aqueous phase, a greater void diameter was

obtained, but at the expense of creating STF on the surface. Bancroft's rule indicates that in an emulsion, the phase in which the surfactant is more soluble constitutes the continuous phase. The simple answer to the STF is that Span 80 is insoluble in cold water (and therefore in the original polyHIPE the surfactant was more soluble in the monomeric phase), but it is soluble in hot water, and a point can be envisaged in which Span 80 is more soluble in the hot water than the monomeric phase, and so the emulsion inverts, causing STF to form. A solution to this can be seen in that changing the surfactant, to one that is not soluble in hot water (easier in theory than practical), would eliminate the STF. Alternatively the aqueous phase temperature could be reduced to one where the Span 80 is not soluble in the hot water (but this would come at the expense of the void diameter).

3.10 References

¹ R.J. Carnachan, M.A. Bokhari, S.A. Przyborski, N.R. Cameron *Soft Matter* (2006) **2** 608

² "Persulfates: Technical Information" datasheet produced by *FMC Corporation*. Available at www.fmcchemicals.com

³ T.E. Williams, S. Nagarajan, P. Selvaraj, C. Zhu *J Bio Chem* (2001) **276** 13283

⁴ J.F. Moulder ed: J. Chastain, R.C. King, E. Prairie *Handbook of x-ray photoelectron spectroscopy : a reference book of standard spectra for identification and interpretation of XPS data* Physical Electronics (1995)

Chapter 4 - Wet Chemical Functionalisation of PolyHIPEs

4.1 Introduction

A “smart material” can be defined as a material, which in some way interacts with its environment or the environment in which it is placed. In general a “smart material” is one which actively changes in some way as a result of a stimulus in its environment. In this instance a smart material is envisaged created with the polyHIPE, in which the polyHIPE is modified in order to release EC23, but only when placed into an *in-vitro* cell culture environment. The next step toward creating a “smart material” for cell culture was to identify potential routes for surface modification. Creating a polyHIPE with alternative monomers containing functionalisable motifs - such as vinyl butyl chloride (VBC) was ruled out as this would have an effect on the previously optimised structure and would possibly reduce the void diameter.¹ Wet chemical routes as set out below were proposed and investigated by XPS, ToF-SIMS and *in-vitro* cell culture.

4.2 Bromination

Powdered PS-DVB-EHA polyHIPE (2.00 g) was placed in dry toluene with anhydrous lithium bromide (1.0 g, 12 mmol), chlorotrimethylsilane (1.4 ml, 13.4 mmol), water (0.12 ml, 6 mmol) and recrystallised (from MeOH) AIBN (0.2 g, 1.2 mmol) was heated to 70-80 °C for 24 hrs. The powder was washed with hot acetonitrile, then rinsed with diethyl ether. Secondary washings were done by extraction with acetonitrile in a Soxhlet apparatus for 48 h then dried *in-vacuo* overnight. Polymer turned pale yellow after reaction and retained pale colour upon drying.

A paper by Mercier et al² claims that a polyHIPE composed of 100 % divinylbenzene (DVB) can contain up to 40 % unreacted vinylic bonds. To take advantage of the reactivity of the surface, and to quantify the number of unreacted double bonds in our polyHIPE, a bromine radical reaction was used. Briefly, 2.00 g of powdered polyHIPE (nP), consisting of styrene, 2-ethylhexyl acrylate (EHA) and DVB in the w/w ratios of 6:3:1, was brominated in toluene using LiBr, chlorotrimethylsilane, water and recrystallised AIBN. The powdered polyHIPE turned pale yellow upon bromination. The extent of bromination was analysed by elemental analysis. The results are shown in table 4.1. Calculations are based on solely monomeric components, as the amount of initiator incorporated cannot be readily measured, as demonstrated in the previous chapter.

Table 4.1. Quantity of bromine from a radical addition and an electrophilic addition reaction

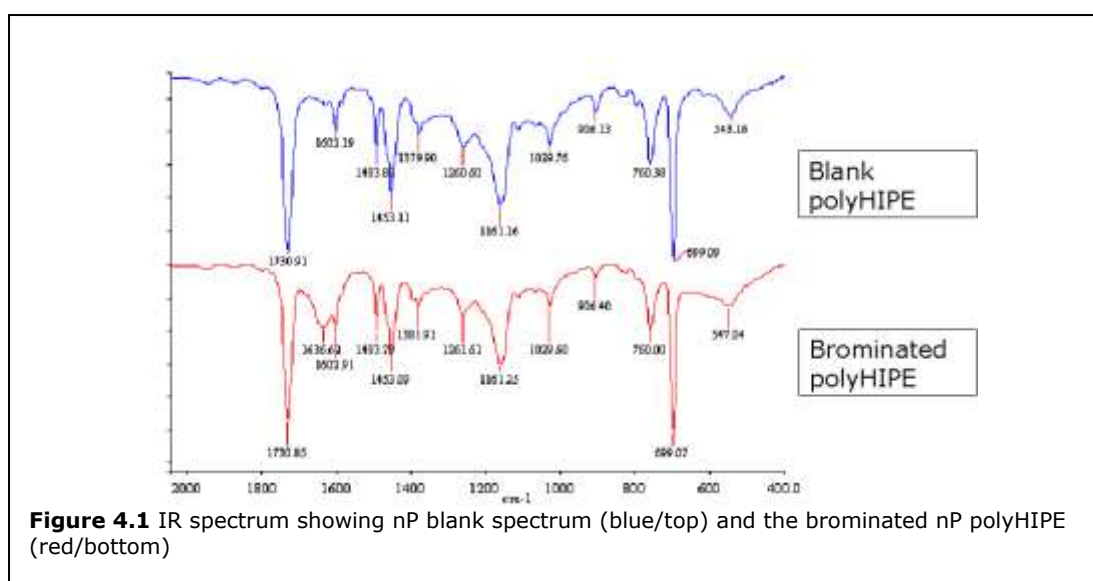
	Amount Br %	Unreacted double bonds %
radical addition	1.7 ± 0.4	29.1 (± 6.85)
electrophilic addition	3.7 ± 0.7	33.5 (± 6.34)

The 1.7 % Br value was in the range expected, as these polyHIPEs contain 10% monomeric DVB. The maximum expected bromination of the DVB (assuming 40 % unreacted double bonds) would be 2.34 % Br. As this maximum is not reached it is assumed that more vinyl bonds are reacted within the polymer in this polyHIPE process or that some of them don't react with Br. From the value of 1.7 it can be calculated that in this case there are a minimum of 29.1 (± 6.85) % unreacted double bonds.

Titration of Br₂ was attempted also to quantify the unreacted vinylic groups. The standard method is undertaken with an aqueous solution of bromine, but as the polyHIPEs are highly hydrophobic, a DCM solution was used. Briefly, titration of bromine was performed into a suspension of polyHIPE in DCM, with the endpoint

based on the visual observation of the last point of decolouration of the solution. This method was unsuccessful due to the inability to seal the apparatus sufficiently and the bromine/DCM dissipated into the atmosphere. However the resulting brominated polyHIPE was analysed and the resulting amount of bromine found was approximately double the initial (radical bromination) experiment at 3.7 ± 0.7 bromine content (see figure 1). This can be back calculated to a value of $33.5 (\pm 6.34)$ % unreacted double bonds. This corresponds well with the previous radical addition reaction as it is roughly double the radical reaction route.

The Mercier paper quoted a peak in the infra-red spectrum at 1261 cm^{-1} as resulting from the bromine. From the literature³⁻⁴ an additional C-Br stretch would appear “right of 667 cm^{-1} ”, which is difficult to observe. With the nP (blank) polyHIPE a peak appears at 1261 cm^{-1} from the carboxylic acid from the EHA of the base polymer as shown in figure 4.1. This would mask any bromine stretch seen at this wavenumber. The IR spectrum of the nP after bromination IR shows an additional peak at 1636 cm^{-1} which could be assigned to a N-H bend or aliphatic C=C. This is unexpected, as it would be assumed that the C=C bond would have been reduced by the bromination.



4.3 Amination

Following the procedure as set out in the original Mercier paper,² brominated powdered PolyHIPE (nP) from the previous radical addition was suspended in a solution of Tris(2-aminoethyl)amine in DMF. The mixture was stirred at 45°C for 24h, then cleaned and dried. Tris(2-aminoethyl)amine was chosen for its high basicity and high nitrogen content (4 nitrogen atoms for every one attachment) which would increase detection and would lead to a lower error in elemental analysis. The results of elemental analysis after the reaction are shown in table 4.2.

Table 4.2 Elemental analysis values from amination experiments (4.3)

	N %	Br %
Brominated	0.00	2.10
Aminated	0.34	2.05

The results show that, although reaction was left for over 24 hours to proceed, the amount of amine attached was minimal, with the amount attached corresponding to less than 0.1 % attachment.

4.4 Thiolation

Due to the disappointing amount of amine attachment, direct thiolation of the vinyl bonds was tried. This involved both powdered polyHIPE (nP) and also small cubes (10 mm³) of monolith. The secondary purpose of this was to investigate the permeability of the monolith to the reactants. The thiol used was aminoethanethiol. The method involved suspending the polyHIPE powder/cubes in DMF, adding a large excess of aminoethanethiol and AIBN as an initiator, heating to 80 °C then stirring under N₂ for 48 hours. The powdered polyHIPE and the cubed polyHIPE gave a elemental analysis of 0.54 % and 0.40 % sulfur respectively. This figure is

the same as the blank polyHIPE (no treatment) of 0.50 % sulfur, and this is probably accounts for the margin of error of elemental analysis.

4.5 Bromination of 100 % DVB PolyHIPE

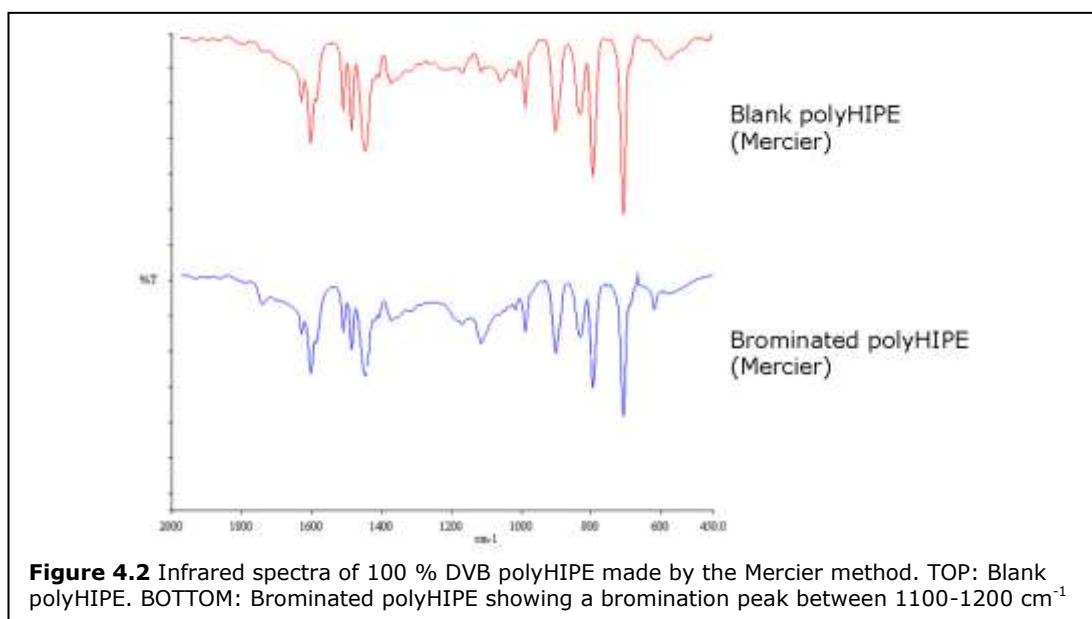
To investigate if the initial radical addition methods could be optimised, the 100% DVB polyHIPE from the Mercier paper was made. The 100 % DVB polyHIPE was prepared by two methods, one taken from the original paper and one derived from our previous method, with the whole monomer mixture comprising of 100 % DVB as opposed to the mixture of styrene : DVB : EHA mixture. The main differences were that the Mercier polyHIPE was a 95.7 % porosity polyHIPE with a slightly lower surfactant level and NaCl stabilising salts as opposed to the “nP” method which consisted of a 90 % porosity polyHIPE with an increased aqueous phase temperature (80 °C) and shorter addition and mixing times.

Both the polyHIPEs were very brittle and weak with a chalk-like texture. Extraction of the intact monolith from the curing tubes was not possible as the structure significantly degraded upon removal from the tube. The polyHIPEs were therefore ground up and used as powders. The powder was not graded, but was ground up to a uniform powder, with no large pieces visually observed (above 2 mm²). The results of the bromination are shown in table 4.3. Both 100% DVB polyHIPE structures showed a greater addition of bromine than the 10 % DVB material, and a large increase (over 100 %) was observed with the electrophilic addition. The amount of reacted double bonds calculated from this are 14.9 % (radical) and 24.1 % (electrophilic addition) for the nP polyHIPE and for the Mercier polyHIPE 18.3 % and 30.1 % respectively.

Table 4.3 Bromination data showing the difference in amount of bromine incorporation between nP and PolyHIPE made by the Mercier paper route

	Br % (radical)	Br % (electrophilic addition)
nP polyHIPE	7.31	19.76
Mercier polyHIPE	8.94	24.65

With the 100 % DVB PolyHIPE the IR spectrum of the brominated material can be taken, without intrusion from the EHA, and a peak was seen in the fingerprint region at 1116.5 cm^{-1} after bromination as shown in figure 4.2.



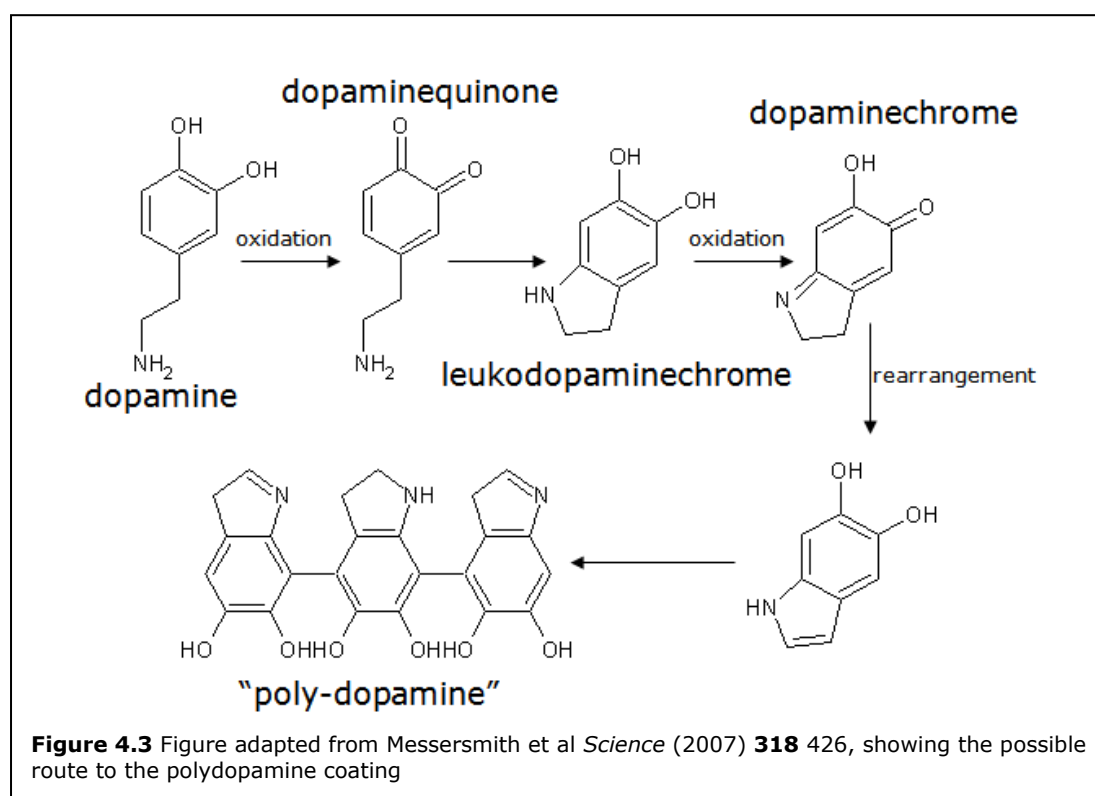
4.6 Poly-Dopamine Coating of PolyHIPEs

As the reactions with the vinyl groups gave very low values of surface functionalisation, with many too low to be measured accurately using elemental analysis, it was decided to try to adsorb a coating onto the polymers. This would result in a much larger amount of reactive groups to further functionalise the polyHIPE. This coating must be stable and non-toxic to cells once adsorbed. A paper by Philip Messersmith's group⁵ describes a bio-inspired coating produced from dopamine, which spontaneously polymerises at pH 8.5 and irremovably coats any immersed object. The dopamine-based coating was shown to be further

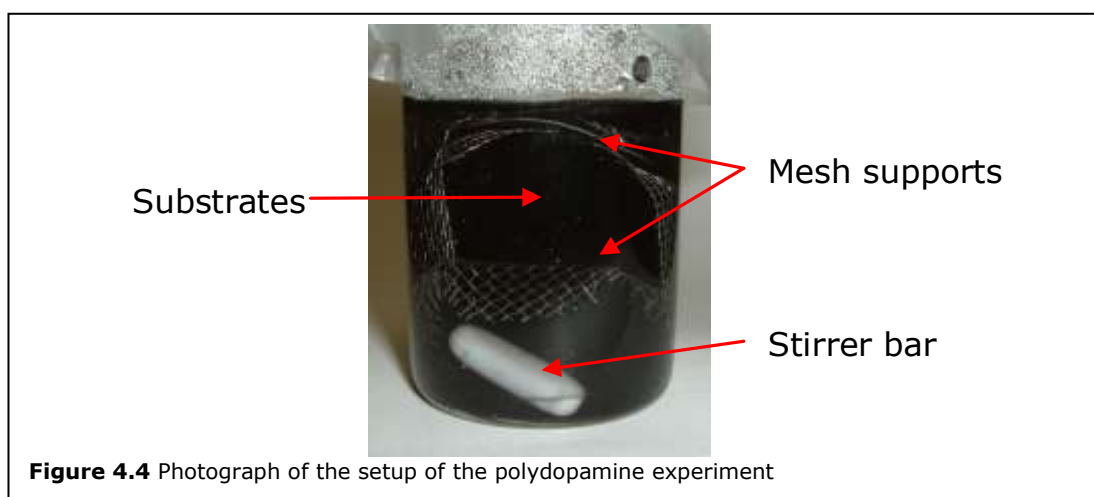
reactive to amine and thiol containing groups so seemed ideal for the proposed purpose of coating the polyHIPE, and, being present in a natural environment, promises to show limited toxicity.

The process of coating an object involved an aqueous Tris-Cl buffer solution and adding dopamine hydrochloride at a defined concentration, and ensuring that all the dopamine was dissolved whilst maintaining the pH at 8.5. Within 1 minute of total addition the substrates to be treated were immersed in the liquid, and after about 5 minutes, with continuous, vigorous stirring, the solutions turned black, coating the side of the reaction vessel, the stirrer bar, and the immersed substrates.

The proposed route to the polydopamine moiety is shown in figure 4.3 (adapted from above paper), and also the resulting ToF-SIMS is, from which the above route was proposed.

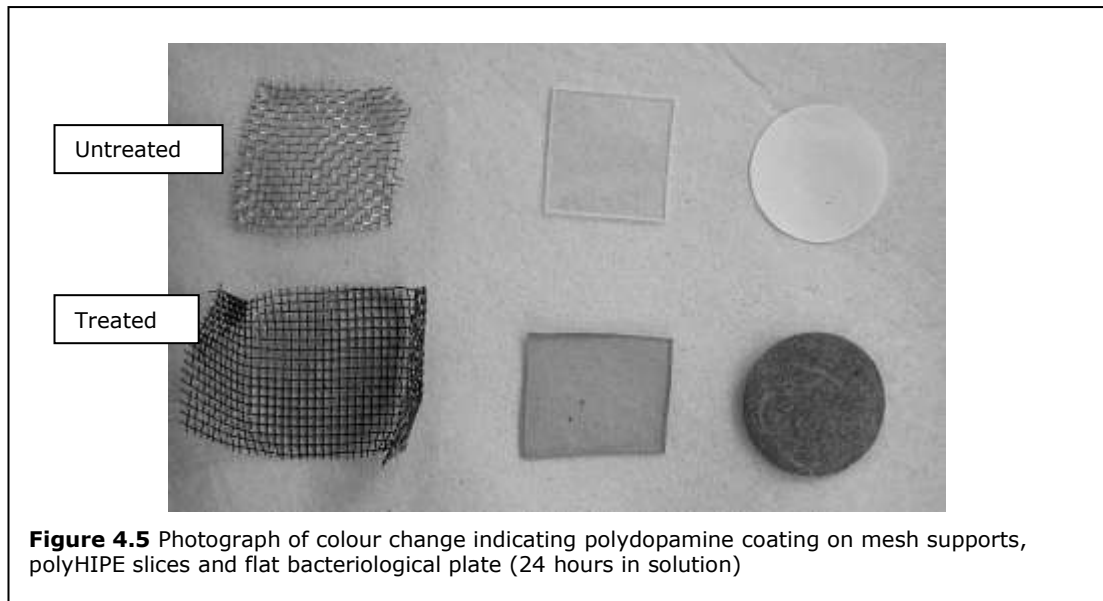


The procedure described in the Messersmith paper assumes that the object in question was able to be immersed fully in the aqueous solution. The polyHIPE slices were very hydrophobic, consequently they float in an aqueous solution. Upon “forced” immersion, the pores of the polyHIPE did not become saturated with the solution. The mechanical stirring tended to break up the polyHIPE slices quite brutally. The polydopamine did not form sufficiently with shaking or moderate stirring. A modification was made to the setup of the stirrer and polyHIPE, the reaction vessel was sectioned into two parts with wire mesh, allowing free circulation of the solution, whilst maintaining a distance between the mechanical stirrer and the polyHIPE slices as shown in figure 4.4.

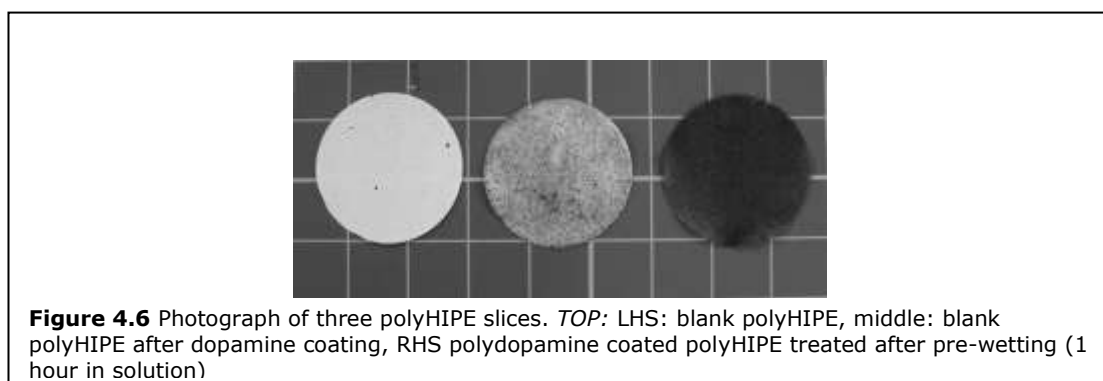


Metal mesh was used to stop the polyHIPEs floating on top of the aqueous solution, and to prevent mechanical damage of the slices by the magnetic stirrer. Photographs were taken of the apparatus set up, and the resulting coating on the wire mesh, polyHIPE and bacteriological plate (BP). The bacteriological plate was used as it was composed of predominantly untreated polystyrene, which could be utilised as a flat control. The photographs are shown in figure 4.5. It is clearly seen that, after treatment, the substrates and mesh are darkened, although the

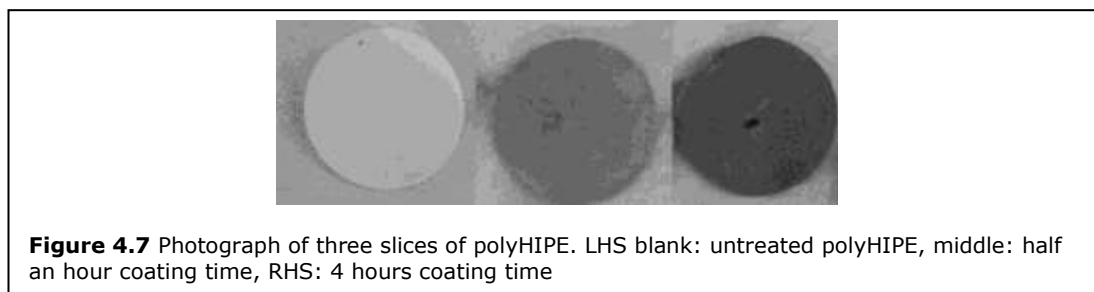
coverage on the polyHIPE is partial, and incomplete as the internal surface is not coated.



The polyHIPE was not totally covered due to the hydrophobic nature of the polyHIPE, and although immersed, the aqueous solution did not have contact with the internal surface of the polyHIPE slice. Two pre-treatments were tried, firstly “pre-wetting” the slices with 70 % ethanol and gradually exchanging this with water/buffer and secondly by plasma treating the polyHIPE slices (see chapter 5 for more detail), which made them hydrophilic, so the dopamine containing buffer solution fully saturated the surface of the polyHIPE. Both of these methods lead to a darker, more complete coating of polydopamine, even after extensive washing. A photograph of an example of the effect of pre-wetting is shown in figure 4.6.



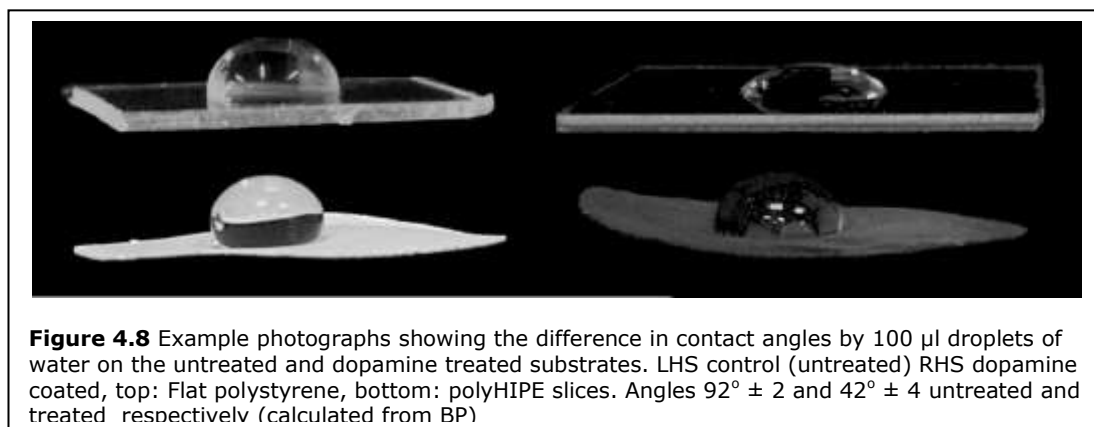
The time of reaction was found to be an important factor in the durability of the coating. The stirring solution, if left stirring overnight, polymerised dopamine formed discrete particles of polymerised dopamine in the water and they were also deposited on the surface of the substrate. These were undesirable as they tended not to be removed by the thorough washing, but instead desorbed over a period of days after thorough washing if the substrates were left in solution. In a cell culture setting this is not desirable. The ideal period of time for the solution to be left stirring in order to get a reasonable coating, with minimal droplet formation, was 4 hours. The judgement of this was by eye, observing the maximum colour change in minimum time. This was judged by the visual integrity of the coating on the polymer substrates. The differences of colour are shown in figure 4.7 which shows two treatment time points with differing length of time in solution. In this case the slices were pre-wet.



4.7 Contact Angles

Contact angles were measured using a setup of a pipette suspended 5 cm above the substrate to be measured. A camera was set up level to the substrate surface with a 2 second timer to reduce camera shake. The camera timer was activated at the same time as the droplet was released from the pipette. Contact angles were measured with the flat bacteriological plates (BP) and photographs were also taken of the polyHIPE slices to compare. The contact angles on the polyHIPE

slices, were related to the flat contact angles, but as these are dynamic contact angles, they are not exact. The contact angle is affected by the porous/non flat surface, as outlined in the experimental section. Example photographs, taken from a higher viewpoint are shown in figure 4.8 to relate the behaviour of the droplet between the BP and the polyHIPE slice.



The static sessile contact angles measured for the BP were 92° (blank) and 42° (dopamine coated), the dopamine coated corresponds well to the contact angles measured in the Messersmith paper (average 47° static).

4.8 X-Ray Photoelectron Spectroscopy (XPS)

The XPS wide scans showed that there was an increase in nitrogen and oxygen on the surface after dopamine treatment. The wide scans are plotted from the XPS showing increase in size of the oxygen peaks as well as the appearance of nitrogen in figure 4.9. The corresponding table is shown in table 4.4.

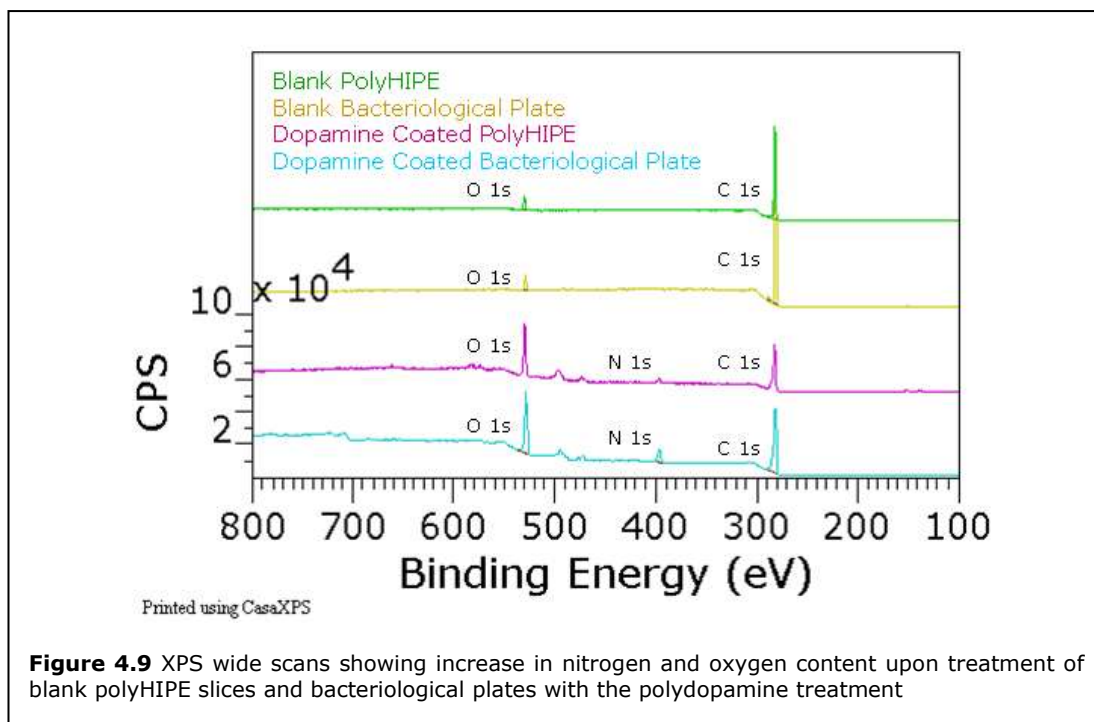


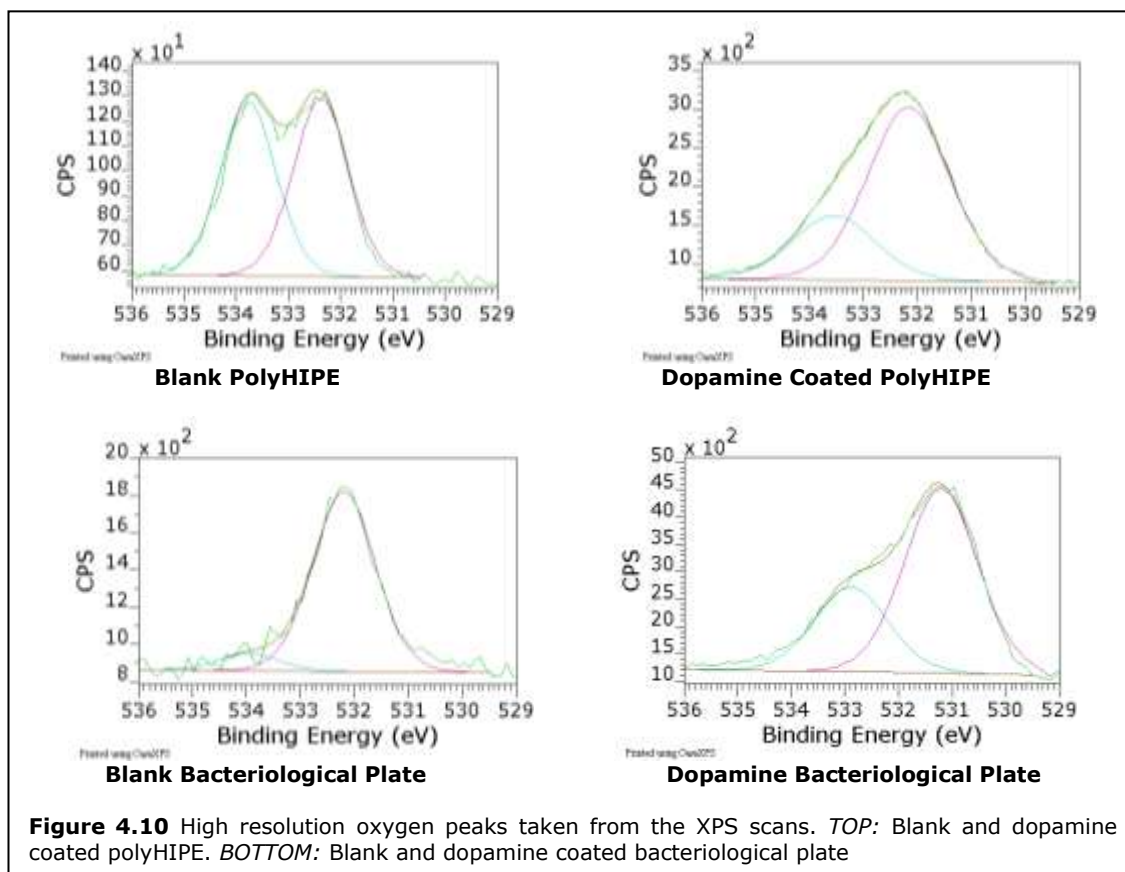
Table 4.4 Corresponding table of values from the XPS wide scans plotted in figure 4.9

	%	Average	S.D.
Blank PolyHIPE	C 1s	95.02	0.08
	O 1s	4.98	0.07
Dopamine Coated PolyHIPE	C 1s	73.93	1.31
	O 1s	18.58	1.11
	N 1s	3.69	0.45
	Zn 2p	1.57	0.06
	Zn 2p	0.73	0.04
Blank Bacteriological Plate	C 1s	95.83	0.96
	O 1s	2.91	0.69
	Si 2p	1.23	0.26
Dopamine Coated Bacteriological Plate	C 1s	76.43	0.09
	O 1s	16.32	0.21
	N 1s	6.13	0.11
	Si 2p	0.03	0.05
	Zn 2p	0.68	0.04
Zn 2p	0.41	0.02	

The XPS is very surface sensitive and silicon and zinc show up as contaminants in the polyHIPE slices. In the bacteriological plates the silicon is present in the composition or manufacture of the plate, but this gets “covered” by the dopamine coating, and only detected at very low levels in the coated substrate. The zinc is assumed to come from the metal mesh that was used to protect the polyHIPE slices from being broken up by the stirrer bar. This is seen in very low

concentrations (generally < 2 %) and shouldn't affect the further surface functionalisation of the polyHIPE, but is worth noting as a contaminant.

Further investigation using a high resolution nitrogen peak was not undertaken as the nitrogen peak is not sufficiently defined. The oxygen high resolution peaks however were investigated, as shown in figure 4.10.

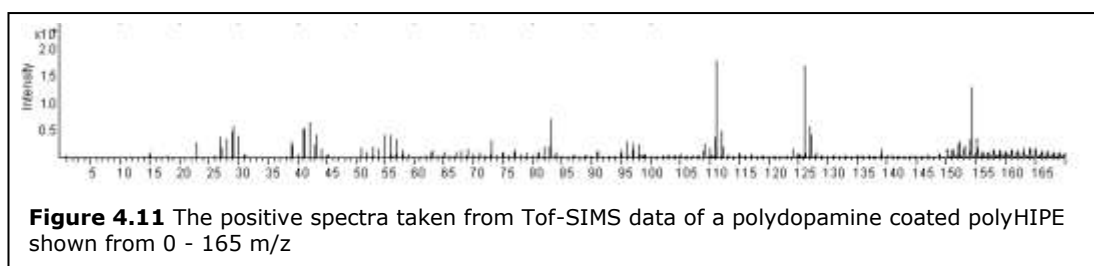


The oxygen high resolution peaks were fitted assuming that the original substrate was fully covered. The peaks show a widening and increase of the O 1s peaks. Synthetically two distinct two peaks can easily be fitted. The fitted peaks are not constrained to appear in the same place for the different coated substrates. The polydopamine peaks for the polyHIPE and the BP fall at different eVs with the dopamine coated BP having peaks at 531.202 (68.45 %) and at 532.883 (31.55 %) whereas the dopamine coated polyHIPE peaks fall at 532.189 (71.24%) and at 533.527 (28.76 %). This of course is a simplification as there are possibly more

than two oxygen environments, but even with this simplification and by looking at the overall peak shape, it is obvious that the underlying substrate is showing through, which leads to two hypothesis, either the polydopamine coating is not completely covering the surface, or it is thinner than the 10 nm of the surface that the XPS analyses, therefore some polyHIPE base structure is showing through. For future reference, depth profiling would be a useful techniques to establish which one of these hypothesis this is, although this would have to be done on a similar substrate, but one which was as flat as possible, as the polyHIPE has three dimensional edges. A flat substrate could possibly be prepared using spin casting. The Messersmith paper compared the nitrogen to carbon (N/C) ratio to compare to the theoretical value of dopamine (0.125), but does not compare the coating on a polystyrene plate. In this case the ratio is 0.05 for the polyHIPE slice and 0.08 for the BP.

4.9 Time-of-Flight Secondary Ion Mass Spectrometry (ToF-SIMS)

The positive spectra from the ToF-SIMS analysis of the polydopamine coated surface is shown in figure 4.11 up to 165 m/z. After 150 m/z the signals are less easy to distinguish.



Large peaks are seen at 111 and 126 m/z which could correspond to nitrogen-containing $C_6H_9NO^+$ and $C_7H_{22}NO^+$ correspondingly. Peaks attributed to the

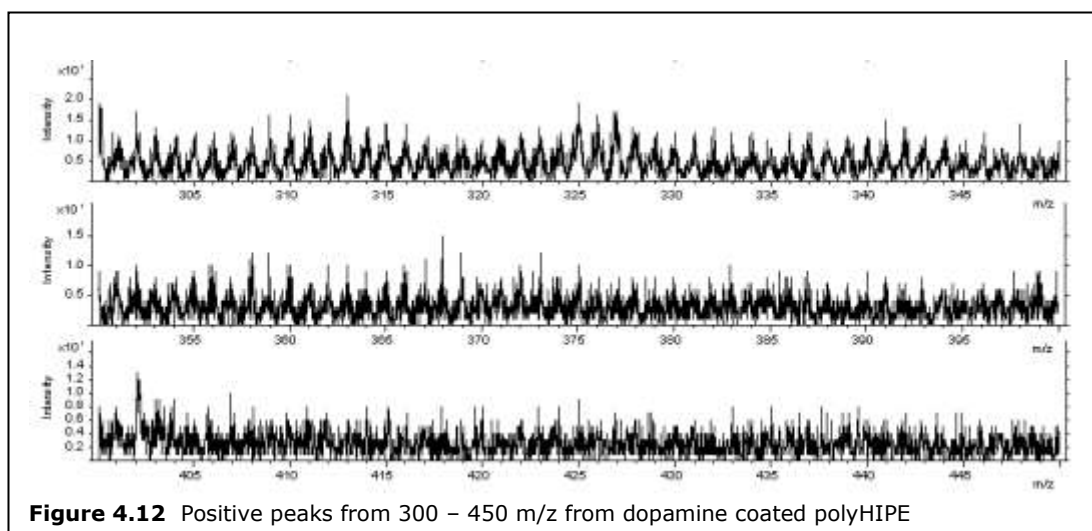
dopamine-coating are highlighted in blue in table 4.5. Some peaks attributable to polystyrene are still visible.

Table 4.5 Table of peak assignment from ToF-SIMS data of analysis of the dopamine treated PolyHIPE. Peaks attributable to the dopamine treatment are apparent and are highlighted blue

Ion	Mass	Deviation (ppm)
CH ₃	15.026	170.9
NH ₃	17.0258	-43.4
NH ₄	18.0395	285.3
Na	22.9917	81.8
CH ₂ N	28.0246	210.6
CH ₄ N	30.0402	195.1
CH ₆ N	32.0524	73.2
C ₂ H ₄ N	42.037	61.6
C ₄ H ₃	51.0223	-23.9
C ₃ H ₄ N	54.0358	27.2
C ₅ H ₃	63.0235	0.7
C ₆ H ₅	77.0353	-49
C ₅ H ₉ N	83.0502	-280.8
C ₇ H ₇	91.0581	36.6
C ₅ H ₆ NO	96.0413	-38.3
C ₅ H ₇ NO	97.0524	-4
C ₅ H ₈ NO	98.0536	-70.9
C ₈ H ₇	103.0472	-73.9
C ₆ H ₉ NO	111.0831	131.9
C ₉ H ₇	115.0442	-92.1
C ₇ H ₁₂ NO	126.0978	47.2
C ₇ H ₁₃ NO	127.1013	12.9
C ₁₂ H ₉	152.0443	-120.6
C ₉ H ₁₆ NO	154.1203	-18.9
C ₁₃ H ₉	165.0517	-113.6

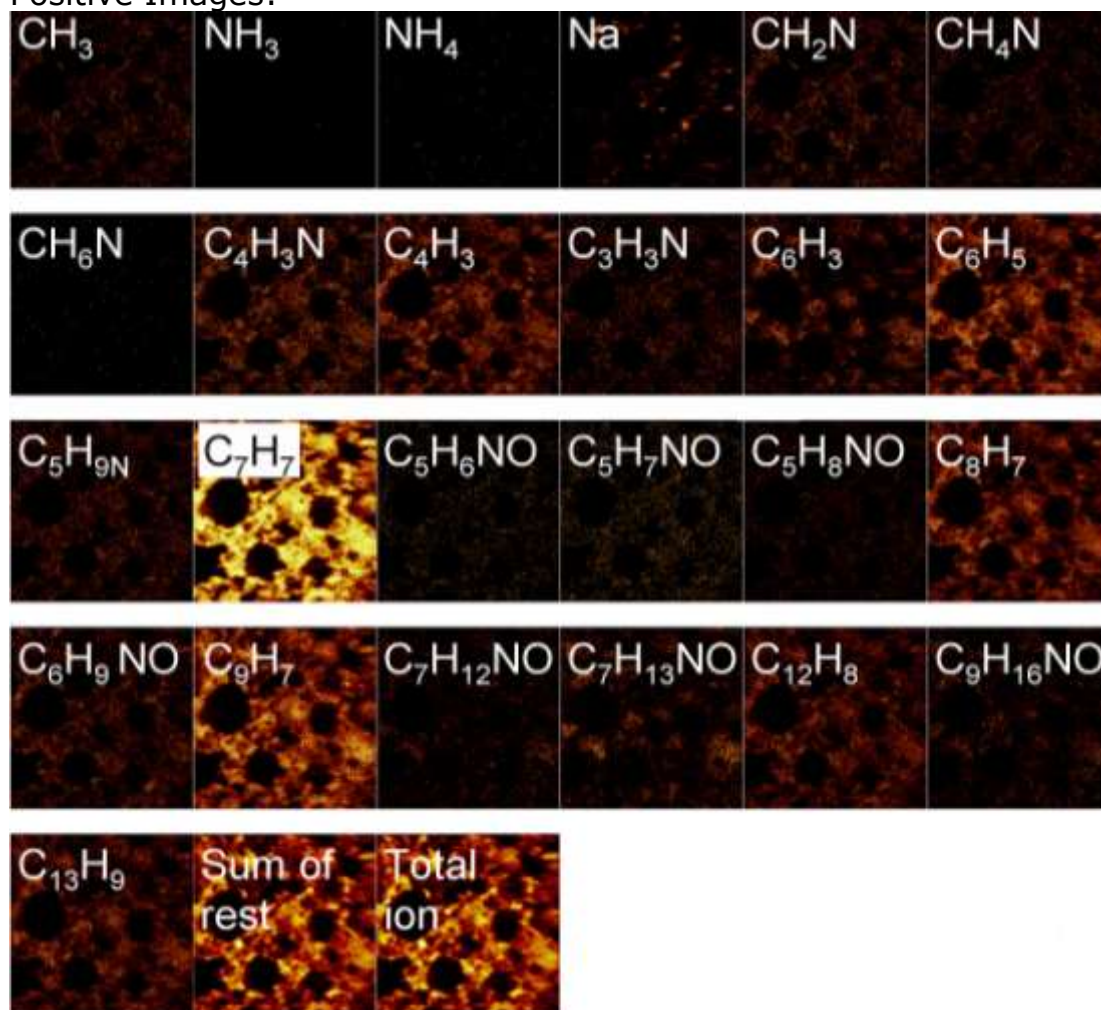
= Polystyrene
 = Contamination
 = Due to polydopamine treatment

Positive spectra were examined between 300 - 450 m/z to try and identify similar the M⁺ peak. In the Messersmith paper, the M⁺ peak was identified at 445 and immediately below was identified a set of peaks indicating a typical α - α - β splitting pattern for the liberation of hydroxyl groups and a portion of the phenyl group from the proposed “polydopamine” molecule. Unfortunately the spectra gained from the polyHIPE slices did not show a definite pattern, with the spectra above 325 being mainly noise. The spectra gained from the polyHIPE between 300-450 m/z are shown in figure 4.12.



The composite images, both positive and negative, in figures 4.13 and 4.14 show that many of the polystyrene peaks are suppressed by the dopamine coating, but not all. This indicates the coating is adsorbed onto the surface, but does not form a complete layer over the surface, or it has less than 10 nm thick coating. There are obviously greater amounts of nitrogen-containing species on the dopamine coated surface than the blank polyHIPE.

Positive Images:



Negative Images:

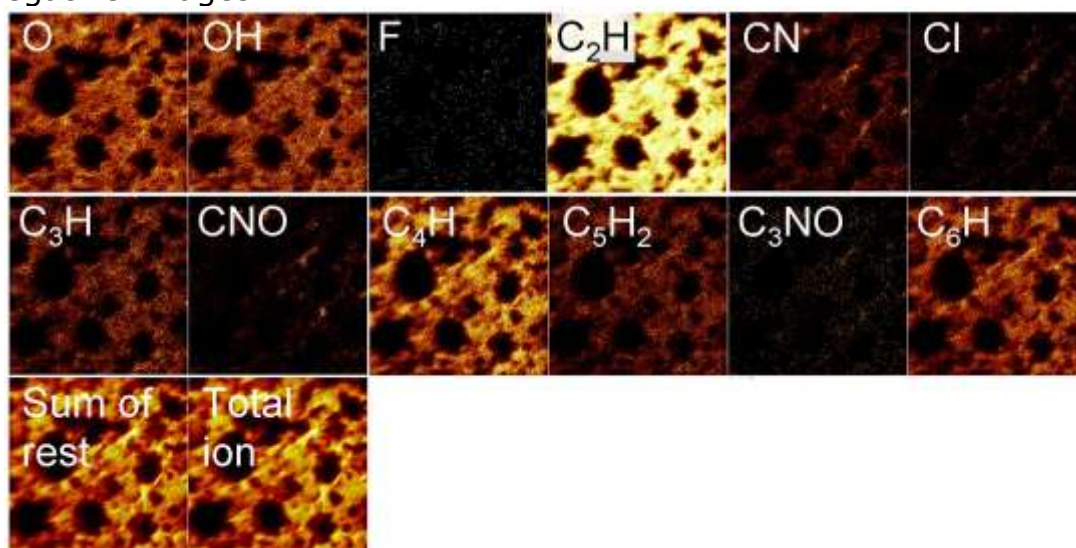
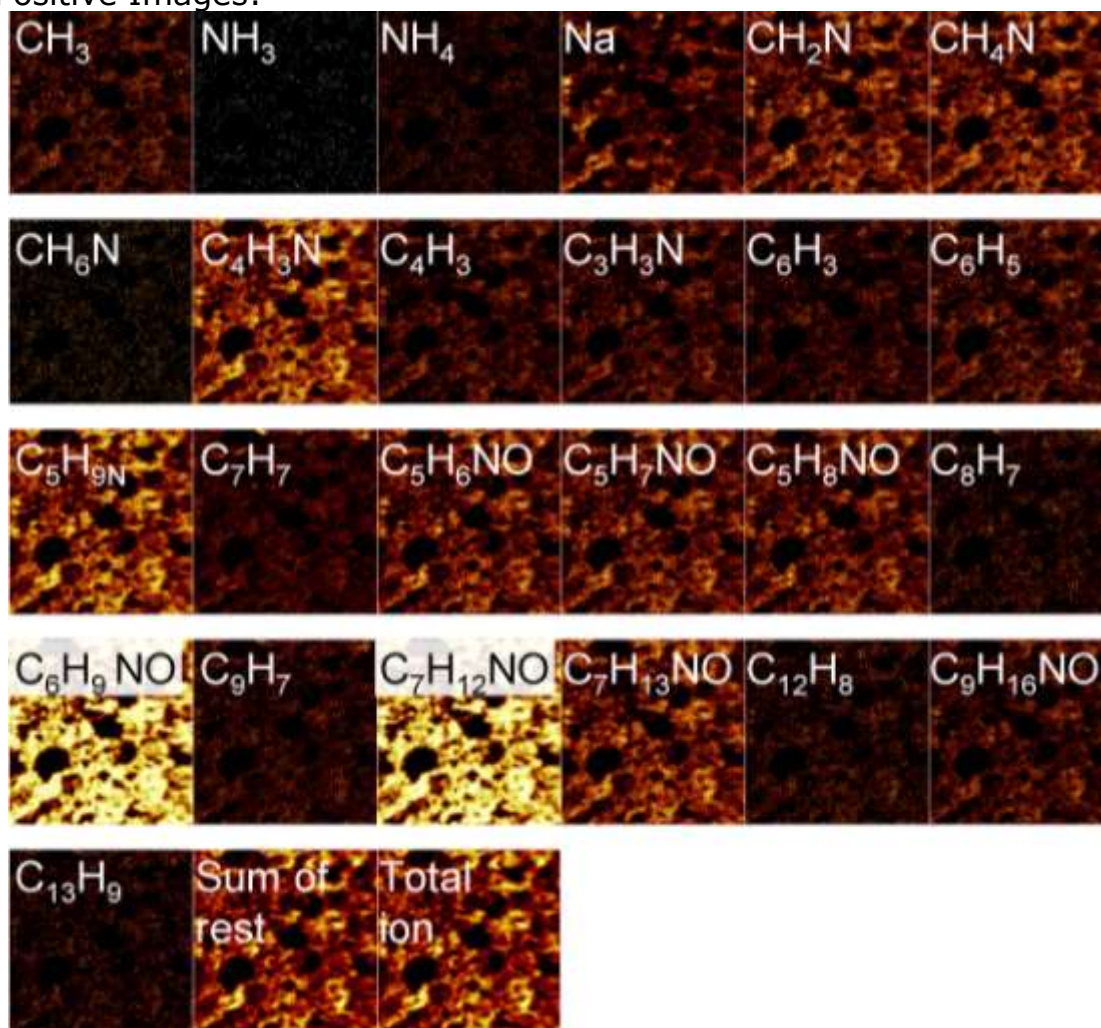


Figure 4.13 ToF-SIMS composite images and corresponding ion assignments for blank polyHIPE (LHS)
TOP: positive images. *BOTTOM:* negative images

Positive Images:



Negative Images:

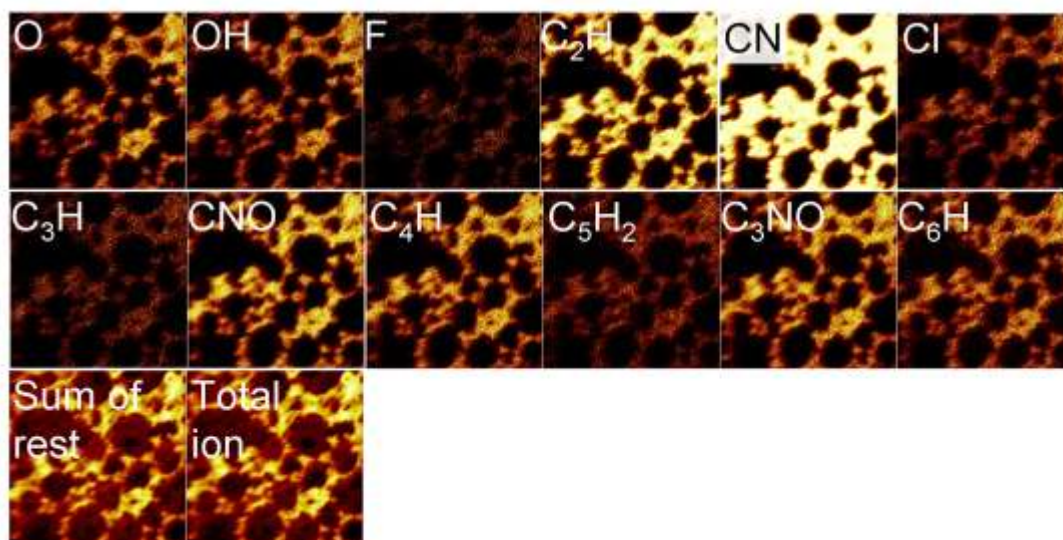
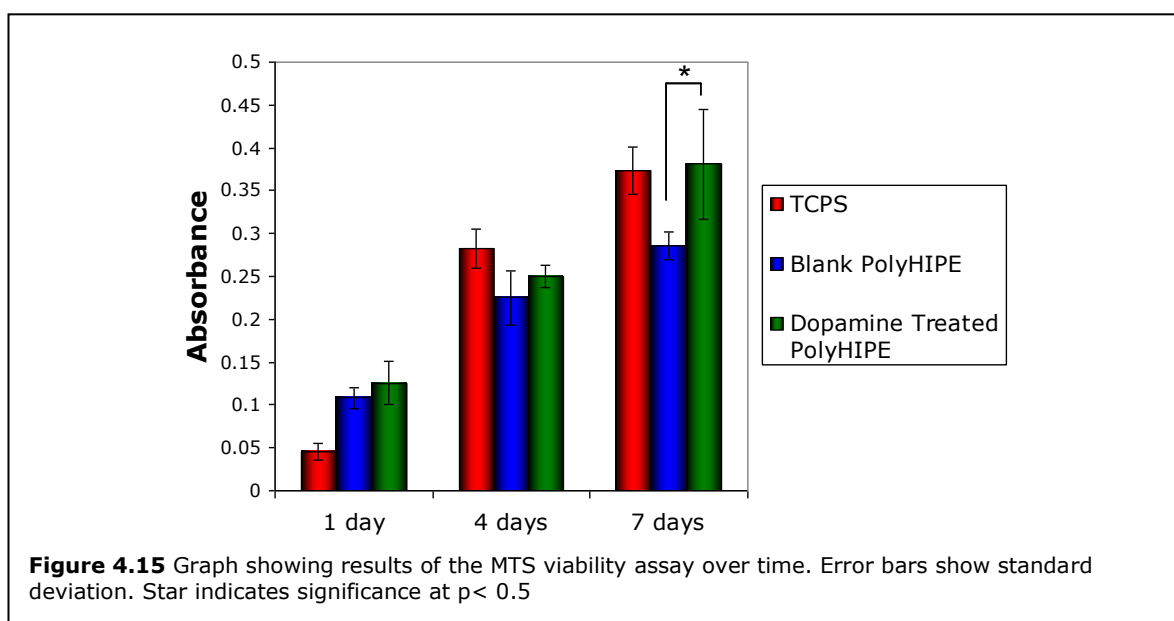


Figure 4.14 ToF-SIMS composite images and corresponding ion assignments for dopamine coated polyHIPE. *TOP*: positive images. *BOTTOM*: negative images

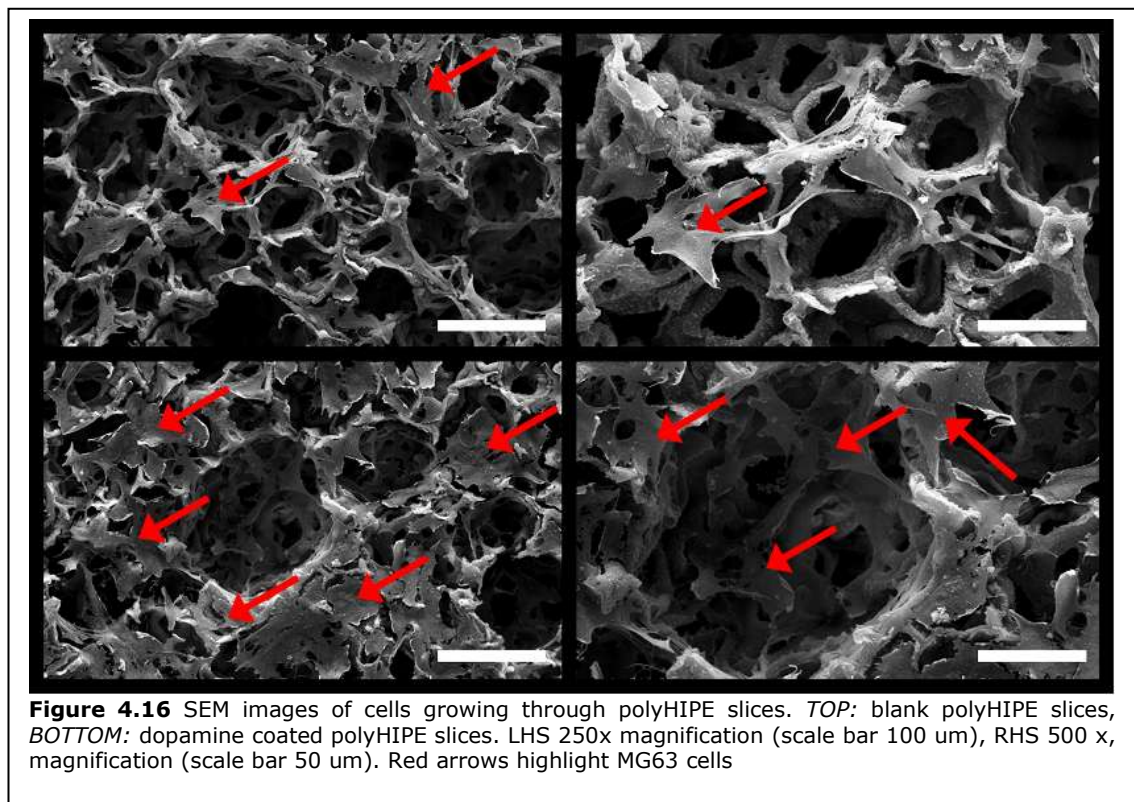
4.10 *In-Vitro* Cell Culture on Polydopamine Treated PolyHIPEs

We have shown that polyHIPE slices can be functionalised by polydopamine adsorption. Before any further functionalisation takes place, it is needed to establish whether the polydopamine is toxic to cells. It is known that dopamine is a neurotransmitter and any unreacted or non-permanently adsorbed dopamine could affect the viability of the cells. To investigate this, polyHIPE slices were prepared with the polydopamine coating and MG63 osteoblast-like cells were cultured on the prepared plates, alongside blank polyHIPE slices and flat TCPS pieces as a control to ensure the cells were growing as expected. A MTS assay was run at 1, 4 and 7 days to highlight any differences in cell viability between the blank slices and the polydopamine coated slices.



The results were non-parametric and with a normal distribution (as determined by 1 sample Kolmogorov-Smirnov (K-S) test) so significances were calculated using a one-way ANOVA calculation with a TuKey post-hoc analysis (SPSS). The results of the MTS assay are shown in figure 4.15, these show there are no significant differences at 1 or 4 days between cells growing on blank polyHIPE and

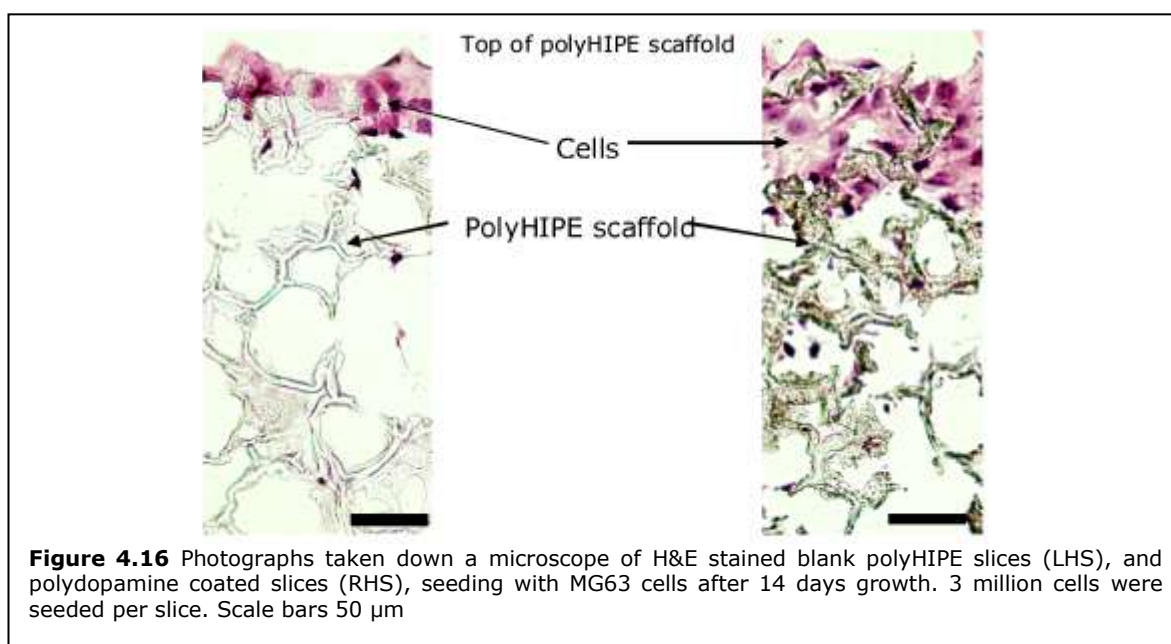
polydopamine coated polyHIPE. At 7 days the cells show a significant ($P < 0.5$) increase in viability. Cells were fixed at 7 day time point with 4 % PFA, dried using the critical point dryer and sputter coated with gold, and examined under SEM. 7 day SEM images are shown in figure 4.16, which show very little, if any, cell death. Cell death can be observed in osteoblasts with the observation of small, rounded cells. In this case the cells are flat and “star-shaped” and are seen spreading into the support (see red arrows in Figure 4.16). There visually appear to be more cells on the dopamine coated polyHIPE support, which is supported by the MTS data. This could be due to the increased “wettability” of the polydopamine coated material allowing the cells to spread more easily through the polyHIPE.



4.11 Histology

MG63 cells were grown on blank and polydopamine coated polyHIPE scaffolds for 14 days before preparation for staining. The slices of blank polyHIPE show the

cells mainly sitting on the surface of the polyHIPE, with not much ingress into the polymer slice, as shown in figure 4.16. The dopamine coated sample (RHS) shows the cells primarily on the surface, but showing more ingress than the blank polyHIPE slices. This backs up the MTS assay and the SEM images, in terms of there are more cells on the dopamine coated polyHIPE slice (and thus a greater viability reading). This difference is small, but in terms of coating affecting the viability of the cells, the coating does not appear to have a detrimental effect.



4.12 Conclusions

Several different methods were used to attach functional molecules to the surface of the polyHIPE. Direct attachment was successful, although with fairly low yields, and an inability to react the species further. A promising adlayer formed was the dopamine coating, and some steps were made to optimise the setup. However, even with the modifications, the dopamine does not seem to cover the surface in its entirety, and the base polymer, whether polyHIPE or bacteriological plate can be observed using characterisation techniques. The polydopamine coating,

however non-complete, provides a promising adlayer for the further attachment of molecules, as discussed in chapter 6, as it is not detrimental to cell viability.

4.13 References

¹ J.F. Brown, P. Krajnc, N.R. Cameron *Ind Eng Chem Res* (2005) **44**(23) 8565

² A. Mercier, H. Deleuze, O. Mondain-Monval *React Funct Polym* (2000) **46** 67

³ N.B. Colthup, L.H. Daly, S.E. Wiberley *Introduction to Infrared and Raman Spectroscopy 3rd Ed* Harcourt Brace Jovanovich (1990) 385

⁴ E.F. Mooney *Spectrochimica Acta* (1963) **19**(6) 877

⁵ H. Lee, S.M. Dellatore, W.M. Miller, P.B. Messersmith *Science* (2007) **318** 426

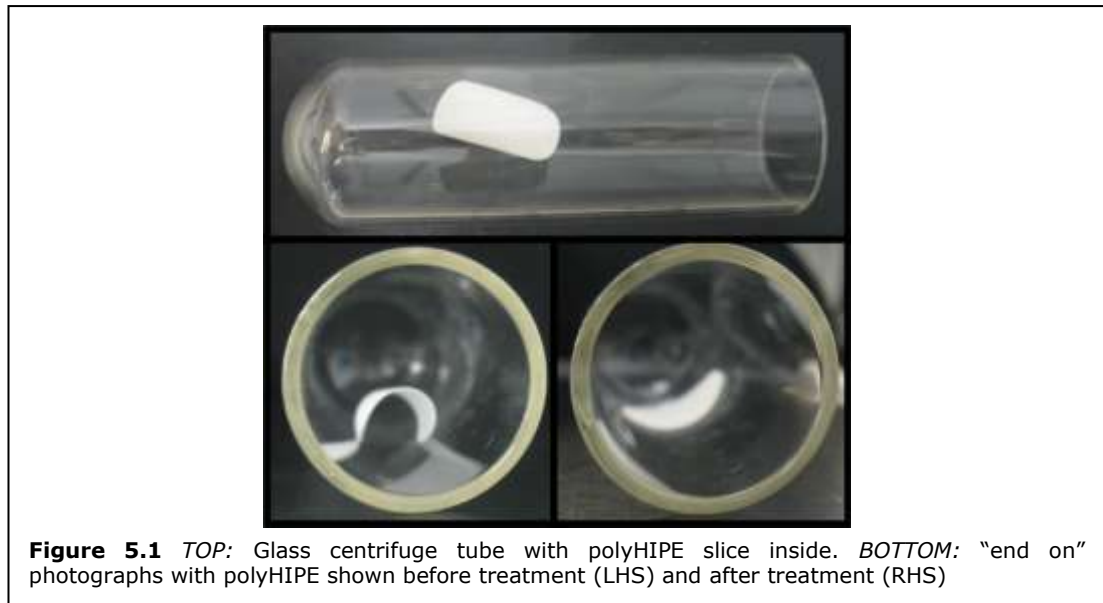
Chapter 5 - Plasma Treatment

5.1 Introduction

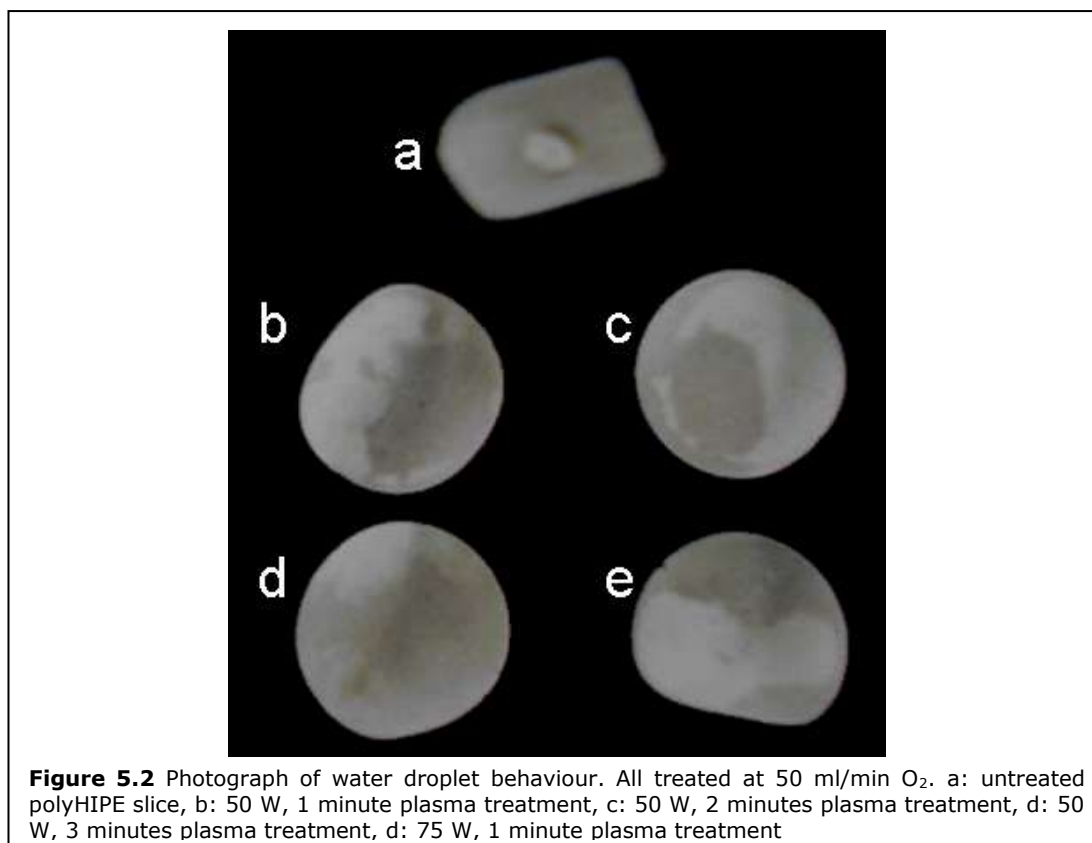
Plasma treatment is known to be used in the plastics industry for treating polystyrene plates for cell culture.^{1,2} Plasma treatment was therefore investigated to find a suitable process for plasma treating the polyHIPE slices. The projected outcomes should be two-fold. Firstly the plasma process should create oxygen containing groups on the surface of the polyHIPE slice which should promote cell viability, and secondly to create, and identify, the oxygen groups for further attachment of larger biologically active molecules.

5.2 Optimisation (machine)

Two machines were considered with which to plasma treat the polyHIPE slices. A batch (vacuum) process, as opposed to an atmospheric or flame gun treatment, was deemed to be suitable for a non-specialised laboratory environment, as the process was controlled and contained within a small area. The two machines that were considered were a PVA TePla Microwave Asher (300) and an Emitech Plasma Asher (K1050X). Initial trials were held with the K1050X during which the polyHIPE slices were plasma treated at a variety of power settings (between 50 - 75 W) for a variety of times (between 1 - 3 minutes). In order for the slices to remain in place when the system was under vacuum, they were treated in a glass centrifuge tube as shown in figure 5.1.



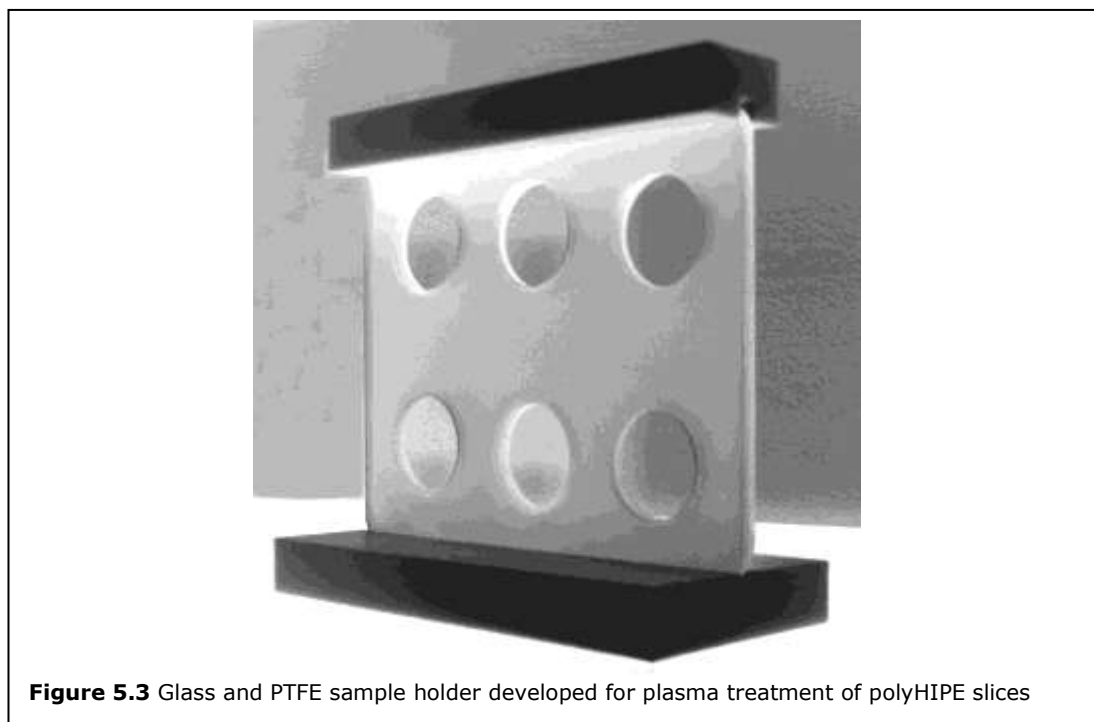
As can be seen in figure 5.1, only one slice could be treated at a time, and the conditions of the treatment, even when mild, caused the polyHIPE to change shape, and after treatment rest on the bottom of the glass tube. To assess qualitatively the effects of the treatment, droplets of water were used. When a droplet of water was placed on the top surface of an untreated polyHIPE disc, its hydrophobic nature ensured that the droplet remained on top and was not absorbed by the polyHIPE. After plasma treatment it was hoped that the polyHIPE would lose some of the hydrophobic character and therefore the droplet would change shape. The water droplet treatment was used to assess the success of the plasma treatment. The initial trial results are shown in figure 5.2 where 100 μm water was placed on the top of the polyHIPE slice, and a photograph taken within 1 minute of the droplet being placed.



The photos show a difference with the water flowing into the polyHIPE material after plasma treatment, as opposed to sitting on the surface as shown in the untreated material (a). The darker areas on the slices in figure 5.2 show the regions into which the water flowed within the treatment. This showed promising results, although was not an ideal treatment as the slices appeared still to have hydrophobic as well as hydrophilic areas, showing the treatment was not homogeneous.

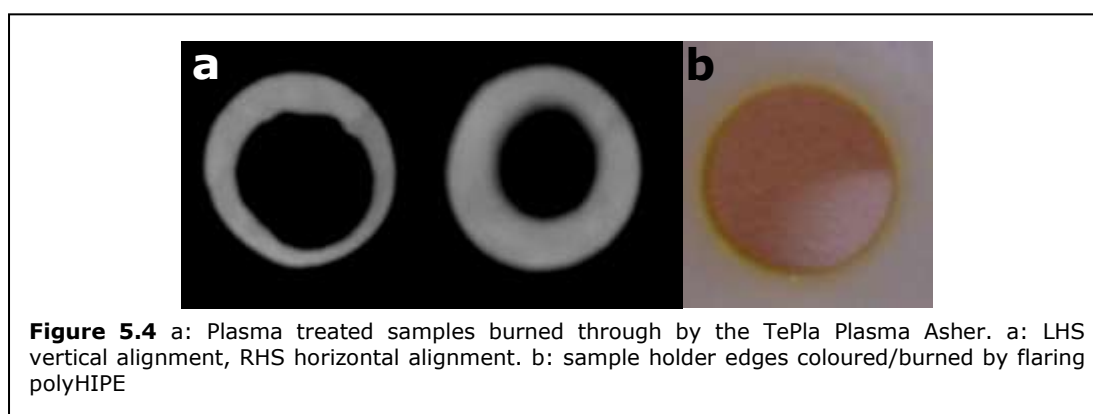
Trials were then held with the more powerful TePla Asher. The TePla is capable of up to 1000 W and a vacuum of at least an order of magnitude greater than that reached by the K1050X (6×10^{-1} mbar). The TePla plasma asher is primarily used for cleaning silicon wafers in the semiconductor industry and has capabilities far superior to the K1050X such as in-line temperature and pressure monitoring. In the initial trials, when the polyHIPE slices were placed into the chamber, even when

supported at the edges by thin glass cover slips, the polyHIPE slices were sucked into the vacuum pump. Various methods were tried to restrain the slices, with the eventual result of the creation of a sample holder. A photograph of this is shown in figure 5.3.



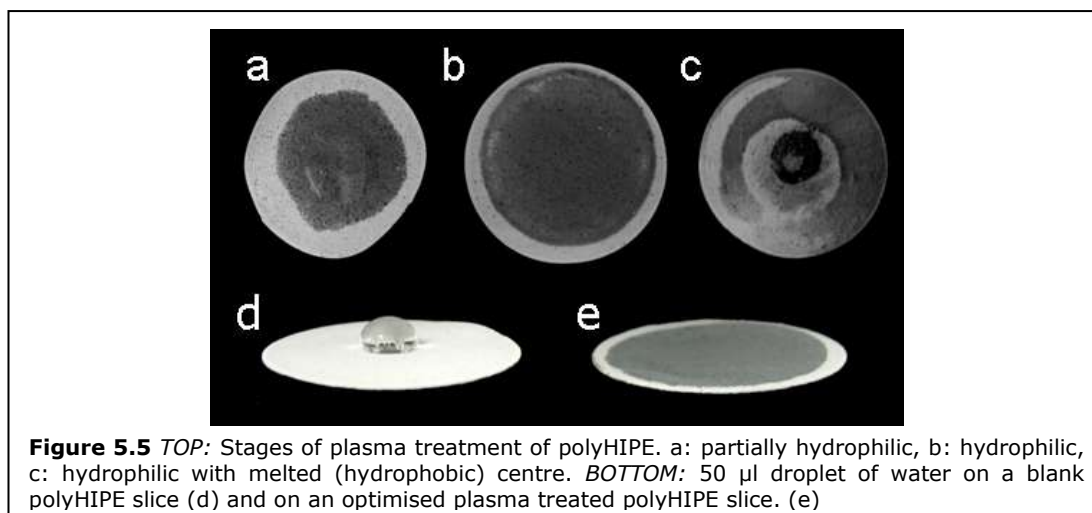
The sample holder was composed of two pieces of glass, with 6 holes 4 mm smaller in diameter than the smallest polyHIPE slice to be used, drilled through both glass plates. The glass was held together by two pieces of PTFE blocks with ridges cut out in the centre of the block, into which slid the two slices of glass when held together. The PTFE blocks were used at the top and the bottom of the glass plates, holding them together. The polyHIPEs sit between the two slices of glass and most of the polyHIPE would be exposed to the plasma, whilst the slices maintained their place during the pump down cycle and plasma treatment.

The holder was tried on the TePla machine. It was found that if the holder was positioned vertically in the plasma chamber, (60 s, 150 W, 250 ml/min O₂) the polyHIPEs flared and burned through on the plasma ignition. If the holder was placed horizontally, the samples still burned through, but to a slightly lesser degree. The results of the flaring using the new holder are shown in figure 5.4. Lower power settings and lower oxygen flows were tried, but settings lower than 150 W, 200 ml/min O₂ flow, the plasma failed to ignite.



The next step was to try the slice holder, developed for the more powerful TePla, to hold and align the polyHIPEs more favourably in the K1050X. In this case the PTFE edges were not used, and the polyHIPEs were sandwiched between the two glass plates and aligned horizontally across the K1050X sample holder. The weight of the glass was sufficient to hold the slices in place.

A set of variables were tried, changing the time (5 s - 30 min), power (5 - 25 W) and O₂ flow (0 - 30 ml/min). Some of the initial trials resulted in the partial creation of hydrophilic patches but also the melting of the polyHIPE slice centre as illustrated in 5.5. However, moderate conditions such as 10 W, 15 minutes and 30 ml/min O₂ flow demonstrated that the K1050X with the modified polyHIPE holder could create uniformly hydrophilic slices, as shown in figure 5.5 (b and e).



5.3 Optimisation (Parameters)

The surface characteristics of plasma treated surfaces change over time, and this is a documented phenomenon, often termed “hydrophobic recovery”.^{3,4} This result is seen, most often with oxygen plasmas, where the hydrophilicity of the surface, imparted by the plasma treatment, decreases over time. The conclusion of the papers is that this is probably due to reorganisation of the surface, with the higher energy groups changing orientating with respect to the polymer: air interface. To determine how long the polyHIPEs would retain their hydrophilicity after treatment by the K1050X, a selection of slices were prepared. The variables were; O₂ flow from 5 - 50 ml/min, time from 15 - 120 minutes and power from 5 W - 30 W. The “drop test” was again used as a qualitative guide to the hydrophilicity of the material. The results were categorised into three groups, a: where the water flowed into the material in less than 1 s, b: the water took 1 - 10 s to flow into the material, and c: the water remained on the top of the material after 10 s. 3 repeats of 6 slices were prepared for each O₂ flow, time point and power. These were observed over 6 months storage at room temperature and the results are shown in table 5.1.

Table 5.1 Hydrophobic recovery of the plasma treated polyHIPE slices assessed over time. Categories are defined as; a: where the water flowed into the material < 1 s, b: the water took 1 - 10 s to flow into the material, and c: the water remained on the top of the material > 10 s. Where the material visibly thinned, is denoted with an x in the "burn" column

10 W, 30 min

O ₂ Flow (ml/min)	burn	immediately	1 week	2 weeks	1 month	2 months	6 months
5		a	a	a	a	b	b
10		a	a	a	a	a	b
20		a	a	a	a	a	b
30		a	a	a	a	b	c
50	x	a	c	c	c	c	c

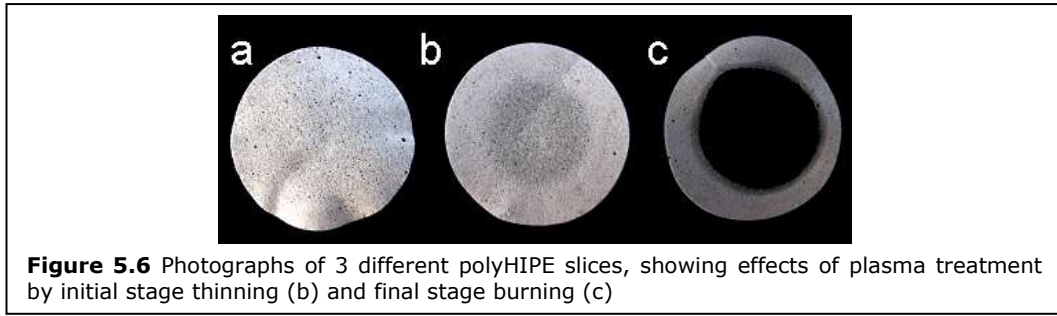
10 W, 30 ml/min O₂ flow

Minutes	burn	immediately	1 week	2 weeks	1 month	2 months	6 months
15		a	b	b	c	c	c
30		a	a	a	a	b	c
60		a	a	a	a	a	b
90	x	a	a	a	a	b	b
120	x	a	a	a	b	b	c

30min, 30 ml/min O₂ flow

Wattages	burn	immediately	1 week	2 weeks	1 month	2 months	6 months
15		a	c	c	c	c	c
30		a	a	b	b	c	c
60		a	a	a	a	b	b
90	x	a	a	a	a	b	b
120	x	a	a	a	a	a	a

Table 5.1 gives a good outline of the parameters that would treat the polyHIPE slices sufficiently for a hydrophilic nature to be imposed, and by choosing specific parameters, could keep the apparent hydrophilicity for enough time to grow cells or attach further molecules. An outcome of producing the tables was to look more closely at the thinning of the samples, denoted with an "x" in the "burn" column in table 5.6. This column was added to the table as it was observed at the higher level parameters the treatment produced visually thinned samples as shown as "b" in figure 5.6.



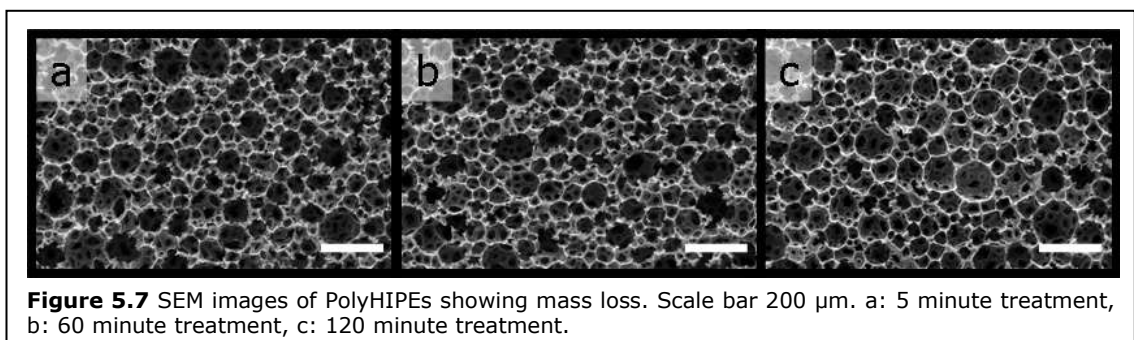
Sometimes this thinning or melting is very difficult to detect visually, either by the eye, or by SEM. The most reliable way to tell if the polyHIPE slice has thinned is by mass difference.

Three conditions were chosen: 5 W, 30 ml/min O₂ and 5, 60 and 120 minutes respectively. The mass of six slices was weighed before and after each treatment. The masses (of six slices) before and after treatments are shown in table 5.2.

Table 5.2 Table of mass loss of polyHIPE slices after different time points of plasma treatment at 5 W, 30 ml/min O₂.

Time of treatment	Mass before treatment (mg)	Mass after treatment (mg)	change (mg)	% change
5 min	64	63	1	3
60 min	64	50	14	22
120 min	64	46	18	28

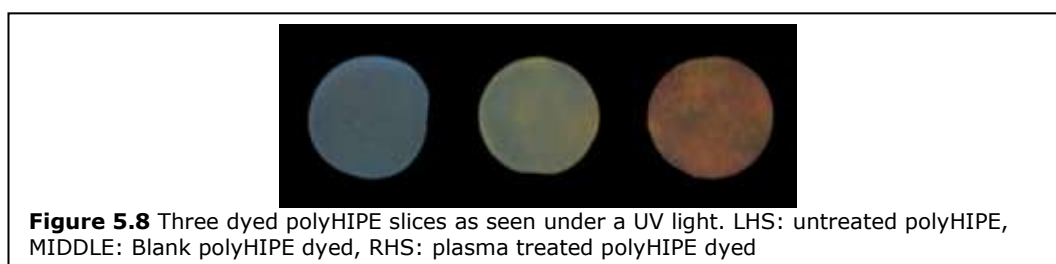
There was no significant mass loss at 5 min, but almost 30 % mass loss after 60 minutes. Each of the polyHIPE slices was also were imaged using SEM and the corresponding images are also shown in figure 5.7. The thinning of the slices can be visually observed, but the image analysis on SEM images reveals no significant change in void or interconnect diameters.



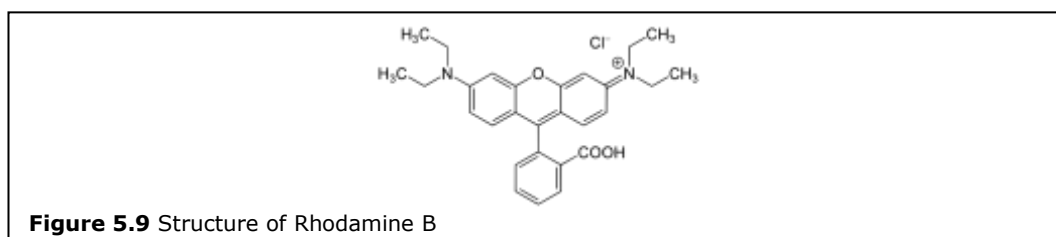
The images in figure 5.7 show that it is very hard to detect plasma burning by SEM alone.

5.4 Chemical Markers

Chemical markers were used to visualise the plasma treatment on the surface of the polyHIPE slices. Rhodamine B was dissolved in ethanol and both blank and plasma treated substrates were immersed in the solutions overnight. The slices were then thoroughly washed (5 x 20 ml EtOH washes), and examined under a standard TLC UV lamp, and a photograph taken. The results of this are shown in figure 5.8.



The blank polyHIPE fluoresces blue under the UV light and this can be seen on the LHS. The fluorescence is caused by the largely aromatic content of the polymer backbone. The middle picture is a blank polyHIPE that has been immersed in the dye. The rhodamine b has reacted with the carbonyl of the EHA, and a light yellow fluorescence can be seen. The RHS is the plasma treated polyHIPE slice after dying. This is much darker in colour, showing a greater number of reactive groups on the surface of the plasma treated slice. The structure of Rhodamine B is shown in Figure 5.9 below.



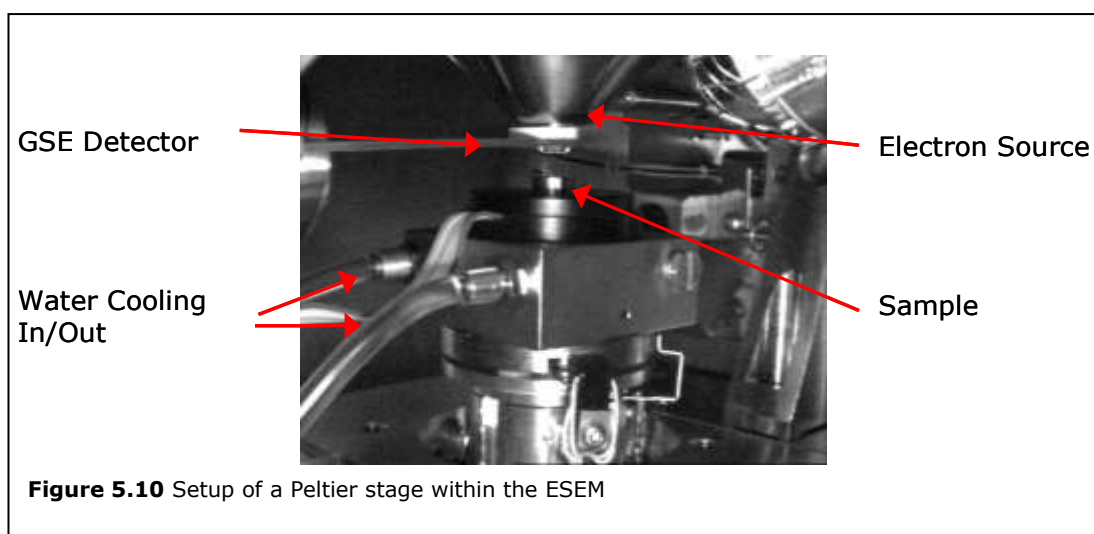
5.5 Contact Angles and Wet Mode SEM

A common method to examine the surface energy of a material is by observing advancing and receding contact angles. As polyHIPEs are a porous substrate, static contact angles cannot be taken with usual equipment (for example a goniometer). The behaviour of water on an untreated polyHIPE and a plasma treated polyHIPE is stark as demonstrated in figure 5.5. Whereas the water on the untreated polyHIPE beads up (d), on the oxygen-plasma treated polyHIPE slice, the water flows into the polyHIPE in less than 1 second (e). This test has been used to assess qualitatively the stability of the plasma treatment over time, as shown in table 5.1.

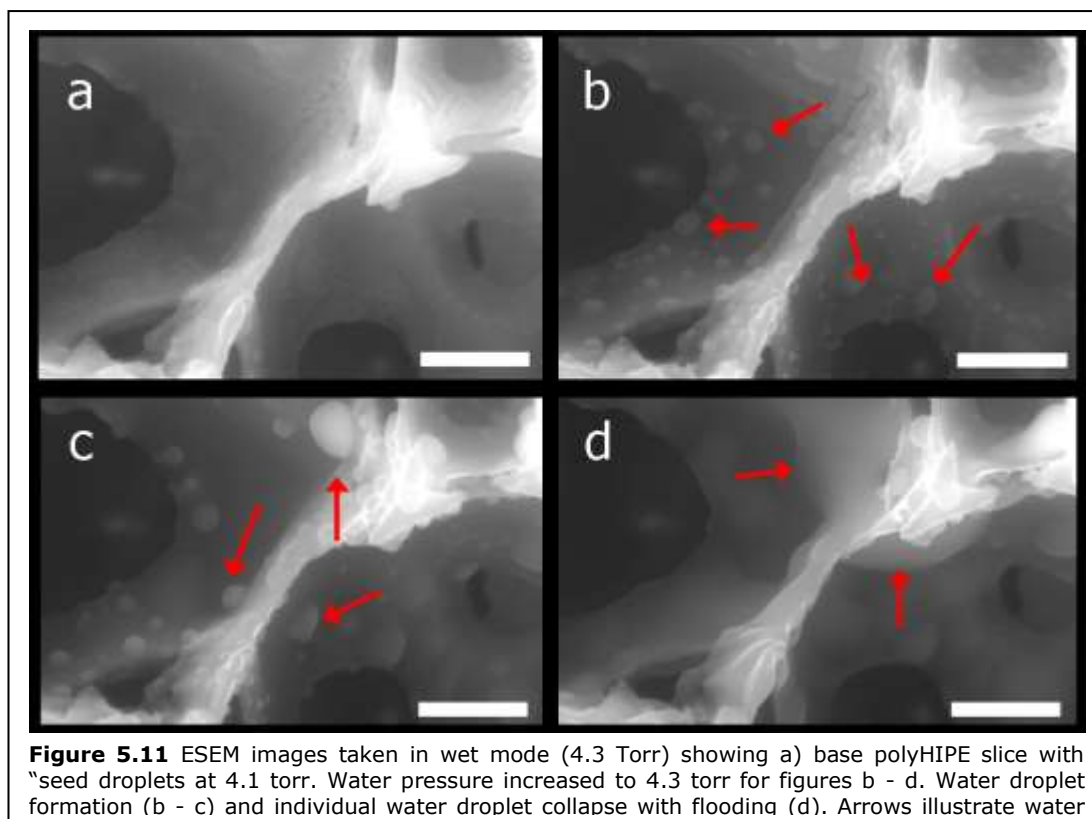
Contact angles cannot be measured accurately using traditional sessile drop methods on porous materials. However the difference in how the water drop sits on the surface of the polyHIPE before and after plasma treatment is so great, that it demonstrates that the surface has been modified in some way. In outlining the specifications for the plasma machine, samples were tried in different plasma machines at a range of rates and times, with the end results primarily being assessed by eye, looking at how a droplet of water (typically 50 -100 μ l) behaved on the surface of the slice.

To take this idea further, the ESEM was utilised in “wet-mode” to create very small droplets of water, observed at a high enough magnification that the internal surface of the polyHIPE creates a flat surface, and in principle advancing and receding angles can be measured by varying the moisture content in the ESEM chamber. In order to do this, very thin (< 30 μ m) polyHIPE slices were placed in a ESEM under “wet-mode” on a cooled Peltier stage, using either a GSED 500 or 1000 μ m

detector, and observed using the gas secondary electron (GSE) detection mode. The setup of the Peltier stage within the ESEM is shown in figure 5.10.



After a few unsuccessful attempts, a polyHIPE monolith was made with a high proportion of EHA that had a smaller pore distribution and a “flatter” internal surface (i.e. no STF) to test the setup and method. The successful method involved polyHIPE slices ($< 10 \text{ mm}^2$) held to the stage using a layer of silver paint. Carbon containing putty was also tried, but did not conduct sufficiently well to allow water droplets to form on the polyHIPE. The layer of silver paint was allowed to dry partially before the polyHIPE slices were attached. This prevented the silver paint from ingress into the polyHIPE itself and giving a false reading due to the paint coating the internal surfaces of the polyHIPE. The stage was cooled to $5 \text{ }^\circ\text{C}$. This was then left for an hour to chill the sample fully. The ESEM was then set to purge between 2 and 10 Torr for 10 cycles. When the preparation was complete the vapour pressure was brought up to 4 Torr and allowed to equilibrate for half an hour.

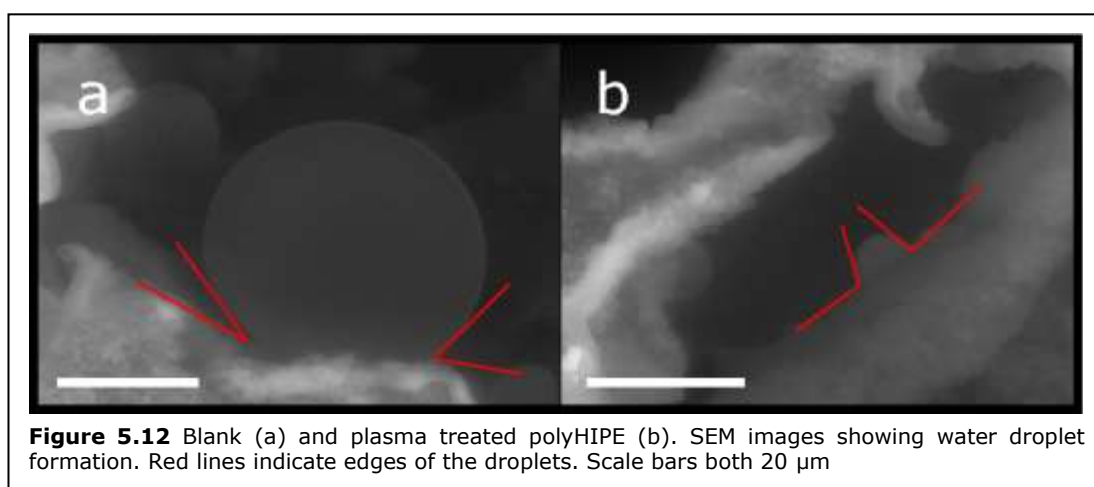


The water pressure was very slowly increased so that small water droplets formed on the surface of the polyHIPE. Several images were taken at each site of droplet formation to ensure that the features observed were water droplets (and growing/changing shape accordingly) as opposed to any surface features (STF). An example of this is shown in figure 5.11, with obvious water droplet formation (and subsequent collapse of the individual droplets).

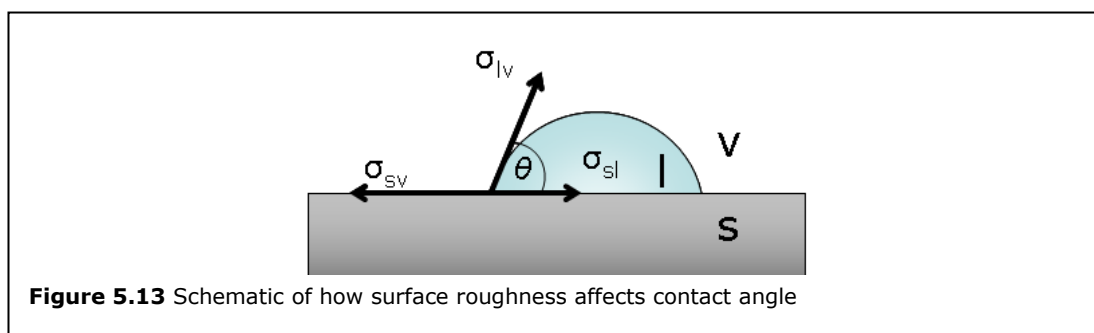
Upon trying to observe a receding contact angle, the image became unstable, with electron charging and a clear image was impossible to take. This was assumed to be surface damage of the polymer from the electron source. Images therefore were limited either to the advancing or receding contact angle at each area, with both readings being unable to be taken on the same area of polyHIPE.

With the "standard" polyHIPE (nP) the method was slightly adjusted with more time allowed to equilibrate at temperatures and between each step of increasing or decreasing the vapour pressure. Advancing contact angles were repeated both on

the untreated nP and the plasma treated nP slices, and the contact angle was taken of at least 10 droplets and was averaged. This gives a better indication of the actual contact angle of the surface, although as STF were present in some cases, the surface energy cannot be calculated as the readings were not taken on a fully flat surface. They do, however, give a comparison between the two surface types. An example of each surface type is shown in figure 5.12. The angles calculated were $122^{\circ} \pm 6$ and $76^{\circ} \pm 7$ respectively.



This is a less obvious change in contact angle than the stark contrast as shown in figure 5.5. This is due to the surface roughness, which affects the contact angle. This can be explained by the rearrangement of Young's equation (as illustrated in figure 5.13) and the subsequent addition of a factor " r " to show that the contact angle will be exaggerated upward, if over 90° , and downward, if under 90° , by surface roughness.⁵



This can be explained in terms of Young's equation $\gamma_{sv} = \gamma_{sl} + \gamma_{lv} \cos \theta$, the rearrangement of which rearrangement gives:

$$\cos \theta = \frac{(\gamma_{sv} - \gamma_{sl})}{\gamma_{lv}}$$

In the Wenzel equation, surface is ratio of true surface area to the geometric area, for a rough surface, both the solid-vapour and solid-liquid areas are increased by a "roughness" factor r , but the liquid-vapour remains unaffected. Wenzel proposed that the contact angle in the rough surface, θ^* , was:

$$\cos \theta^* = \frac{r(\gamma_{sv} - \gamma_{sl})}{\gamma_{lv}} = r \cos \theta$$

Therefore plotting a $\cos \theta$ curve, the angles are exaggerated, with the "turning", or exaggeration point being 90° .

5.6 X-ray Photoelectron Spectroscopy (XPS)

To obtain quantitative measurements of the hydrophilicity of the surface, XPS was run on polyHIPE slices after selected oxygen plasma treatments. To gain an understanding of the ageing process, settings were chosen (15 W, 30 ml/min O₂, 15 minutes) and the treated polyHIPEs were allowed to age for a set period of days at room temperature and pressure, before XPS analysis. These parameters were chosen with reference to the initial trials; with the parameters chosen, the slices were expected to lose most of their hydrophilicity after 1 week (category "c") and this therefore would give a indication of how much plasma treatment oxygen species were still on the surface of the polyHIPE. XPS analysis was undertaken on times after treatment every 7 days for 4 weeks, and labelled as 1 week, 2 weeks, 3

weeks and 4 weeks. The high resolution oxygen 1s scans, with the corresponding composition table are shown in figure 5.14 and tabulated in table 5.3.

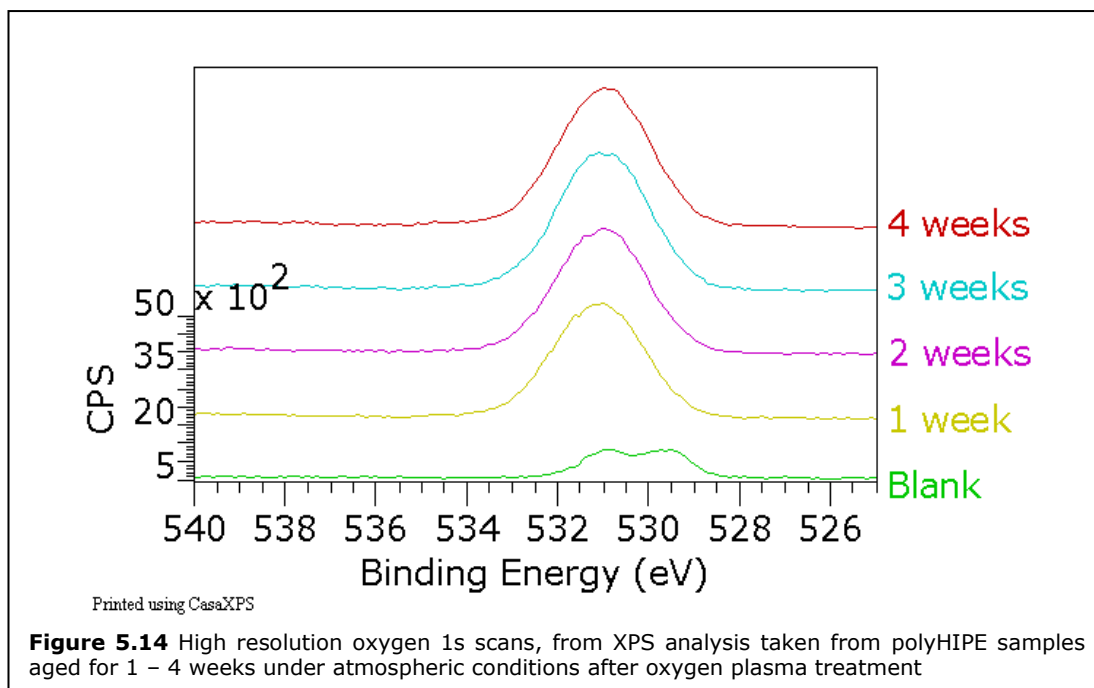


Table 5.3 Elemental compositions of the plasma treated polyHIPE over 4 weeks as analysed by XPS

	Blank polyHIPE	Plasma Treated polyHIPE (1 week)	Plasma Treated polyHIPE (2 weeks)	Plasma Treated polyHIPE (3 weeks)	Plasma Treated polyHIPE (4 weeks)
C 1s	94.7	79.9	80.0	79.7	79.7
O 1s	5.3	20.1	20.0	20.3	20.3

As the table shows, the oxygen content was not lost over the 4 weeks. The oxygen peaks all appear in the same eV range after treatment, and the relative oxygen amount does not decrease over the 4 weeks. This was unexpected, as it was presumed that the slices would lose the effects of the plasma treatment over this time. The slices were also tested with the “drop” test, and this time, all the slices were in group “a” - ie. the water immediately flowed into the material. Several different suggestions of why this happens would be due to the difference in season, and therefore the room temperature, or humidity. The samples were run on different machines - one on loan from the manufacturer, and one that was

purchased. The setup was identical and the physical settings also were the same. The difference therefore could be attributed to the variability of individual plasma ashers, but is still open to interpretation.

A second set of variables were tried, all analysed by XPS one week after treatment, to evaluate the effect of treatment time on the oxygen content and also on the thinning (mass loss upon treatment) of the slices. The parameters chosen were 5 W, 30 ml/min O₂ flow, and the treatment times varied from 5 to 60 minutes. The slices treated for 60 minutes were visibly thinned. The XPS results are shown in figure 5.15 and table 5.4.

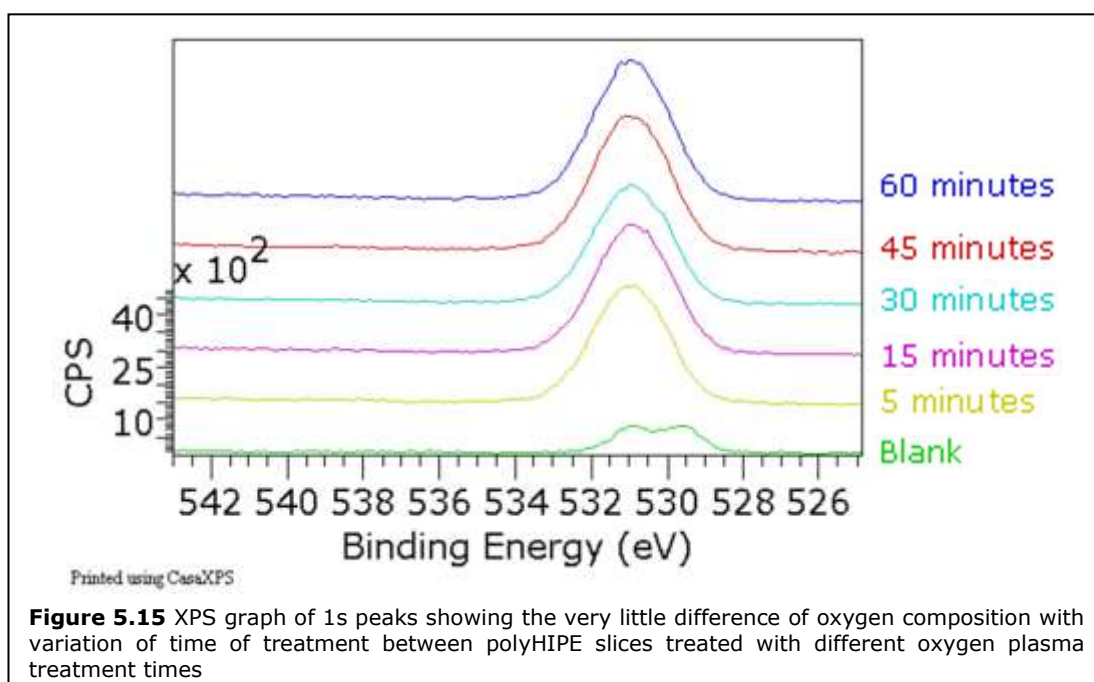


Figure 5.15 XPS graph of 1s peaks showing the very little difference of oxygen composition with variation of time of treatment between polyHIPE slices treated with different oxygen plasma treatment times

Table 5.4 XPS table of oxygen percentage composition of the surface of the polyHIPE variation with changing oxygen plasma treatment time

Atomic %	Blank polyHIPE	Plasma Treated polyHIPE (5 min.)	Plasma Treated polyHIPE (15 min.)	Plasma Treated polyHIPE (30 min.)	Plasma Treated polyHIPE (45 min.)	Plasma Treated polyHIPE (60 min.)
C 1s	94.7	79.2	78.4	78.0	78.5	78.4
O 1s	5.3	20.8	21.6	22.0	21.5	21.6

As figure 5.14 and table 5.14 show, there is very little variation in the values obtained from the XPS analysis between treatment times. The oxygen composition remains at approximately 20 % for all time points. The fact that even the visually thinned polyHIPE (60 minute treatment time) had approximately 20 % oxygen composition, and the oxygen peak occurs at the same binding energy, and interestingly suggesting that the type of oxygen groups formed are not affected by the polyHIPE “burning”. It also can be implied that ~ 20 % surface oxygen is the maximum obtainable for the polyHIPE slices, and that any higher incorporation burns/thins the slice. A suggestion from this set of results is that the oxygen incorporation is administered in the very first “burst” of the plasma ignition (in igniting, the wattage can increase up to 80 W in the first 5 seconds), whereas the longer time points (as shown for the initial results in table 5.4) leading to a higher stability over time could be due to an increase in crosslinking of the polyHIPE slice surface, and leading to less rearrangement at the surface over time. In chapter 3, low levels of unreacted vinylic groups were shown to exist from the DVB, and these could potentially be crosslinked by the low level plasma. Crosslinking is a well known result of plasma treatment.⁶

To investigate the effect on the oxygen content in terms of reaction to common solvents (eg. ethanol), freshly plasma treated polyHIPE slices were immersed in ethanol, allowed to air dry and then analysed by XPS. The results are shown in table 5.5.

Table 5.5 Table of XPS analysis of plasma treated slices before and after ethanol immersion, and the results of the drop test on each slice

	Blank polyHIPE	Plasma Treated polyHIPE	EtOH/Plasma Treated polyHIPE
C 1s	94.6	78.9	82.7
O 1s	5.4	20.8	16.2
other	0	0.3	1.1
a/b/c	c	a	c

As is shown in table 5.5, the oxygen content is decreased by the immersion in ethanol, but not to the same levels as the blank polyHIPE as the “drop test” measurements (a/b/c) would suggest.

To get a more specific picture of the reactivity of the plasma treated substrates, certain fluorine-containing molecules were selected to react solely with one type of oxygen containing group - and to determine the relative amounts of reactive carbonyl, hydroxyl and carboxylic acid surface groups. The protocol was followed directly from the literature⁷ with the only exception that in the literature carbonyl derivatisation took place with the addition of *N,N*-Di-*tert*-butylcarbodiimide, and this was not carried through as this would give a falsely high reading as it would react with the carboxyl groups also.

Two types of setup were used, “wet” and “dry”. The “wet” phase relates to the fact that the functional molecules (either in solution or liquid reactant) were in contact with the polyHIPE slices, and the “dry” phase relates to the setup with the polyHIPE suspended above the reaction mixture.

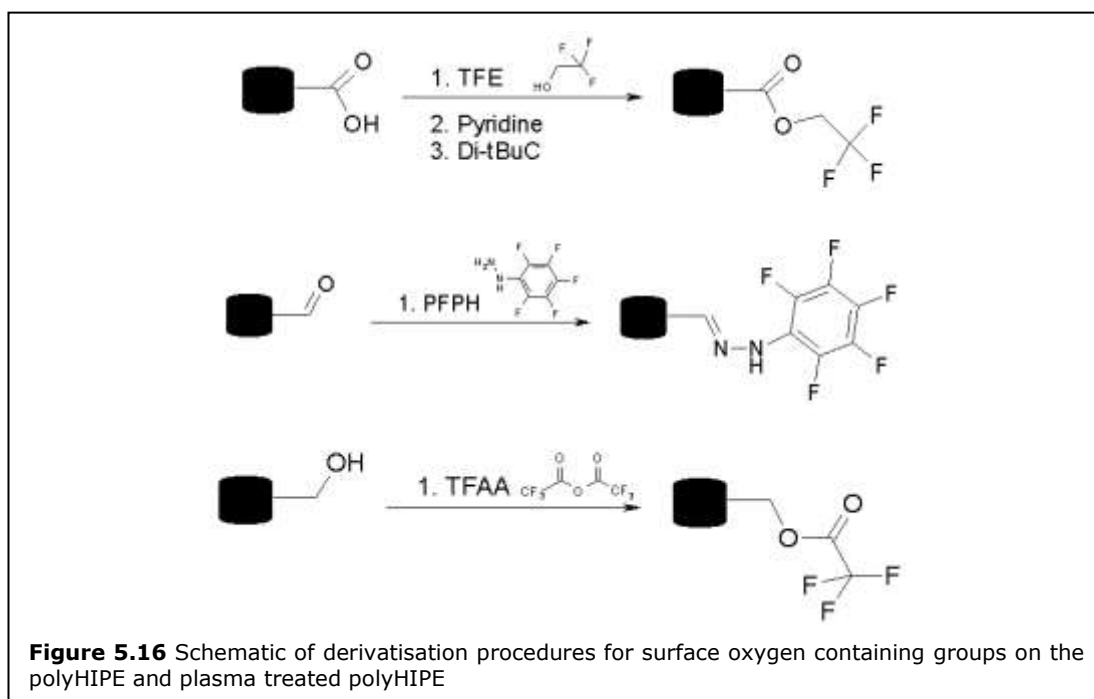
Briefly, the **carboxyl derivatisation** used Trifluoroethanol (TFE), pyridine and *N,N*-di-*tert*-butylcarbodiimide (Di-tBuC) injected down the side of a sealed container containing freshly plasma treated polyHIPE slices, each at 15 minute intervals. The reaction was left to proceed at ambient temperature for 18 hours. The differences

between the “wet” and “dry” procedures are: the “dry” reactants were injected under the suspended polyHIPE slices; and with the “wet” run, the TFE was dissolved in ethanol first, then the TFE/ethanol mixture was injected straight onto the polyHIPE slices, saturating them, with the further liquid reactants added after the set amount of time.

The **carbonyl derivatisation** briefly consisted of pentafluorophenyl hydrazine (PFPH) dissolved in ethanol (4 % by weight) and either placed under the freshly plasma treated suspended polyHIPE slices (dry) or in direct contact with the slices (wet). These were sealed and kept at a maintained temperature for 12 hours at 50 °C.

The **hydroxyl derivatisation** briefly consisted of trifluoroacetic anhydride (TFAA) injected into a sealed container, either in direct contact with the slices, or below the suspended slices. These both were left to proceed for 40 min at 35 °C.

A schematic of these procedures is shown in figure 5.16.



The polyHIPE slices were cleaned; the “wet” samples for the carbonyl and carboxyl functionalisation were washed with 3 x 20 ml ethanol then dried *in-vacuo*. The other samples were all (individually) cleaned by removing the samples from the sealed container and placed in an oven *in-vacuo* for at least 48 hours to remove any unattached reactant. The samples were then subjected to XPS within a week of being treated. Readings were taken twice for each sample and the results shown in table 5.6.

Table 5.6 Tables of tabulated XPS data showing the degree of attachment to plasma treated polyHIPE slices for each fluorine containing functional molecule

	position (eV)	Carboxyl Dry		Carbonyl Dry		Hydroxyl Dry	
		average	average	average	s.d.	average	s.d.
O 1s	530	13.7	8.9	8.9	0.94	17.7	0.99
C 1s	282	76.8	71.9	71.9	0.47	66.0	0.08
F 1s	685	5.6	11.5	11.5	0.33	10.7	0.46
other	-	3.8	7.6	7.6	1.08	5.6	0.44

	position (eV)	Carboxyl Wet		Carbonyl Wet		Hydroxyl Wet	
		average	s.d.	average	s.d.	average	s.d.
O 1s	530	13.5	0.04	9.3	0.66	12.7	0.52
C 1s	282	82.3	0.55	75.7	0.00	79.6	2.84
F 1s	685	1.9	0.08	9.3	0.28	3.2	2.37
other	-	2.3	0.60	5.7	0.94	4.6	0.99

This table shows there are carbonyl, carboxyl and hydroxyl oxygen species on the surface of the polyHIPE from oxygen plasma treatment. The table shows that all the derivatisation reactions caused a lowering of the amount of oxygen, particularly with the carbonyl derivatisation. With all the “dry” reactions there is a greater amount of fluorine observed, in comparison to the “wet” reactions.

The greatest amount of derivatisation took place with the hydroxyl groups, followed closely by carbonyl groups. Carboxyl groups are also present, but in a lower concentration. These are not quantitative measurements as this would have to take into account the any surface of the polyHIPE analysed and also the composition of the individual molecules., but this still provides a qualitative

comparison to the type of oxygen containing groups on the surface after plasma treatment.

Through personal anecdotal communication with Emily Smith at Nottingham University, it was established that TFAA can give a falsely high reading as it “buries” itself into the surface of the material, instead of reacting with the oxygen groups, and is not removed in-vacuo, either by the vacuum oven, or in the ultra-high vacuum of the XPS machine.

It was therefore decided to run these tests again, with a blank control, only using the “dry” conditions, but expanding the initial runs with an investigation of the effect of ethanol on the surface of the polyHIPE after oxygen plasma treatment, to see if the ethanol affected one particular oxygen containing group, or all equally. The freshly plasma treated polyHIPEs were immersed in ethanol and then allowed to air dry for 24 hours. The tabulated data from the secondary runs is shown in table 5.7.

Table 5.7 Tabulated XPS data after derivatisation reactions

Blank PolyHIPE

	position (eV)	Carboxyl		Carbonyl		Hydroxyl	
		average	s.d	average	s.d	average	s.d
O 1s	530	5.40	0.26	6.57	1.15	6.89	0.79
C 1s	282	94.43	0.43	92.82	1.61	91.64	0.84
F 1s	685	0.14	0.2	0.21	0.13	1.45	0.22
Other	-	0.0	-	0.4	-	0.0	-

Plasma Treated PolyHIPE

	position (eV)	Carboxyl		Carbonyl		Hydroxyl	
		average	s.d	average	s.d	average	s.d
O 1s	530	15.43	0.3	7.97	0.31	14.24	0.68
C 1s	282	73.52	0.42	69.59	0.06	78.86	1.72
F 1s	685	8.47	0.16	16.62	0.14	4.06	0.42
Other	-	2.6	-	5.8	-	2.8	-

Ethanol treated plasma treated polyHIPE

	position (eV)	Carboxyl		Carbonyl		Hydroxyl	
		average	s.d	average	s.d	average	s.d
O 1s	530	14.77	0.34	7.36	0.28	13.99	1.01
C 1s	282	76.32	1.17	73.94	0.41	80.41	1.39
F 1s	685	6.55	0.31	13.98	0.36	3.45	0.36
Other	-	2.4	-	4.7	-	2.2	-

The base polyHIPE contains 2-ethylhexyl acrylate (EHA), so the fluorine incorporation into the blank polyHIPE could be due to reaction with the surface EHA, as well as an indication of adsorption of the reactants. As such, there is a relatively low value of fluorine incorporation into the blank polyHIPE. The “final” amount of attachment at the surface was calculated from the fluorine content on each of the samples, minus the amount of fluorine incorporated into the blank polyHIPE slices to establish the amount of oxygen incorporation induced by the oxygen plasma treatment. The values are shown in table 5.8.

Table 5.8 XPS data showing the degree of attachment calculated from the amount of fluorine present from blank polyHIPE, for plasma treated and ethanol immersed plasma treated polyHIPE

Sample	Carboxyl	Carbonyl	Hydroxyl
Freshly treated Plasma	2.78	3.28	0.87
EtOH Treated Plasma	2.14	2.75	0.67

Table 5.8 shows that the amount of hydroxyl groups is much lower than the initial runs. This could either be due to the time taken to analyse the samples (8 weeks after treatment) due to technical problems, or a lower amount of hydroxyl groups present. In terms of deterioration, it could be due to the amount of “buried” fluorine components changing or being lost over time.

The data also shows that the amount of attachment is lower for the ethanol treated plasma treated polyHIPE, but the difference overall is lower with respect to all three oxygen containing groups on the polyHIPE surface, with no one group being “destroyed” by the ethanol. This gives weight to the theory that the ethanol plasticises the polyHIPE surface slightly, leading to a quicker rearrangement of the surface, with all the oxygen containing groups being “removed” from the surface reasonably equally.

5.7 Cell Culture

To see if the plasma treatment and subsequent oxygen group incorporation affects cell growth, MG63 osteoblastic cells were grown on polyHIPE slices. 1 million cells were seeded on each slice. The blank polyHIPE slices, were prepared by soaking in 70 % ethanol then placed into graded solutions into PBS buffer. This had the dual effect of sterilising the slices and “pre-wetting” the slice, so the cell seeding solution (aqueous) soaked into the slice instead of sitting on the top of the slice. With the plasma treated substrates the “pre-wetting” effect was not needed, but as the step had to be undertaken with the blank slices, two plasma slices were seeded as controls. Both a plasma slice soaked in ethanol and a dry slice, purely sterilised by UV radiation were used. These were labelled “wet plasma” for the soaked polyHIPE slice, and “dry plasma” for the UV sterilised slice. A MTS assay was run (3 technical repeats and 3 biological repeats) for each of the slices; blank, dry plasma, wet plasma, and a square of TCPS plastic from the bottom of a 6 well plate. The cells were grown and a MTS test was administered at 1, 4 and 7 days. The results are shown in figure 5.17.

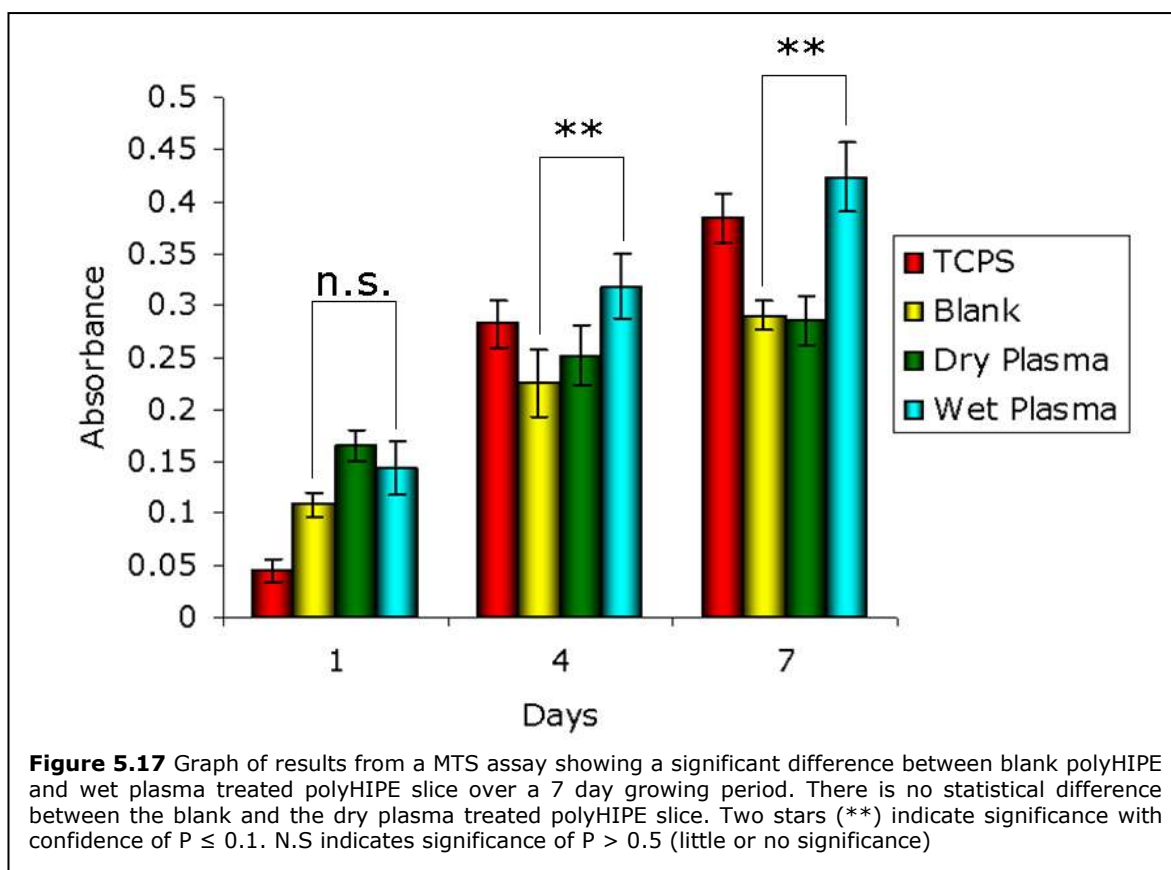


Figure 5.17 shows that the cells growing as expected on TCPS, with an increase of viability over the 7 days. The cells grown on the blank polyHIPE also grow as expected over the 7 days, and there is no significant difference between the viability of the cells grown on the blank polyHIPE and either of the plasma treated polyHIPEs at 1 day.

At 4 days and 7 days the cells grown on the wet plasma treated slices have a significantly ($P \leq 0.1$) greater viability than the blank substrates. This is validated by SEM images at 7 days shown in figure 5.18.

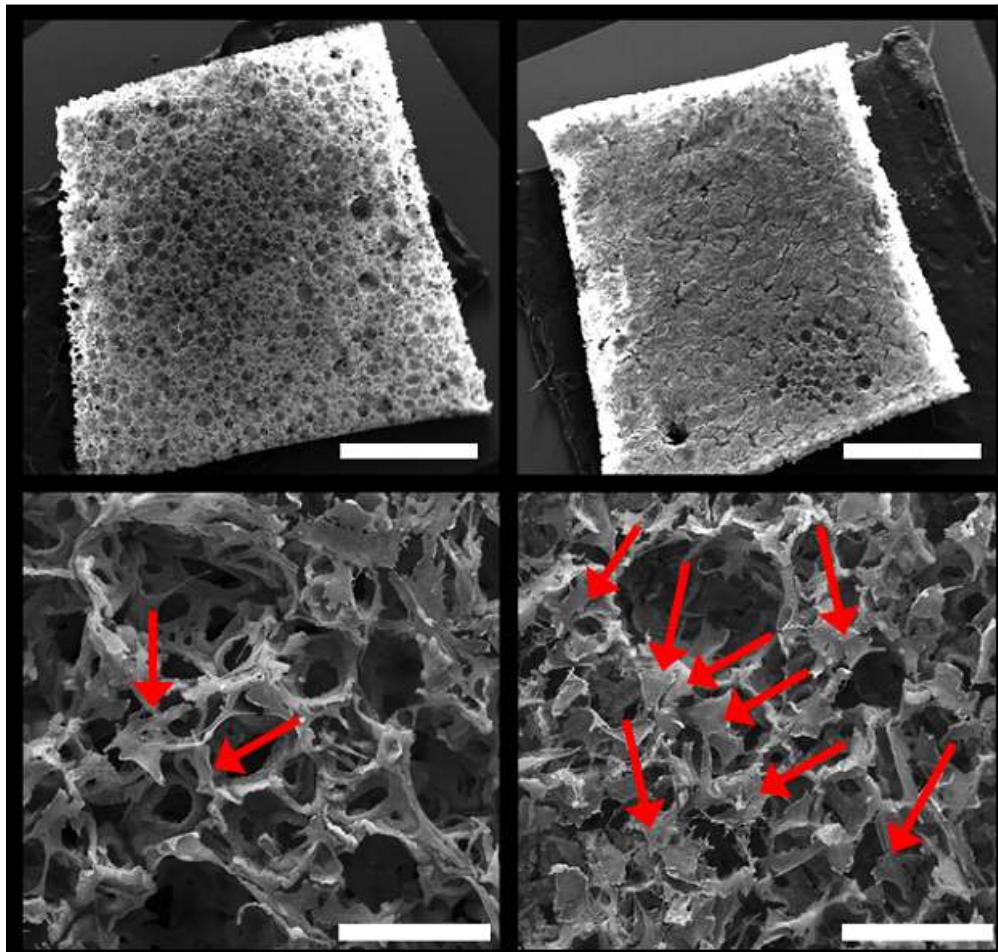


Figure 5.18 SEM images of 7 day time points showing increased cell coverage on the wet plasma treated polyHIPE slice (RHS) as compared to the blank polyHIPE (LHS). Top scale bar is 1 mm, lower scale bar is 100 μm . Red arrows indicate individual MG63 cells.

The MTS assay of the “dry plasma” shows an initial large increase in viability between 1 and 4 days, but then appears not to greatly increase between 4 and 7 days. It was observed that with the “dry plasma” samples, the aqueous media containing the seeding cell suspension was “pulled” into the polyHIPE slice, due to its high hydrophilicity. Upon osmium dioxide staining for SEM, it was observed that the cells had formed a column through the polyHIPE slice, but this high concentration of cells had not spread from the centre of the slice, although permeating all the way through. It was proposed therefore, for future experiments, to increase the amount of aqueous media when forming the cell suspension, in

order to fully saturate the polyHIPE slice with the cells. This is envisaged to give a more even, continuous coverage.

5.8 Comparison with Commercial TCPS

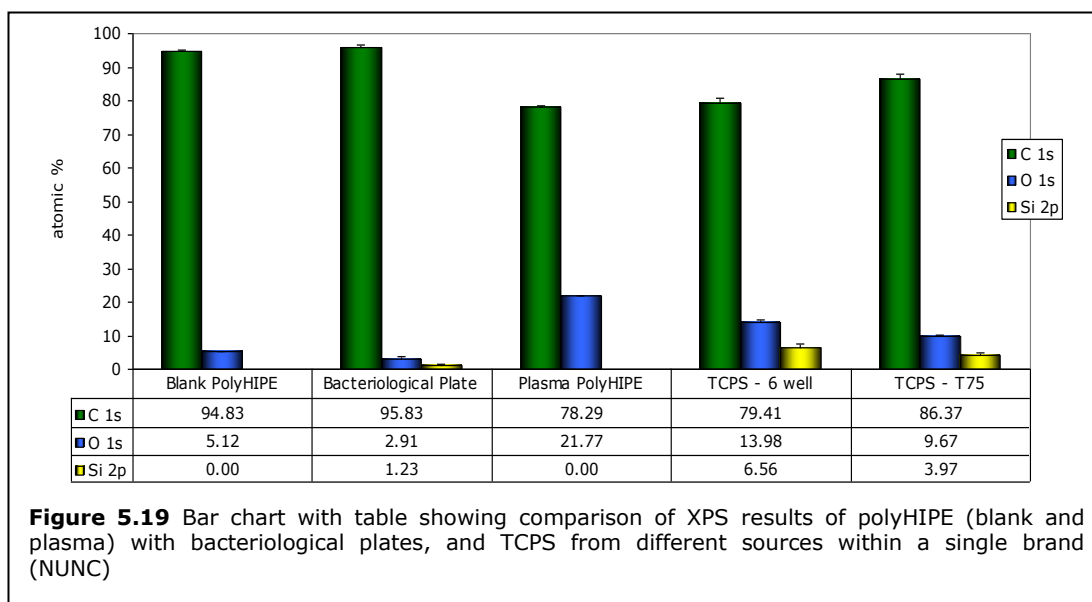


Figure 5.19 shows the results of polyHIPEs, both blank and plasma treated, run against commercial samples of plastics (predominantly polystyrene) used for cell and bacterial culture practices (BP/TCPS). These samples were interesting to indicate whether the plasma treated polyHIPE had similar surface characteristics to the commercial (flat) plastics. The results show that the blank polyHIPE and the bacteriological plate (BP) show similar composition, in terms of being predominantly carbon, with a low level of oxygen. The commercial sample (BP) shows low levels of silicon, which is increased in the tissue culture plastics. The presence of the silicon in the BP, increasing in the TCPS samples could be from two sources - either the presence of silicon in the base material, that migrates to the surface during plasma treatment, or, more likely, is a contaminant from silicon grease used in manufacturing equipment. The plasma treated polyHIPE shows a

greater amount of oxygen compared to the TCPS samples, with the oxygen content approximately double the TCPS T-75.

This shows that the plasma treated polyHIPE slices created in the laboratory are similar in terms of composition to the TCPS. The results also show that there is a great deal of variation between TCPS, even from the same manufacturer, and a greater standard deviation within the commercial samples show that the variation even within the same vessel is great.

5.9 Conclusions

PolyHIPE slices have been plasma treated successfully and a K1050X was purchased for use on polyHIPE slices. Initial problems have been solved by identification of appropriate parameters and holders within the chamber. The plasma treated surface has been defined, predominantly by XPS, and by reacting specific molecules to identify the surface groups. A method has been proven to identify conditions of the plasma machine which created unwanted effects such as thinning, or mass loss and to measure qualitatively the hydrophilicity of the materials by the drop test. Plasma treatment is a very promising treatment for the polyHIPE slices as not only does it provide a stable treatment to enhance cell viability, it also produces a defined surface that can be used for further attachment of biologically active molecules. With plasma treatment of polyHIPEs, what was once a very hydrophobic surface becomes hydrophilic, and also reduces the time spent on the “pre-wetting” ethanol step when undertaking cell culture. IT is anticipated that in the case of “wet” plasma vs “dry” plasma, the cells could be “pulled” into the structure, and grow over a wider area, throughout the polyHIPE, if the cell seeding suspension was more dilute - ie diluting the seeding suspension up to 500-1000 μ l before seeding.

5.10 References

- ¹ S.L. Barker, P.J. LaRocca *J Tiss Cult Meth* (1994) **16** 151
- ² C.F. Amstein, P.A. Hartman *J Clin Micro* (1975) **2** 46
- ³ A. Baszkin, M. Nishino, L.T. Minassian-Saraga *J Coll Int Sci* (1976) **54**(3) 317
- ⁴ F. Truica-Marasescu, S. Guimond, P. Jedrzejowski, M.R. Wertheimer *Nucl Instr Meth Phys Res B* (2005) **236** 117
- ⁵ R.N. Wenzel *J Phys Chem* (1949) **53**(9) 1466
- ⁶ M.J. Owen, P.J. Smith *J Ad Sci Tech* (1994) **8**(10) 1063
- ⁷ A. Chilkoti, B.D. Ratner, D. Briggs *Chem Mater* (1991) **3**(1) 51

Chapter 6 - Further Functionalisation

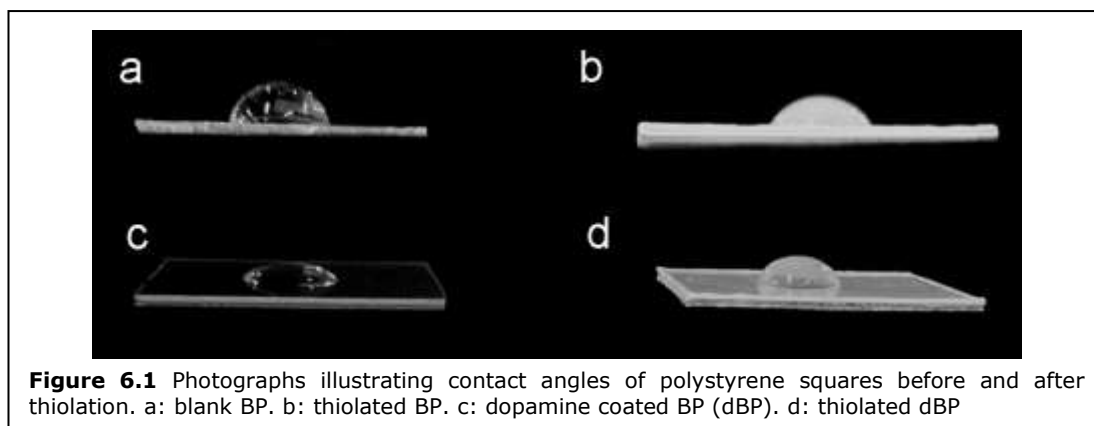
6.1 Introduction

This chapter investigates whether the surface treatments developed and described in the previous two chapters are able to react further, to form “smart” materials - materials that react in some way to their environment. Briefly, the aim of this chapter is to investigate whether the plasma or polydopamine treatment enabled the polyHIPEs to be further functionalised. Initially this was investigated through controlled reactions with simple, chemically distinct molecules with the functionalised substrates. When satisfied that the surface treatments can be functionalised, with defined molecules through defined reactions, smart molecules, in this case, synthetic retinoids, were synthesised to attach to the functional surface.

6.2 Thiol Attachment to Dopamine Treated Substrates

Literature states that the polydopamine layer is reactive to thiols.¹ Squares of bacterial culture plastic (BP) and blank polyHIPE slices were treated with the polydopamine as set out in chapter 3. Initial trials were run by reacting 1-dodecanethiol to the dopamine coated polyHIPE slices. The experiment was run overnight with dopamine coated substrates immersed in a solution of 1-dodecanethiol in DCM. As a control, untreated squares of BP were also immersed in a solution of the thiol. Contact angles were compared between the dopamine-coated BP (dBP) and the blank BP before and after thiolation (figure 6.1). The contact angle of the blank BP decreased after thiolation, from $52 \pm 2^\circ$ to $42 \pm 5^\circ$ (a

and b) whereas the contact angle of post-thiolation dBP increased from $22 \pm 2^\circ$ to $48 \pm 3^\circ$.



The increase in the contact angle of the BP to within a few degrees of each other suggested that the base BP either was equally as reactive as the dBP to the thiol, or the BP was affected by the solvent. The photographs in figure 6.1 clearly show a change in both the base samples after thiolation (turning from transparent to opaque). This would lead to the conclusion that contact angles are not the ideal method to use to identify change in BP slices, as the base material does not withstand physical change when using DCM. Alternative solvents were tried, including hexane, DMF, diethyl ether, but all caused the BP to become opaque or dissolve. Contact angles therefore between BP squares with any solvent apart from ethanol, IPA or water are not directly comparable.

The polyHIPE slices were analysed using XPS and the results are shown in figure 6.1.

Table 6.1 XPS analysis of dopamine coated polyHIPE substrate before and after thiolation

	Blank PolyHIPE	Dopamine coated PolyHIPE	Dopamine coated PolyHIPE post-thiolation
O 1s	4.98	18.11	11.58
N 1s	0.00	4.52	2.53
C 1s	95.02	77.37	85.31
S 2p	0.00	0.00	0.58

The XPS analysis shows a low percentage of sulfur after thiolation, with no sulfur present on the untreated surface. The oxygen and nitrogen components are reduced by the reaction, which suggests the DCM is partially removing the polydopamine coating. The reaction demonstrates that the polydopamine coating is receptive to a sulfur reaction but in low yields. Due to the very low yields of this reaction, the plasma treated polyHIPEs were not subjected to the same treatment.

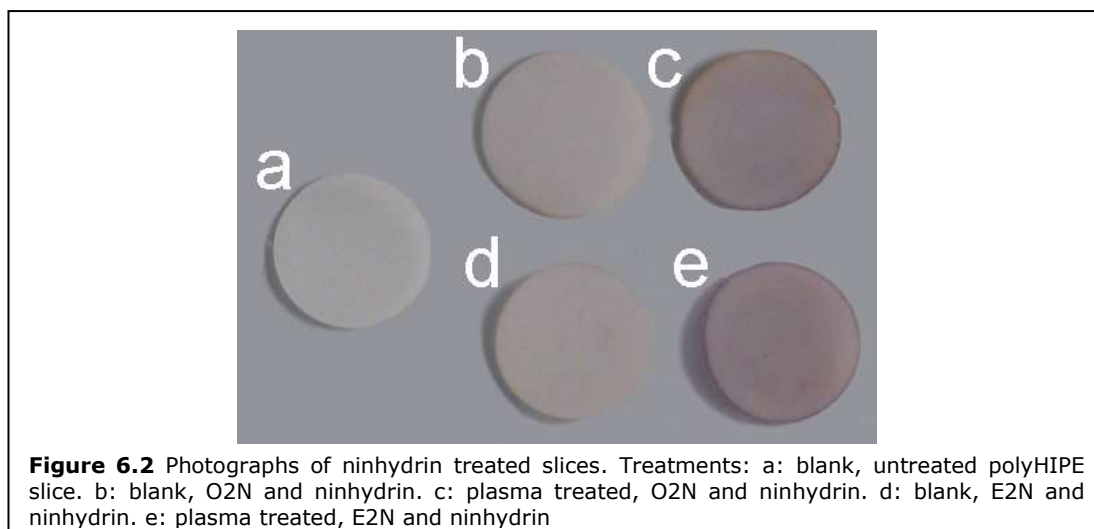
6.3 Diamine attachment

Diamines were proposed as potential di- reactive molecule. A molecule such as diamino-PEG could be used as a 'spacer' to decouple molecules from the surface, as well as providing resistance to non-specific protein adsorption.²

PolyHIPE slices were submerged in a solution containing either a large excess (1 mg/ml) of ethylenediamine (E2N) or 1,8-octanediamine (O2N) in ethanol. Both plasma treated polyHIPEs and dopamine coated polyHIPEs were treated in this way, alongside blank polyHIPE slices.

To observe visually if the diamine was attached, and the second NH₂ group was available for further reaction, the treated polyHIPE slices were subjected to a ninhydrin test. Ninhydrin reacts with amines and turns blue (from yellow).

Ninhydrin (1 mg/ml) was dissolved in ethanol, which was then added in excess to polyHIPE slices and left for 5 minutes. The slices in solution were then placed in a water bath at 60 °C for 15 minutes. All the substrates were then thoroughly washed in ethanol and allowed to air dry. The dopamine treated substrates were dark grey at the start of the test, and no colour change was able to be observed. Photographs of the results for the plasma treated samples are shown in figure 6.3.



As figure 6.2 shows the plasma treated substrates are reactive to the diamines, and the amine is available for further reactions. The central slices are blank polyHIPEs also treated with the corresponding diamine, then immersed in the ninhydrin solution. The slight colour change corresponds to a low level of attachment of the diamines onto the blank polyHIPE slices. The blank polyHIPE slices contain acrylate groups from the 2-ethylhexyl acrylate (as demonstrated in chapter 5) which react with the diamines, causing a slight colour change in the ninhydrin test.

Visually there was a slight difference between the O₂N coated substrates and the E₂N coated substrates and it was proposed that a greater colour difference could be observed if a greater surface area was in contact with the reagents and the ninhydrin. The tests were therefore also run on powdered polyHIPE. The powders were then subjected to plasma treatment followed by the ninhydrin test. The results of this are shown in figure 6.3.



Figure 6.3 Photographs of ninhydrin treated powders after reaction with octanediamine (RHS) and ethanediamine (MIDDLE), compared against untreated polyHIPE powder (LHS)

The powders were treated in a centrifuge tube in the plasma asher at 5 W for 30 minutes in order to obtain visual hydrophilicity with the previously explained (chapter 3) “drop test”. Variation of powder colour within each of the samples is probably due to the fact that the plasma process had not been optimised for powder. Both types of amine attachment cause a blue colour to occur even after extensive washing. From visual observation of the colour difference, it can be suggested that there is a greater amount of diamine attachment on the O2N treated substrate than the E2N treated substrate.

As there was clearly a blue colour seen on the slices and the powders, XPS was used to quantify the diamine attachment, both on the plasma treated and dopamine treated slices. The results are shown in Table 6.2.

Table 6.2 Averaged surface components after diamine attachment taken from XPS analysis

Substrate	Treatment	C %	O %	N %	other* %
Blank	ethanediamine	94.54	5.46	0.00	0.00
	<i>change</i>	- 0.06	0.01	0.00	
Blank	octanediamine	93.75	5.69	0.40	0.16
	<i>change</i>	- 0.85	0.24	0.40	
Dopamine	ethanediamine	77.69	13.32	7.88	1.11
	<i>change</i>	0.69	- 5.79	3.99	
Dopamine	octanediamine	79.93	11.60	6.56	1.91
	<i>change</i>	2.94	- 7.51	2.67	
Plasma	ethanediamine	82.44	13.44	2.91	1.21
	<i>change</i>	3.49	- 7.31	2.91	
Plasma	octanediamine	84.22	10.42	4.67	0.69
	<i>change</i>	5.27	- 10.33	4.67	

* impurities: Cl, Zn, Fe, S, Si

As table 6.2 shows, there is very little residual adsorption onto the blank polyHIPE slices, but there is an increase of nitrogen - signifying diamine attachment onto both the dopamine (+3.99/+2.67) and plasma (+2.91/+4.67) treated surfaces with both (ethyl/octyl) treated surfaces. Change from the previously quoted XPS values for the treated substrates is quoted below the XPS data. The plasma treated surfaces show a greater attachment of nitrogen for the octanediamine slices, as predicted with the ninhydrin test above.

6.4 Fluorine Attachment

As the dopamine surface contains nitrogen and has been shown not to be a uniform coating, an alternative attachment was proposed using a fluorinated molecule, which gives a chemically distinct group that can be detected by XPS ensuring minimal error associated with any non-uniformity of the polydopamine surface. Two molecules were used for attachment, both trifluoro containing species with a short attachment linker ((CH₂)₂). To examine the reactivity of the surface, both a thiol and an amine linker were used (2,2,2-trifluoroethanethiol (FES) and 2,2,2-trifluoroethylamine (FEN)). Slices were treated with plasma or dopamine treatment and immersed in a solution of FES or FEN in DMF. Blank slices were also run at the same time. The results, as a table from analysis of the XPS scans, are shown in table 6.3 and graphically represented in figure 6.4.

Table 6.3 Table of XPS assigned percentages from plasma treatment and polydopamine treatment reaction with fluorine containing thiols and amines

Substrate	Treatment	C %	O %	N %	F %	S %	other* %
Blank	FES	94.56	5.45	0.00	0.00	0.00	0.00
	change	-0.04	0.00	0.00	0.00	0.00	
Blank	FEN	95.03	4.98	0.00	0.00	0.00	0.00
	change	0.43	-0.48	0.00	0.00	0.00	
Dopamine	FES	80.55	11.96	3.46	2.60	0.85	0.60
	change	3.55	-7.16	-0.44	2.60	0.85	
Dopamine	FEN	80.53	13.62	4.06	1.05	0.00	0.75
	change	3.53	-5.50	0.17	1.05	0.00	
Plasma	FES	84.51	13.17	0.00	0.99	0.48	0.86
	change	5.56	-7.59	0.00	0.99	0.48	
Plasma	FEN	83.97	12.54	1.05	2.19	0.00	0.27
	change	5.02	-8.22	1.05	2.19	0.00	

*impurities: Cl, Zn, Fe, Si

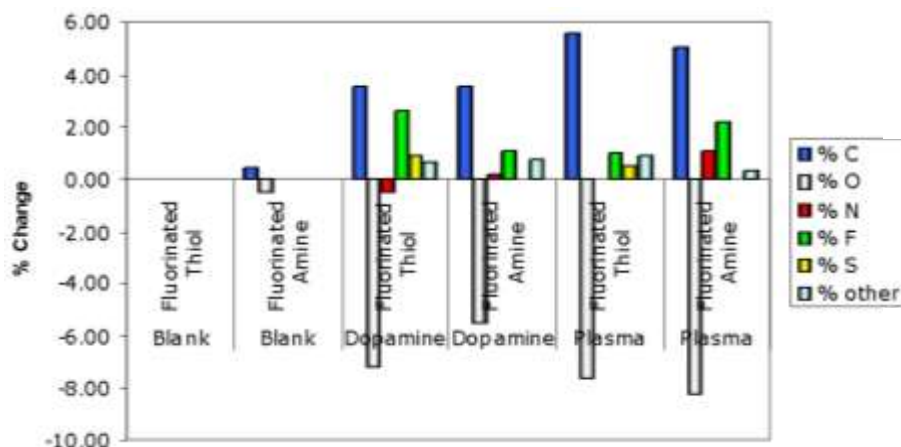


Figure 6.4 Percentage change of each component after fluorination for each of the three types of substrate and two types of treatment before and after reaction with fluorine containing molecules

As table 6.3 shows there is a small amount of attachment of both FES and FEN onto both the plasma treated and the dopamine treated surfaces. The greatest amount of fluorine (2.6 %) is seen on the FES treated dopamine substrate, followed by FEN (2.2 %) on the plasma treated surface. In all cases, for the dopamine and the plasma treated surfaces, the percentage of oxygen significantly decreased.

This analysis shows us that neither the amine nor the thiol react to any great extent with the surface of the blank polyHIPE (as shown in chapter 3). There is a little

amount of incorporation of the amine and the thiol in both the plasma treated and the dopamine treated substrates, but this is still at very low levels, generally below 3 % levels of fluorine. The oxygen composition of the substrates also appears to have been very much depleted by the treatment. This could be attributed to the solvent effects, which will be examined in the next section.

6.5 Solvent Effects

The DMF has been shown above to affect the composition of BP (non crosslinked polystyrene) by turning it opaque. As the polyHIPE slices were already opaque, and it is difficult to observe any change due to DMF, it was suggested that if the DMF used for the attachment was altering the surface of the polyHIPE in some way, it would cause loss, or rearrangement of the surface, so less oxygen was present for attachment of reactive molecules. The “drop test” was used to observe visually the change of the surface of the polyHIPE after plasma treatment to demonstrate the effect of DMF on the surface.

The regaining of a hydrophobic nature was particularly evident in the plasma treated substrates, where a simple immersion of the hydrophilic slice into a bath of DMF and subsequent removal and drying, rendered the slice hydrophobic. To take this solvent effect into account also with the previous reactions with the diamines in ethanol, plasma treated slices that had been immersed in ethanol or DMF for 15 minutes then dried were analysed by XPS. The results of this are shown in table 6.4.

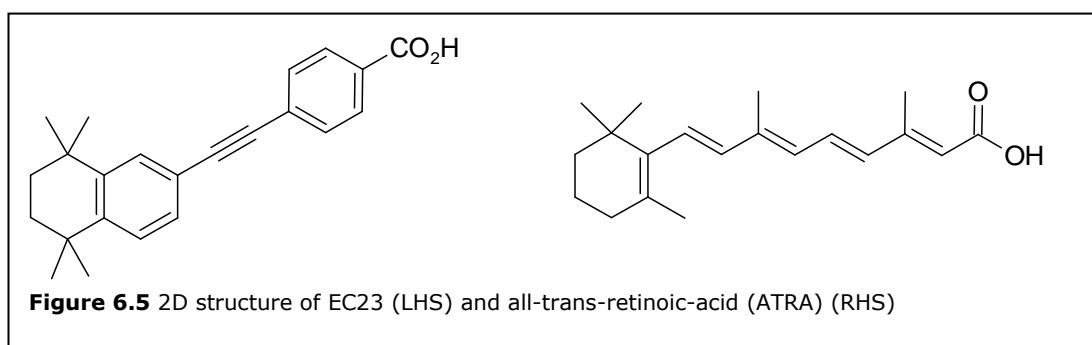
Table 6.4 XPS analysis of solvent effects of DMF on plasma treated polyHIPE slices. (ethanol in chapter 5)

Atomic %	Blank polyHIPE	Plasma Treated polyHIPE	EtOH/Plasma Treated polyHIPE	DMF/Plasma Treated polyHIPE
C 1s	94.6	78.9	82.7	85.4
O 1s	5.4	20.8	16.2	12.9
other	0.0	0.3	1.1	1.7

The table shows that the solvents have a great effect on the plasma treated polyHIPE surface. The slices that had been immersed in DMF had an increase in the percentage of carbon by 6.5 % and a decrease in oxygen of 7.9 %, with the ethanol immersed slice, the results were less stark, with the increase of carbon at 3.8 % and the decrease in oxygen at 4.6 %. This could account for the low attachment of the fluorine-containing molecules. However, with the larger biologically active molecules discussed next, vapour phase reaction was not feasible. A class of molecules which illicit a response in mammalian cells at very low concentrations was chosen, and these are discussed in the next section.

6.6 Introduction to Retinoids

Retinoids are a class of biologically active molecules. Synthetic retinoids, such as EC23, have a great advantage over natural retinoids due to their stability to factors such as heat and UV light. Very low concentrations of EC23 have been shown to illicit a change in cell morphology similar to the change seen with all-trans-retinoic acid (ATRA).³ The structures of EC23 and ATRA are shown in figure 6.5.



The stability of the molecule, combined with the very low concentrations needed to illicit a response, provide an ideal molecule to test the attachment of small molecules to the polyHIPE surface. Stem cell lines have previously been grown on polyHIPE slices, and treated with EC23 in solution resulting in changed morphology and exhibiting specific markers indicating neural phenotypes.⁴

EC23 binds to the nuclear receptors, namely the retinoic acid receptors (RAR/RXR), and therefore any static surface modification would not be suitable. In order to provoke a response, the EC23 needs to be free in solution in order for it to be passively transported across the cell membrane and into the nucleus. Much work has previously been done with EC23 and other synthetic molecules demonstrating structure - receptor relationships, and very small changes in the structure of EC23, such as a change in the position of the carboxylic acid group, from *para* to *meta* position changes the effect of the molecule on *in-vitro* cell culture, changing the observed phenotype.⁵ Therefore to illicit a ATRA-like response, the molecule in solution must have a clearly defined structure. Taking these factors into consideration, a easily hydrolysable thioester based linker was proposed, attached covalently at one end to the plasma-treated polyHIPE, with the EC23 attached forming a thioester linkage, which, when exposed to the aqueous cell culture solution, would reform the carboxylic acid of the EC23 and release the reformed EC23 into the cell culture solution.

6.7 Adsorption of EC23 onto polyHIPE slices.

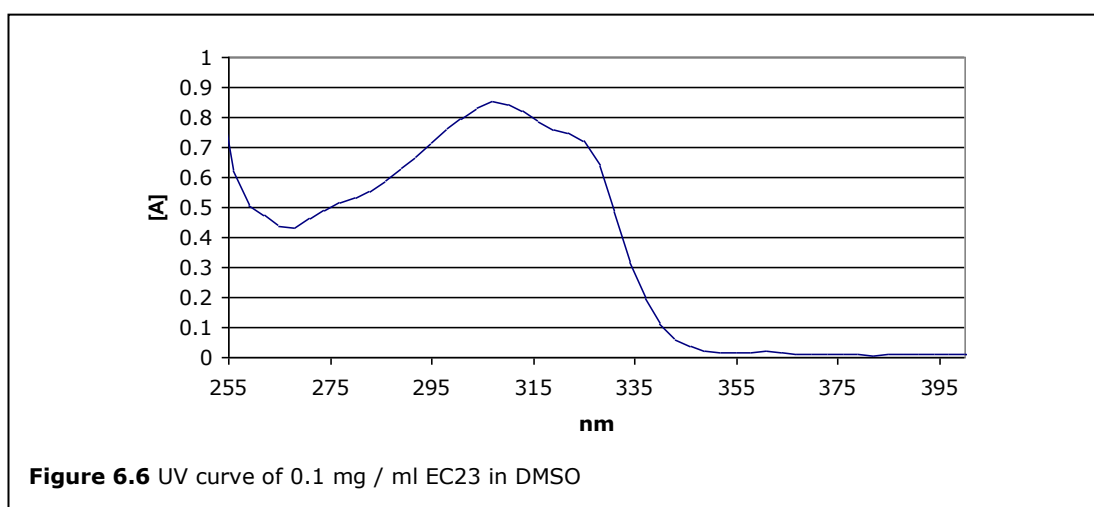
Due to the fluorescence of the EC23 when exposed to UV, it was proposed that attachment of EC23 to a surface could be observed visually under a standard UV lamp. To evaluate this option, EC23 was adsorbed onto plasma treated polyHIPE (10W, 15mins, 30ml/min) by immersing the slices in 1 ml of 1 mg/ml EC23 in THF

solution, for 30 minutes. The slices were then taken out and allowed to dry at room temperature over 2 hours. The EC23 treated slices, alongside blank and plasma treated slices, were photographed under a standard UV lamp to observe any adsorption. There was very little observed difference between the slices, due to the fluorescence of the blank polyHIPE also being visually observed as “blue”. There was no quantifiable difference in intensity.

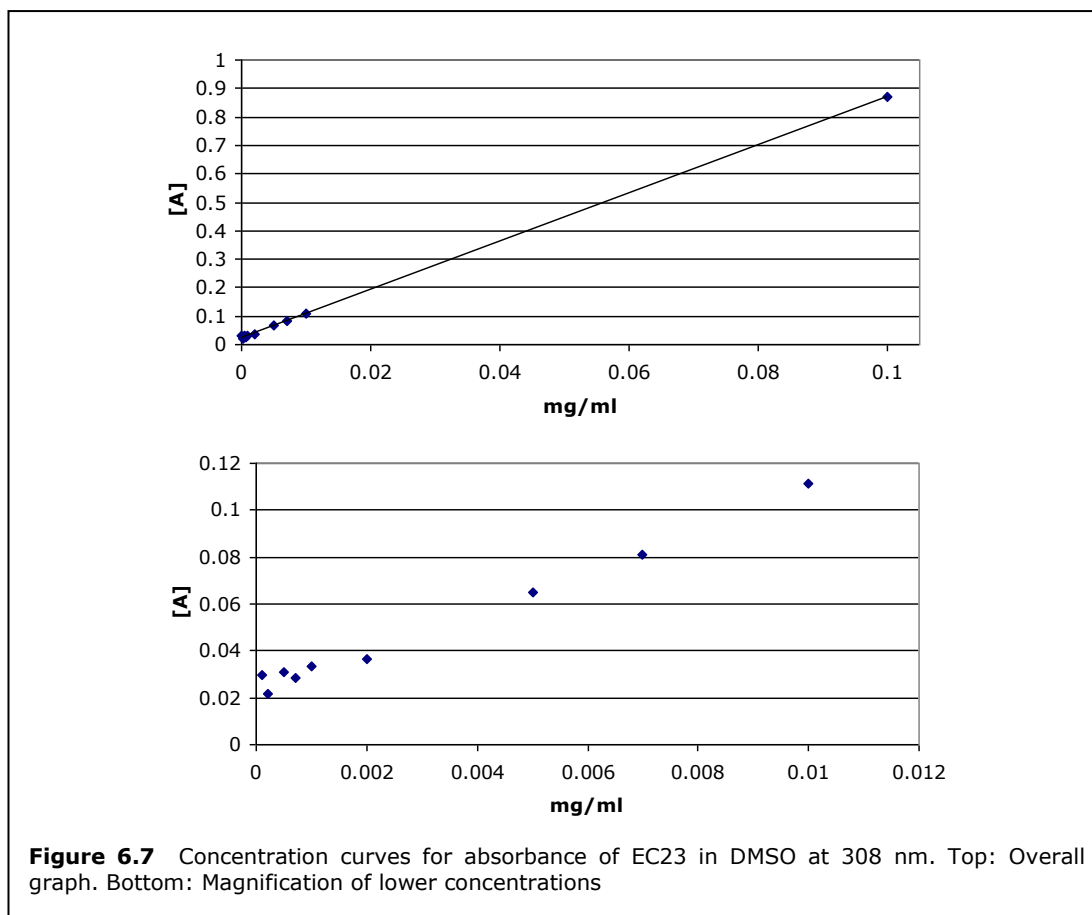
As the EC23 was not able to be visually observed, a solution phase measurement was investigated.

Initial UV observations

Figure 6.6 shows the UV spectrum of EC23 in DMSO taken using 2 μm of solution, measured on the Nanodrop photospectrometer. The peak of the EC23 curve is at 308 nm.



A concentration curve can be plotted from a range of concentrations of EC23 in DMSO. The plot of the concentrations is shown in figure 6.7. The curve appears to be linear below 0.1 mg/ml concentrations



The bottom graph in figure 6.7 shows that any readings below 0.06 are subject to large error on the Nanodrop, so ideally the concentration of EC23 should be above 0.005 mg/ml in DMSO to ensure accuracy.

Different Solvents

DMSO is “readily absorbed through the skin” and “may carry dissolved material through the skin”.⁶ In the case of EC23 which, at very least, affects stem cell development, other solvents were investigated. PolyHIPE slices were prepared with adsorbed EC23 and THF as the previous section. These slices were then (3 slices in each solvent), placed in different solvent systems namely DMSO, water, Water:DMSO in a 100:1 ratio, phosphate buffered saline (PBS), THF and DCM.

These solvents were chosen as the literature² states the EC23 is dissolved into DMSO (at a concentration of 1 mg/ml) and then added to the aqueous cell culture

solution at specific concentrations. The PBS is a water based solution (containing sodium and potassium as chlorides or phosphate salts) commonly used in biological practices as a dilutant or a wash medium. THF and DCM were chosen as EC23 is thought to have some solubility in these solvents.

2 μm of each solution was measured for absorbance at 308 nm using a Leica Nanodrop UV Detector, with samples taken before, and after, the slices were immersed. Readings of the solutions were then taken at time points after immersion at 5 minutes, 30 minutes and at 24 hours. The Nanodrop was blanked beforehand with each appropriate solvent. The tabulated results are shown in table 6.5 and graphically in figure 6.8.

Table 6.5 UV absorption at 308 nm by solvent

Time and (nm)	1 minute	5 minutes	30 minutes	24 hours
Solvent	308	308	308	308
DMSO	1.169	1.080	1.452	1.656
water	0.022	0.017	0.011	0.000
water:dmsso 100:1 ratio	0.013	0.005	0.012	0.000
PBS	0.016	0.053	0.012	0.003
THF	-	-	-	-
DCM	-	-	-	-

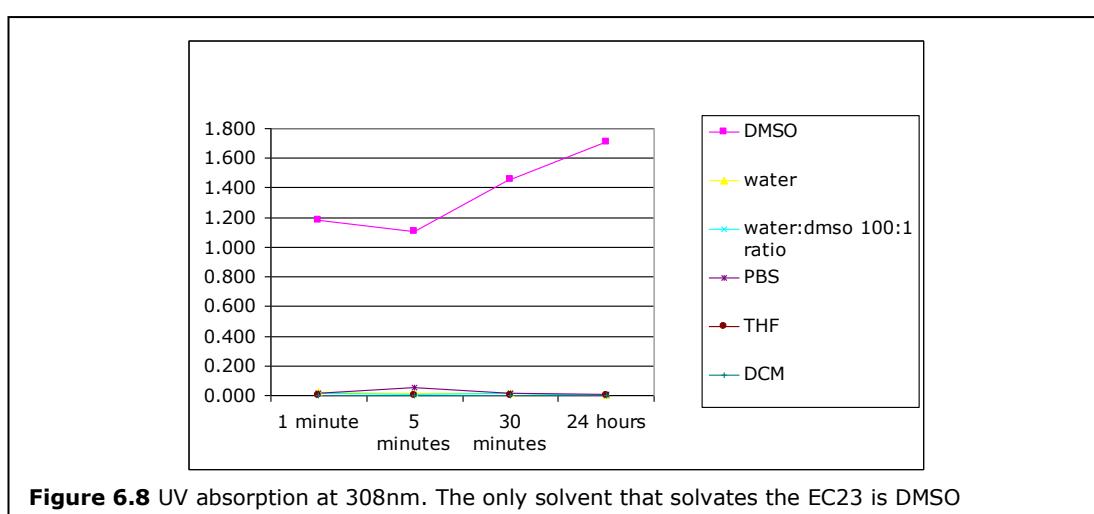


Figure 6.8 UV absorption at 308nm. The only solvent that solvates the EC23 is DMSO

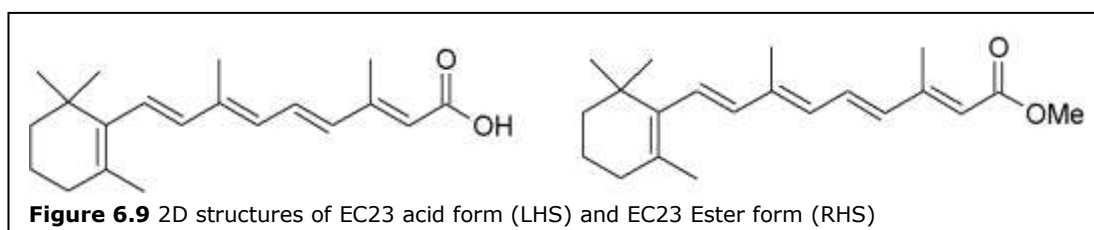
As mentioned, the EC23 is very toxic, even at very low concentrations, so constraints were imposed to ensure safe practice when handling the EC23,

especially when in a DMSO solution. The Nanodrop spectrometer is small, light, is easily moved, and is able to fit into a fume hood. The Nanodrop reads the absorbance using 2 μ l of solution. With respect to table 6.10, the THF and DCM readings are zero due to physical constraints. The volatile solvents evaporated before a reading could be taken, so although it is known that EC23 dissolves in THF, it is not easily measured using available equipment.

Table 6.10 shows that the best, and only practical, solvent, for which to observe the EC23 in solution is DMSO, as it removes the most adsorbed EC23 from the surface of the polyHIPE, and is also easily, measurable. The water:DMSO mixture did not appear to remove the EC23 from the surface. In previous papers it has been noted that EC23 does illicit a cellular response when used in an aqueous environment (once dissolved in DMSO), in concentrations similar to the 100:1 water:DMSO dilution used and therefore it is surprising that the Nanodrop does not record any dissolution into this medium. Consideration has to be taken of the sensitivity of the Nanodrop, as the lowest levels needed to illicit a cellular response have not yet been quantitatively determined, and this potentially could be below the detection limit of the Nanodrop.

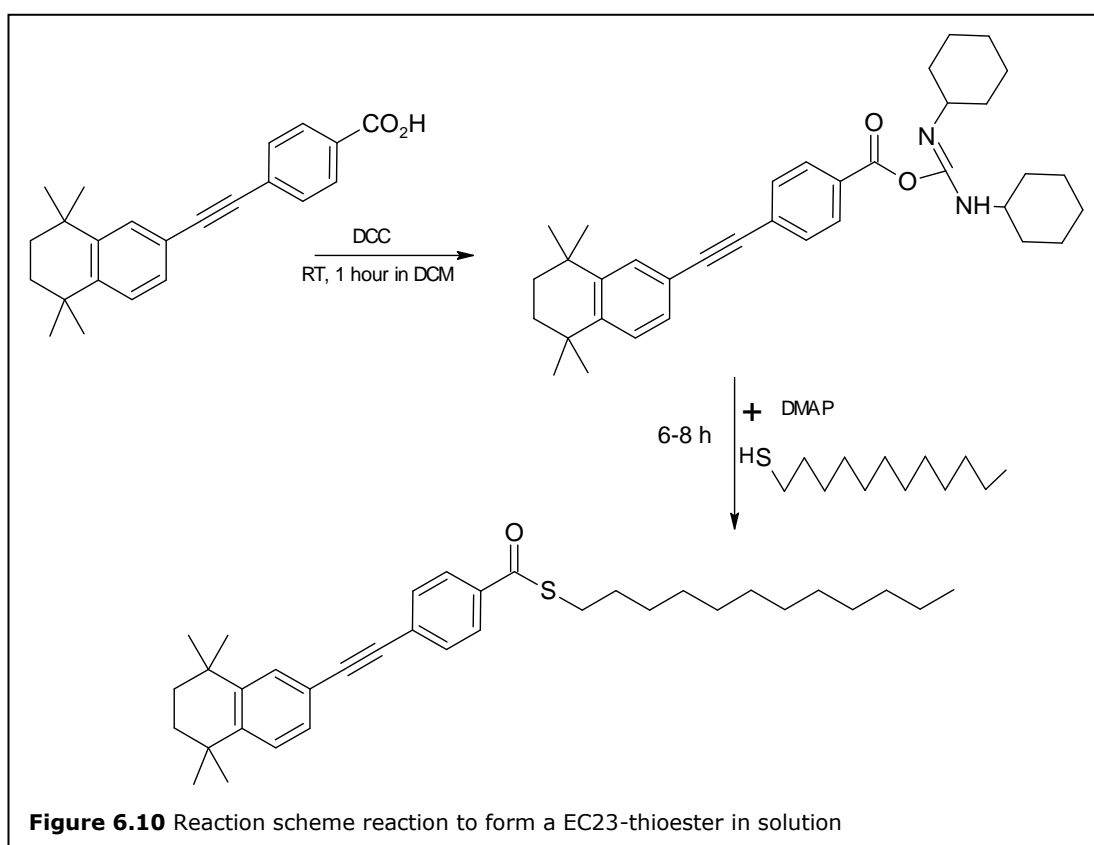
6.8 Solution Phase Thio-ester Formation.

Preliminary trials were run with the precursor to EC23 - the EC23 ester, as shown in figure 6.9, as this is much less toxic a starting material, and the EC23 acid would be formed *in-situ*.



These attempts were unsuccessful, and the synthesis focus returned to the EC23 in its acid form.

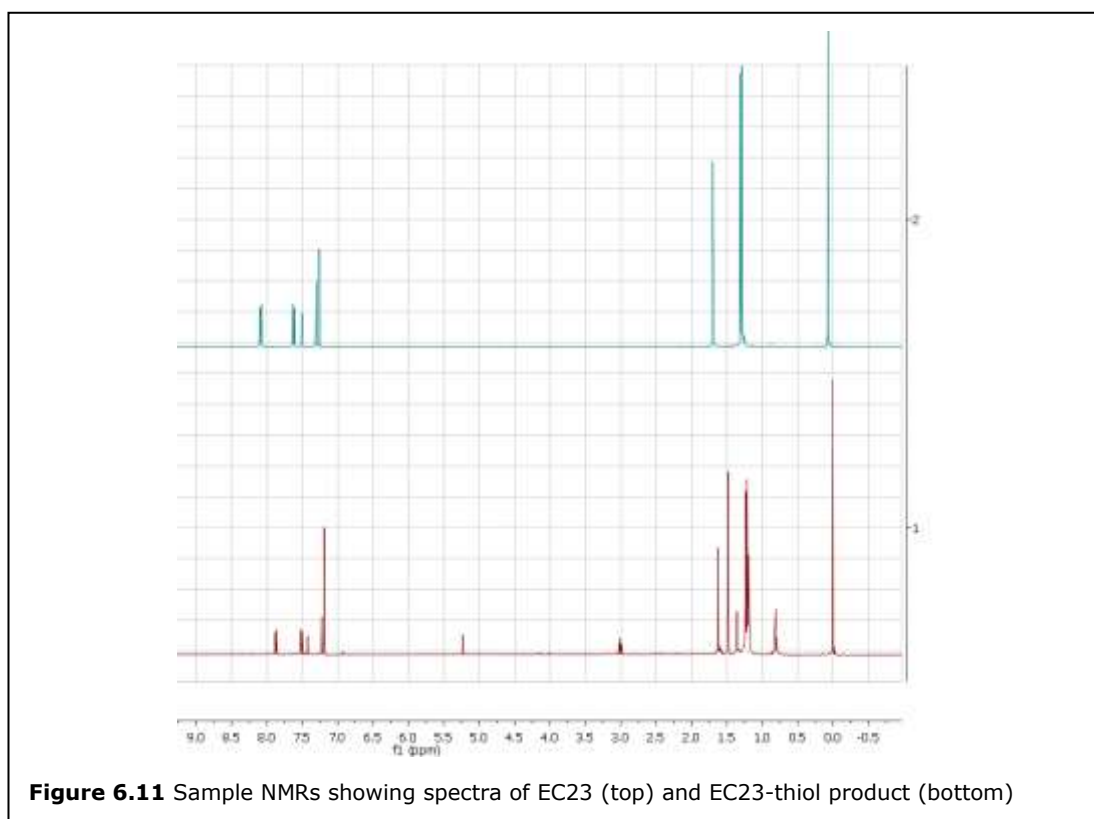
The reactions were initially formed in a solution phase, as this could be monitored by NMR. 1-dodecanthiol was used as a uncomplicated substitute to di-functional molecules (such as ethyldiamine or cysteamine). In order to demonstrate the feasibility of thio-ester formation a procedure to form thio-esters was adapted from the literature.⁷ It was anticipated that a solution phase reaction would be easier to monitor than a solid phase reaction, and that in the solution phase the reaction conditions could be demonstrated, and then related to solid phase. The reaction scheme is shown in figure 6.10.



Briefly, EC23 was reacted with a large excess of DCC (as coupling agent and dehydrating agent) in dry DCM, monitored over time by thin layer chromatography (tlc). It was noted that on the tlc plate, the EC23 and EC23 containing spots can be

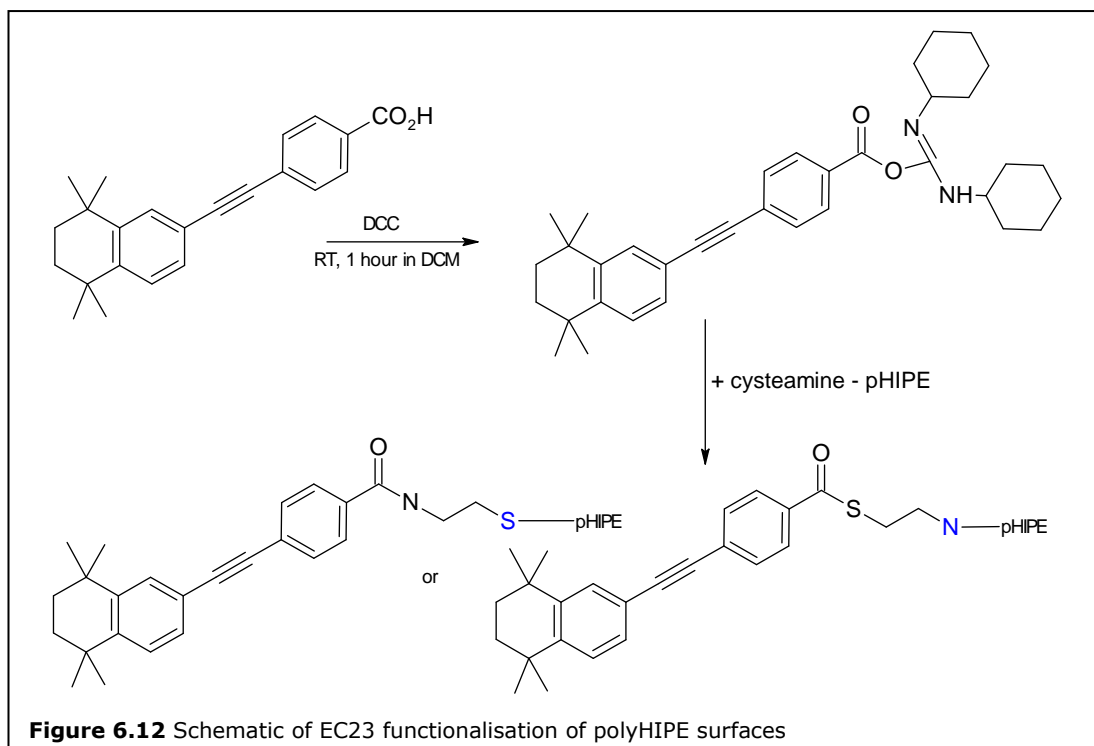
easily identified by autofluorescence under a UV light, with no development treatments needed, either to distinguish the spots, or to identify the EC23 containing fractions. After 1 hour, 1-dodecanethiol and DMAP were added and the reaction stirred. After 6-8 h, the solution was subjected to analysis by NMR. No further purification steps were carried out, due to the reactivity of the thioester.

The thioester linkage was confirmed by ^1H NMR, showing a movement upfield of the 2H closest to the sulfur ester upon attachment. Purification via column was attempted, but the thio-ester hydrolysed on the column and a thio-ester product was not obtained. The NMR quoted has excess thiol in the solution. Sample NMRs are shown in figure 6.11



As the solution phase reaction indicated a thio-ester linkage, the reaction was carried out onto the solid polyHIPE.

See figure 6.12 for a schematic of the reaction with cysteamine, ethylenediamine and ethylamine were reacted in the same manner.



Stage 1

PolyHIPE slices were plasma treated at 10 W for 15 minutes under 30 ml/min O₂ flow.

Stage 2

The plasma treated polyHIPEs were functionalised by cysteamine (SEN), ethylenediamine (E2N) and ethylamine (EN) by exposing them to the respective vapours (diluted to 4% in ethanol, containers sealed at 60 °C for 24 hours). Any unreacted reactants were removed in vacuo for 24 hours (at 60 °C).

These reagents were used to form a defined linkage between the plasma treated surface and the EC23-molecule. The EN was chosen as the surface composition of the polyHIPE will affect its surface energy. This in turn will affect the adsorption of EC23 onto the surface of the polyHIPE, so the adsorption effect will differ. The

EN was reacted to create a control surface to establish whether the EC23 is reacting with, or adsorbing onto, the activated surface, as this will create a similar surface to the SEN and the E2N reacted surface.

Stage 3

The EC23-DCC linker was formed by stirring EC23 and DCC in dry DCM for 1 hour, at a concentration of 1 mg/ml until a third fluorescent spot was seen by tlc. The solution was then decanted, to remove any DCU formed, diluted to 0.1 mg/ml and 3 ml of solution was transferred to a vessel containing the linker-attached polyHIPE slices, which were immersed in the solution.

2 μm samples were taken at 5 min and at 30 min after immersion, and the absorbance measured at 308 nm using the UV Nanodrop. A reading was also taken and analysed from 24 hours after immersion. The results are shown in Table 6.6.

Table 6.6 Comparative UV readings at 308 nm of amount of free EC23 in solution for each of the functionalised surfaces

0.1 mg/ml Sample name	reading at 308 nm			Average change
	5 min	30 min	24 hours	
Plasma + SEN	0.589	0.599	0.593	-0.278
Plasma + E2N	0.562	0.595	0.570	-0.296
Plasma + EN	0.745	0.757	0.807	-0.102

Table 6.16 shows that there is a reduction of the amount of EC23 in solution for all three types of solution, however the amount of reduction is twice EN for the SEN and E2N, indicating that more EC23 is taken out of solution, with the surfaces functionalised by the di-reactive species, so the effect could be attributed to reaction as well as the affect of adsorption. The values do not appear to change over time. The results do suggest a reaction takes place, however with the E2N

this is likely to be an amide linkage, which is more stable than the thio-ester linkage, with only partial hydrolysis expected, and over a longer time period. With respect to the SEN, this could react with the polyHIPE slice at either end of the molecules, with both esters being able to be, at least, partially hydrolysed.

6.10 Conclusions

In terms of an investigation into the potential use of 3D surface releasing retinoids, this is a start. Thio-esters have been formed in solution, and also on the surface of the polyHIPE. The acute toxicity of the EC23 has to be considered when discussing analysis options. Whereas the aim is for hydrolysable esters to be formed, more complex linkers can be envisaged, and form a base for future investigations, with an obvious extension to culture cells on these modified scaffolds.

6.11 References

-
- ¹ H. Lee, S.M. Dellatore, W.M. Miller, P.B. Messersmith *Science* (2007) **318** 426
 - ² S. Patel, R.G. Thakar, J. Wong, S.D. McLeod, S. Li *Biomaterials* (2006) **27**(14) 2890
 - ³ V.B. Christie, J.H. Barnard, A.S. Batsanov, C.E. Bridgens, E.B. Cartmell, J.C. Collings, D.J. Maltman, C.P.F. Redfern, T.B. Marder, S. Przyborski, A. Whiting *Org Biomol Chem* (2008) **6** 3497
 - ⁴ J.H. Barnard, J.C. Collings, A. Whiting, S.A. Przyborski, T.B. Marder *Chem Eur J* (2009) **15** 11430
 - ⁵ J.H. Barnard, S. Fenyk, T.B. Marder, A. Whiting, S.A. Przyborski *Mol BioSyst* (2009) **5** 458

⁶ Material Safety Data Sheet: Dimethyl Sulfoxide *Sigma-Aldrich* updated
11/08/2003

Chapter 7 - Conclusions and Future work

7.1 Conclusions

This thesis set out to create, and optimise a porous, polymeric scaffold for *in-vitro* cell culture.

The first aim was to simplify the use of the scaffold for in-vitro cell culture. This was realised with the plasma processing step, in that the scaffolds no longer need to be wetted out with varying degrees of ethanol progression to PBS.

The second aim was to demonstrate by surface analysis that an adlayer could be created on the surface of the polyHIPE. One successful adlayer of dopamine was developed, and shown to be present on the surface of the polyHIPE. This however was either incomplete or very thin.

The third aim was to demonstrate that this adlayer formed in aims 1 and 2 could be further functionalised with reactive molecules. This was shown to be the case with small, chemically defined molecules and the reactivity of the surface was mapped.

The final, overall aim, which was not fully realised within this thesis, was to attach; and release with at least some semblance of control; bioactive molecules to the surface of the polymeric scaffold, to influence stem cell development *in-vitro*.

These plasma treated polyHIPE scaffolds are currently being sold commercially under the trade name Alvatex by Reinnverate.¹

7.2 Future Work

This could be a vast topic, with possibilities from each chapter. The dopamine coating could be investigated with a suitable flat control, to determine whether the coating is incomplete, or merely thin. The plasma could be vastly expanded upon,

with multilayer holders for the existing plasma machine and also with the K1050X plasma machine alone, which is equipped with a capacitance manometer, and a borosilicate chamber, able to handle many different types of gasses, (an obvious example being nitrogen containing gasses), being able to produce different surface characteristics suitable for cell culture. The optimisation would have to be repeated for each gas, to ensure that the plasma is not destroying the polymeric surface. The plasma treatment is not limited to this particular surface or morphology, and previous scaffolds with smaller voids could now be used more easily to culture cells. The cleavable linker could also be investigated in more depth, and different types of release linkers could be looked at, for example UV cleavable linkers - one that would release the active component upon a specific wavelength, and so create a “hands-off” release of the retinoid. Looking at the release of the retinoid over time (probably using UV) would also be interesting. Other, more complex ideas could include ones such as a linker that cleaves with a certain trigger - either a specific enzyme related to a cell type, or at a certain pH, such as when the culture medium is almost used up, or when fresh culture medium is inserted, or even at particular CO₂ levels. Hydrolysis is a simple idea, as explored in this thesis, but is far from optimal due to the storage conditions needed for an “off the shelf” product, but it is a start to explore the possibilities of controlled release *in-vitro*.

¹ www.reinnervate.com